DEFENSE DOCUMENTATION CENTER

FOR

SCIENTIFIC AND TECHNICAL INFORMATION

CAMERON STATION, ALEXANDRIA, VIRGINIA

63—3—5

405 892

AZUSA PLANT

STRUCTURAL MATERIALS DIVISION

STUDY OF THE EFFECTS OF THICKNESS
ON THE PROPERTIES OF LAMINATES
FOR UNDERWATER PRESSURE VESSELS

A REPORT TO

U.S. NAVY BUREAU OF SHIPS
WASHINGTON, D.C. 40

REPORT NO. 2503 (FINAL) / APRIL 1963 / COPY NO.

AEROJET
GENERAL TIRE
GENERAL

AEROJET-GENERAL CORPORATION
AZUSA, CALIFORNIA

DDC

JUN 10 1963

TISIA D

AEROJET
GENERAL TIRE
GENERAL

STUDY OF THE EFFECTS OF THICKNESS ON THE
PROPERTIES OF LAMINATES FOR
UNDERWATER PRESSURE VESSELS

A Report To

CHIEF, BUREAU OF SHIPS
DEPARTMENT OF THE NAVY
WASHINGTON 25, D.C.
(CODE 634C)

Contract NObs 86406
Project No. SF-01-30503
Task No. 1025
BuShips No. 86-1025-3

Report No. 2503 (Final)   March 1963

AEROJET - GENERAL CORPORATION
A SUBSIDIARY OF THE GENERAL TIRE & RUBBER COMPANY

FOREWORD

This is the Final Report on Aerojet-General Corporation (AGC) Work Order 0623-01, covering the period 15 February 1962 through 15 February 1963, on Contract NObs 86406. This contract is under the direct supervision of the Materials Development and Application Branch, Code 634C, Bureau of Ships, with Mr. William Graner acting as technical monitor.

The program was conducted by the Design Engineering Department of the Structural Materials Division at Aerojet-General Corporation, Azusa, California. Major responsibility for the program resided with R. D. Saunders and R. L. Smith, who are authors of this report. Other significant contributors to the program included T. R. Sakakura, T. E. Anvick, M. Segimoto, and G. Williams.

Approved By:

A. M. Cecka

A. M. Cecka, Head
Design Engineering Department
Structural Materials Division

ABSTRACT

A discussion of the program and a summary of the work conducted is presented. The basic program was to study the effects of thickness on the mechanical and physical properties of fiber-reinforced plastic laminates for deep-submersible external pressure vessels. An analysis of fabrication methods investigated, and problems related to thick-walled cylinders, is given. Methods of testing and test results of cylinders and rings are presented.

CONTENTS

CONTENTS (cont.)

CONTENTS (cont.)

APPENDIX A - CIRCUMFERENTIAL FILAMENT-TENSIONING AND STRESS DISTRIBUTION

CONTENTS (cont.)

I. SUMMARY

The purpose of this program was to determine the effects and relation-
ship of thickness on the physical and mechanical properties of filament-wound
underwater pressure vessels, to determine design criteria, to determine fabri-
cation methods and test methods for thick-walled cylinders by fabricating and
testing small cylinders and test rings, and to compare and correlate actual
fabrication methods and test results with the analytical work.

This relationship was determined by design analysis and by the fabrication
and testing of small cylinders and test rings. Twenty-two cylinders, most of
which had a 6.0-in. ID (several had ID of over 12.0 in.), with wall thicknesses
to 4.00 in. thick, were fabricated. The long cylinders fabricated were
machined into 37 shorter cylinders for hydrotest and into rings for mechanical
evaluation.

Significant highlights of the program are as follows:

In general, no gross changes in the physical and mechanical properties
of the laminate were noted. Composite compressive properties of the cylinders
tested were determined to be: Young's Modulus 5.3×10^6 psi; density, 0.076
pounds per cubic inch, and a maximum circumferential compressive yield stress
of 130,000 psi.

An increase in the maximum circumferential stress level accompanied each
successive change in thickness (as predicted by general instability equations[*])
until a thickness to diameter ratio of approximately 0.1 was reached, after which
failure occurred by material yield or shear at the end plates.

---

[*]See Item 7 of Bibliography.

I Summary (cont.)

The winding pattern selected for the majority of cylinders fabricated was a ratio of 4 circumferential plies of roving to each 2 longitudinal plies of roving. Filaments were placed in the direction of principal stresses. One cylinder, built using a 2-ply circumferential to 1-ply longitudinal ratio of dispersion resulted in an increase in the maximum composite stress level of 20%, indicating that additional effort should be expanded in this area. Displacement of the longitudinal filaments observed after cure in several initial cylinders was determined to be caused by winding of the circumferential filaments in one direction only. Each succeeding circumferential ply should be reverse wound (i.e. alternately wound in the opposite direction).

A theoretical analysis (presented as Appendix A) showed the desirability of incorporating a programed tension pattern in the circumferential filaments. Actual cylinder fabrication, however, showed that the incorporation of a programed tension pattern is difficult to attain because of fiber-relaxation due to lowered viscosity and migration of the resin during cure and because of resin shrinkage. A constant tension pattern was selected for specimen fabrication on this program because of the difficulty in establishing a programed tensioning which would give identical patterns in the concentric cylinders machined from the thick cylinders.

Theoretically, pretensioning the longitudinal plies beyond that tension required to straighten the filaments is not necessary. Undue tensioning results in detrimental residual stresses, if the longitudinals are wrapped on by winding over the heads and then cut off by a circumferential cut.

Another analysis (presented as Appendix B of this report) indicated that scale-up will not affect the properties of filament-wound external pressure structures. This theory has been verified by the fabrication and testing of several subscale cylinders of up to 18.0-in. ID.

Fabrication methods evaluated were based on bulk or one step cure for thinner cylinders and a multi-step cure for thicker cylinders. Step curing was proven to be a feasible method for fabricating thick-wall cylindrical structures of preimpregnated roving material.

I Summary (cont.)

The standard material of construction for this program was U.S. Polymeric E787/HTS 20E Prepreg. This material is 20 End E Glass Filaments with an HTS finish preimpregnated with EPON 1031/EPON 828/MNA/BDMA epoxy resin system.

The standard method of test was external hydrostatic pressurization of cylindrical test specimens mounted on special end closure plates which were stepped to provide support at the inner ends of the cylinder. Test methods were modified during the program to permit testing to stress levels closer to the ultimate compressive yield strength of the material.

Exposure of several test cylinders to 5,000 psi simulated sea water for periods of time up to one month resulted in less than a 5% reduction in the composite stress level with no measurable weight gain.

Mechanical tests conducted on rings and ring segments cut from the ends of test cylinders showed a general increase in horizontal shear stress and axial shear stress with improved fabrication controls. Since thickness was the main variable on this program, horizontal and axial shear mechanical test results were not relatable to the values obtained from the hydrostatic testing of cylinders.

Photomicrographic examination of the composite structure was utilized to determine and improve microscopic construction characteristics such as fiber packing, voids, resin pockets, and general uniformity of construction.

II.   BACKGROUND

The U.S. Navy requires lightweight, high-strength structures such as buoys, mines, torpedoes, and submarines. Performance requirements of deep submergence vessels are exceeding the capabilities of conventional structures and fabrication methods. Glass filament winding, a process which provides the highest strength-to-weight ratio available has been steadily improved, and will continue to be improved, to reliably attain all of the complex material characteristics required for hydrospace use.

An important aspect of the development of hulls for deep-submergence vessels is the effect and relationship of thickness on the properties of filament-wound structures.

This program encompasses research and development in the areas of design theories, fabrication procedures, and evaluation methods for heavy-walled, filament-wound structures.

III. DESIGN ANALYSIS AND PLANNING

The principal tasks during the initial phase of the program, prior to fabrication of test cylinders, were to conduct design analyses regarding the theoretical aspects of such items as pretensioning of the circumferential filaments, and pretensioning of the longitudinal filaments; and to determine the effect of scale (i.e., the correlation between specimens of different size).

Considerable planning and investigation were directed, prior to actual fabrication, to such important considerations as material selection, winding pattern, winding equipment, and mandrels and test equipment. A discussion of these analyses and an evaluation based on the results of specimen fabrication and tests is presented in the following paragraphs.

A. CIRCUMFERENTIAL FILAMENT TENSIONING AND STRESS DISTRIBUTION

1. Theoretical Approach

A theoretical method was derived during the first quarter of this thick-walled cylinder program for deriving an optimum filament tensioning pattern for cylinders that are uniformly loaded by external pressure. This analysis is given in Appendix A; the analysis shows that it is theoretically possible to build a fiber-reinforced plastic external pressure vessel in which the combination of strains arising from external pressure, winding tension, and cure temperatures can be balanced to give an optimum stress pattern throughout the crossection of the vessel, provided the external pressure is known.

2. Correlation

The attainment of an optimized pretension pattern in actual cylinder fabrication is difficult because of variables such as the change in resin viscosity and resin migration during cylinder cure. In addition, the use of high tensions on the inner surface appears to have contributed to damage of the inner plies. Therefore, an alternate method considered practical for incorporating a programed tension pattern (as described in Appendix A) was the use of a pattern wherein mandrel expansion would provide some of the

III Design Analysis and Planning, A. (cont.)

tensioning of the inner plies. This approach was substantiated by the fabri-
cation and test of two cylinders (TW-12 and TW-13). These cylinders were fab-
ricated using 4.0 pounds tension per 20E Roving on the inner layer stepping
up to 8.0 pounds tension on the following circumferential layers and then
progressively decreasing the tension to 4.0 pounds at the outer surface. A
comparison of the test results produced using these programed tension cylinders,
with results of tests of cylinders wound using a constant tension, showed a
small increase (10%) in the mechanical properties and stress levels obtained.
Positive conclusions regarding this parameter are considered premature, however,
because of the limited number of tests and because of the unstable nature
of specimen failure.

3. Conclusion

A constant 5.0 lb of tension per 20E prepreg roving was
selected for most of the cylinders fabricated on this program. This tension
pattern was selected as the standard pattern because:

a. Higher tensions resulted in damaged, or resin-starved,
inner plies (see Section IV).

b. The resolution of such problems as craze-cracking of
the resin at the inner surface, "telescoping" (an excessive axial movement of
the circumferential plies due to circumferential tension), circumferential
ply wrinkling, and mandrel removal dictated the use of a constant tension
pattern to reduce the number of fabrication variables.

c. It was not desirable to use a programed tension pattern
for the thicker cylinders. Since these thick cylinders were machined into
thinner, representative concentric cylinders for test, a programed tension
pattern in these thick cylinders would not have produced the same tension
pattern in each machined cylinder.

III Design Analysis and Planning, A (cont.)

4. Factors Affecting Circumferential Tension

a. Preheating of Preimpregnated Roving

One of the variables affecting tension and the residual stress pattern in a filament-wound composite is the amount of preheating applied to the preimpregnated material immediately before roving payoff onto the part surface. Preheating the prepreg, before and during payoff, softens the resin, and allows the tension (which is applied through the spool of prepreg material) to straighten out any kinks, birdseyes, or patterns present in the roving because it was helically wound onto a spool. Another variable inherent in the prepreg roving is the degree of resin advancement. Advancement of the resin makes the prepreg stiffer, and not only affects the amount of preheating required, but makes a difference in the amount of tension required to produce a consistent, compact laminate.

One problem encountered with some cylinders wound during this program was the difficulty in removing parts from the mandrel. This difficulty was due to the higher effective roving tension resulting from prepreg preheating. Constant tension of 5.0 lb, when used without preheating, resulted in parts which allowed sufficient mandrel expansion to allow easy mandrel removal. The same 5.0-lb/20E tension, combined with the effects of preheating, required forces of approx 20 tons to break the initial part grip the mandrel.

Preheating the prepreg before winding onto the mandrel is highly desirable because of the superior parts which are produced by this method. Tension patterns must be selected, therefore, that will not cause mandrel removal problems, or segmented mandrels may be required. Possibilities include use of the lowest possible tension that will allow payoff of consistent straight fibers (the method used in the fabrication of the thickest cylinders), and use of a programed tension with, say a very low tension on the inner plies only (the method used in fabricating the programed tension Cylinders No. TW-12 and TW-13).

III Design Analysis and Planning, A (cont.)

Specific variables which must be evaluated in association with programed tension include: fabrication processes; manufacturing practicality; mandrel deflection; resin percentage, and the eventual effect on such design properties as short-term, long-term, and cyclic external pressurization.

b. Mandrel Design Considerations

It has become apparent that mandrel design is a critical factor related to tension. The small cylinder sizes presently being fabricated present no problem but do serve to point out that for mandrel scale-up, such as for an 8-ft-dia or larger hull, present methods of fabrication may have to be modified to allow use of lighter weight mandrels.

At present, 6.0-in.-ID and 12.0-in.-ID cylindrical parts are being fabricated on steel mandrels 0.62 and 1.25 in. thick, respectively. The thickness of mandrels was selected to withstand the highest anticipated compressive loads due to winding tension. Mandrel removal difficulty from these 6.0-in.-ID and 12.0-in.-ID parts has been affected by both filament winding tension and part thickness. It would seem, therefore, that a large hull structure may have to be fabricated by some method other than bulk elevated temperature cure, possibly by an in-process room-temperature cure system, or by an elevated-temperature cure performed in steps (several cylinders -- TW-16, TW-18, and TW-20 - were fabricated to investigate the step-cure method.). Both of these methods would provide additional strength to the composite during fabrication and would thereby reduce requirements for mandrel strength.

B. LONGITUDINAL FILAMENT TENSIONING

1. Analysis

An analysis was made during this program relative to tensioning the longitudinal fibers.

This analysis assumed a theoretical cross section having a uniform tension applied to all longitudinals, as in the case of constant tensioned

III Design Analysis and Planning, B (cont.)

longitudinals wound on in an end-over-end manner. When the ends are cut off these parts, thereby forming open-ended cylinders, a redistribution of longitudinal tensile forces occurs to reach equilibrium. This redistribution results in compressive loads being introduced into the resin. When these tensile and compressive loads reach equilibrium, there are resulting undesirable residual stresses in the composite.

2. Factors Influencing Longitudinal Filament Tensioning

Following is a discussion of additional areas of consideration which relate to tensioning of the longitudinal filaments, and supplement this analysis:

a. Smoothness of the circumferential windings, initially and progressively, is a major factor in thick-walled cylinder fabrication. Since the normal fabrication process involves laying down alternate circumferential and longitudinal layers, each longitudinal layer is forced to conform to the contour of the previous circumferential layer by the following circumferential wrap. Optimum smoothness dictates minimum band-width variation of the prepreg roving, and absolute accuracy of roving placement by the winding machine and machine payoff head. The feasibility of winding parts with wall thicknesses of greater than 1.0 in. was demonstrated by the fabrication of a 4.0-in. thick cylinder. This cylinder was fabricated in four 1.0-in. thick steps. Each step was cured and machined smooth before the succeeding step was wound on. The fabrication of this cylinder demonstrated the feasibility of the step cure approach.

b. Low viscosity of resin when heated, and resin shrinkage during cure tends to upset the uniformity of the programed tension pattern. Resin shrinkage can cause residual stresses.

3. Conclusions Concerning Longitudinal Filament Tensioning

a. Longitudinal elements must be straight and uniform in order to carry their maximum load without buckling.

III Design Analysis and Planning, B (cont.)

Although tensioning of the longitudinal elements as well as machining of hoop layers would tend to improve straightness of the longitudinal elements, these factors are not considered to be critical considering the present state of the-art.

b. Programed prestressing of the longitudinals, beyond that tension required for straightness, does not appear to offer major advantages for the fabrication of open-ended cylinders.

C. SCALE EFFECTS

1. Analysis

The effects of scale were investigated on another program at Aerojet running concurrently with this thick-wall study (see Appendix B). The results of this investigation are directly applicable, and satisfy the analysis requirements of this program.

Briefly, it can be said that scale effects will not influence the performance of any cylinders fabricated on this program. Theoretically, scaling does not upset the stress distribution, and the buckling load, when buckling occurs, will only be a function of non-dimensional length and coefficients.

On the practical side, however, there will be a limit beyond which any further scaling-down of the models will begin to produce different stress distributions for the same surface stresses. First, the transition region between laminations or interlaminar shear lines, being a constant uncontrollable thickness, prohibits the application of scale. Second to be considered is the laminate material itself. Each layer is considered as a homogeneous orthotropic material because of the large number of fibers in each layer. Should the scale be reduced to a very small size, however, the individual fibers composing the laminate become comparatively larger and fewer in number. This condition makes it impossible to define an effective modulus, since the averaging process will break down.

III Design Analysis and Planning, C (cont.)

Fortunately, these two cited effects are not of importance for the present state-of-the-art and current manufacturing techniques. Therefore, cylinders of the size utilized on this thick-wall study are theoretically considered free of any effects of scale.

2.   Scale-Up Model Verification

Verification that scaling up filament-wound cylinders does not upset the stress distribution was attempted by the fabrication and testing of three progressively larger cylinders. These three cylinders had inside diameters of 12.0 in., 15.2 in. and 18.4 in., and were machined from one 12.0-in.-ID by 4.0-in. thick cylinder, TW-20. Fabrication details for this cylinder are given in Section IV,A,21. These three cylinders are shown in Figure 1.

Cylinders TW-20-2, TW-20-3, and TW-20-4 were biaxially tested. Specific physical and mechanical properties are given in Section IV, A,21. The maximum circumferential stress values attained with the larger series cylinders were within 10% of the circumferential stress values attained with the 6.0-in.-ID test cylinders. Therefore, the experimental results attained on these three larger-diameter cylinders support the conclusions given in the theoretical analysis (see Appendix B) that scaling does not upset the stress distribution. The effect of scale should be further confirmed by additional model fabrication and testing.

D.   WINDING PATTERNS

1.   Dispersion (Layer Thickness)

A dispersion of circumferential plies to two-ply longitudinal plies was used for all test cylinders fabricated on this program except for four cylinders (TW-1, TW-2, TW-3 and TW-17). A ply is considered as the thickness of one roving or tape; a layer is composed of one or more tapes or plies laid in the same direction without interspersing plies. Although the 2 circumferential plies to 1 longitudinal ply ratio gives a maximum dispersement of layers, a dispersion giving a 4 to 2 ratio was selected to allow fabrication

III Design Analysis and Planning, D (cont.)

of cylinders having the longitudinal filaments either wound on, or laid in by hand using tape. When longitudinal filaments are wound on, the roving discharge roller must be offset from the longitudinal axis to clear the mandrel shaft. In winding the longitudinals, one revolution of the mandrel results in two plies (or thicknesses) of the filament since it is not possible to wind on only one longitudinal ply because of the offset due to the shaft. The dispersement pattern, therefore, for wound on longitudinals, must be in a ratio of four hoops to two longitudinals, instead of two hoops to one longitudinal as in the case of hand laid-up single-thickness longitudinals.

It is possible that layer thickness (dispersion) may be a prime variable in the attainment of optimized filament-wound external pressure vessel mechanical properties.

One cylinder, TW-17, was fabricated specifically to evaluate the effect of dispersion of maximum, or 2:1, circumferential plies to longitudinal plies. Details of construction are given in Section IV,A,18.

The hydrotest of a 5-in. length of this 0.526-in. thick, 6.0-in.-ID cylinder resulted in a maximum circumferential stress value of 115,725 psi without failure. Examination of this cylinder after the test was suspended at 16,000 psi showed what appears to be the beginning of failure at both ends originating at the end plate support areas.

This stress-value indicated that the 2:1 dispersion of circumferential to longitudinal plies produced an increase of approximately 20% in the circumferential stress over 4:2 dispersion cylinders of the same length. Also significant to this discussion of dispersion are the cylinders (TW-2 and TW-3) fabricated before selection of E787 prepreg as the standard material of construction. Test results of these cylinders show a higher maximum circumferential stress level at failure for the same geometry than the cylinders fabricated using E787 Prepreg (TW-4). The mechanical tests (see Section IV,B) performed on rings and ring segments from these two cylinders (TW-2 and TW-3) showed substantially lower values for both horizontal and axial

III Design Analysis and Planning, D (cont.)

shear, than did the E787 material. It appears likely, therefore, that the
2:1 dispersion was the sole factor contributing to higher stress levels on
several cylinders.

It is likely that where bending occurs, such as buckling
due to instability or due to rigid end conditions, that interlaminar shear
may be a controlling factor. A correlation between resin interlaminar shear
strength and maximum composite stress on test cylinders has been noted on the
Resin Study Program (NObs 86307). It appears that cylinders having maximum
dispersion exhibit higher stress levels than cylinders having thicker layers.

2.   Filament Orientation

The orientation selected for this program was based on the
placement of fibers in the directions of the principal stresses, and on obtain-
ing test specimen simplicity. The circumferential or hoop layers were wound
on as nearly normal to the mandrel axis as the minimum lead angle will permit;
the leads used were the width of one prepreg 20E roving, or 0.078 in. The longi-
tudinal layers used unidirectional tape and were laid in by hand parallel to
the mandrel axis.

Hoop filaments were initially wound in one direction only to
avoid fiber cross overs and bridging. Later cylinders had each successive
circumferential layer reverse helically wound (that is, the lead angle was
reversed). This change was required because of the displacement noted in the
longitidunal filaments of several thick-walled cylinders after cure. This
displacement was visible through the outer surfaces of these cylinders. It
was concluded that this displacement was caused by an unbalanced winding due
to winding the circumferential filaments in one direction only, resulting in
an initial circumferential residual stress, before cure, directly proportional
to the winding tension. This residual stress is released during the initial
stages of cure when the resin viscosity is lowered, resulting in an "unwinding"
of the cylinder causing longitudinal fiber displacement.

III Design Analysis and Planning, D (cont.)

        Reverse winding (reversing the helix angle or lead angle of the roving), incorporated in all cylinders after TW-17, eliminated all of the displacement of longitudinal fibers due to an unbalanced stress pattern.

        3.   Cross-Section Layer Dispersement

        Cross-section construction was designed based on the following considerations:

        a.   Need for circumferential filaments at the inner and outer surfaces.

        b.   A pattern that is readily applicable to increased wall thicknesses.

        c.   A pattern that will maintain a 2-to-1, or similar, circumferential-to-longitudinal relationship.

        d.   A symmetrical pattern for consistent scale-up.

        Circumferential layers are four plies thick; longitudinal layers are two plies thick. The longitudinal plies are designed slightly thicker than two regular circumferential plies to attain the 4-to-2 (2 circumferentials to 1 longitudinal) or other desired ratio.

    E.   MATERIALS SYSTEMS AND FABRICATION METHODS

        1.   Materials Systems

        Initial test base cylinders were fabricated using ECG 140-P048 (HTS) 20E Roving, in-process impregnated with DER 332/HHPA/HDMA Resin System in the circumferential direction, and 4-in. wide pre-impregnated glass fiber (with 801 finish) tape (Scotch-ply 1009-26) for the longitudinals. (Specific details of construction are given in Section IV.) After the fabrication of several cylinders, TW-1, TW-2, and TW-3, the need for a different resin system which could be more easily standardized for use by the several companies engaged in fabrication of test cylinders for deep submergence programs became apparent and was requested by the Bureau of Ships. One of the

III Design Analysis and Planning, E (cont.)

requirements set for selection of a new material was that both circumferentials and longitudinal plies be fabricated of the same material

Limited data available suggested that interlaminar shear strength was a big factor in influencing composite stress properties. It was also concluded that such properties as resin percentage, resin advancement, consistency of materials, quality control practices, and ease of fabrication dictated selection of a preimpregnated resin system for this program.

A thorough survey of the available high quality, high horizontal shear strength prepreg materials was made of material suppliers by the Materials and Process group within the Structural Materials Division at Aerojet.

The recommended system was U. S. Polymeric E787/HTS 20E Preimpregnated Roving. This E787 prepreg system, which was being used for First Stage Polaris Rocket Case fabrication and for which much test data was available, was chosen as the standard material of construction. Procurement of this material on this Thick-Wall program has been to the same, stringent, quality control procedures and acceptance tests used on the Polaris Rocket Case Program.

In general, this material has proven to be a good selection as the standard material for these initial phases of the Deep Submergence Programs.

Two problem areas associated with the use of this type of prepreg material are the variation in material strength and material softening characteristics due to the degree of resin advancement, and the "memory" of the roving of the lay of the helically wound bundle. The degree of resin advancement may well be an important factor in obtaining consistent physical and mechanical properties. It has been found, on other programs at Aerojet, that the degree of resin advancement, as determined by the number of days at room temperature, can grossly affect resin interlaminar shear strength. (Since this program is currently in the laboratory evaluation stage, results are not yet available for publication.)

III Design Analysis and Planning, E (cont.)

Degree of resin advancement is a definite factor in cylinder fabrication techniques. Since some rolls of roving are more advanced than others, more heat is required to soften the roving before winding, and additional heat has to be applied to the part surface.

Because of the wide helical pattern in which prepreg roving is currently wound on the storage spools, proper preheating and tensioning are required to make the roving lie flat on the part mandrel. In addition, because of the variation in prepreg roving width, the forming of a tape from several rovings involves exact payoff-roller adjustment and considerable care in winding. It is expected that improvement in this area will evolve with improved heated payoff roller designs, and more experience in pre-impregnating by suppliers. A major improvement is expected with Aerojet's in-situ process preimpregnated roving whereby the roving is vacuum impregnated without removing the material from the spool. Funding is required, however, to increase the capacity of this laboratory process, which, from all indications, will produce a superior, more economical, preimpregnated material.

Roving aging (the amount of time prepreg material on the spool or after winding onto a mandrel can sit at room temperature before cure) is an important parameter of prepreg efficiency. The effect of this aging is currently being evaluated on another program at Aerojet.

2.   Fabrication Methods

The methods evaluated and used for the winding of all cylinders on this program are discussed below.

a.   General Approach

All cylinders after TW-7 were wound on 6.0-in.-OD steel mandrels (except for TW-20 which was wound on a 12.0-in.-dia mandrel) with removable end dams to prevent "telescoping" of the circumferential plies. All circumferential plies were paid off, either two plies or four plies at a time, similar to the method shown in Figure 2, using the tension noted in the sections

III Design Analysis and Planning, E (cont.)

on cylinder fabrication. Unidirectional tape, made of E787 prepreg roving was layed-in by hand parallel to the mandrel axis for the longitudinal elements. A shrink tape overwrap was utilized on all later cylinders. The standard cure (Section III,2,d) was monitored and controlled by thermocouples.

        b.   Longitudinal Plies

        Unidirectional tape was fabricated of E787 prepreg by winding in a circumferential direction, onto a plastic-film-covered 12.0-in.-dia aluminum mandrel heated to approximately 150°F. Two E787 prepreg 20E rovings, tensioned at the spool, are wound at one pass using a lead which will give the desired layer thickness to obtain the desired finished composite ratio of two circumferentials to one longitudinal. The finished thickness of each longitudinal ply is approximately 0.016-in. After winding a length of the 12.0-in. mandrel sufficient to wrap the circumference of the test cylinder, the windings are cut through, parallel to the mandrel axis, and removed from the mandrel as a flat sheet.

        c.   Circumferential Plies

        Several changes in the method of winding the circumferential plies were incorporated during this program. Initially, the circumferential windings were wound in one direction only (no reversing of the helix or lead angle). The circumferential windings were unrestrained at the ends, reflecting a practice common to thin wall cylinder winding.

        With the increasing wall thickness of cylinders being fabricated, two new problem areas developed: telescoping of the circumferential plies and displacement of the longitudinal plies.

        "Telescoping" of the circumferential plies was concluded as being caused by an unwinding action of the circumferential filaments during cure. This unwinding action results from the lowered resin viscosity during cure and the initial filament tensioning. Addition of dams to the ends of the mandrel eliminated the telescoping.

III Design Analysis and Planning, E (cont.)

The unwinding action of the tensioned circumferential filaments during cure also caused displacements of the longitudinal elements. This displacement was especially evident after the addition of the end dams to prevent telescoping. This displacement of the longitudinal filaments was concluded as due to winding the circumferential filaments in one direction only. The incorporation of a winding pattern wherein each succeeding circumferential layer was reverse helix wound from the previous layer eliminated the displacement of the longitudinal filaments.

Cylinder fabrication on this program was transferred from a cam-hydraulic controlled winding machine to a new machine having a lead-screw controlled roving-payoff head in order to obtain improved roving application for linear patterns. In both machines, tensioning of the circumferential filaments is applied at the roving spool.

d.   Cure

Both bulk and step cures were evaluated and used for cylinder fabrication during this program. In both cases, the final cure of the entire composite thickness was carried out as follows: 2 hours at 200°F; 15 min at 225°F; 15 min at 250°F; 15 min at 300°F; and 8 hours at 325°F.

For cylinders cured by the step cure method, this standard cure cycle was followed for the first step except that the time at 325°F was reduced to one hour so that the final cure of the entire thickness would result in a uniform time at temperature relationship. All temperatures noted above are part temperatures controlled by thermocouples which were wound in close to the inner surface at part mid-length. After completion of the cure cycle, the part is slowly cooled to room temperature. For thick, step-cured parts (TW-16 and TW-18), the first step, after cure, was machined to obtain a smooth surface and concentric diameter before the second stage is wound on.

III Design Analysis and Planning, E (cont.)

A significant improvement in attaining an even, stress-free cure was noted during this program by placing the heat sensing thermocouples close to the inner surface. Craze-cracking of the inner surface was experienced on many of the initial cylinders. Since the thermocouples have been used close to the inner surface, no craze-cracking has occurred, indicating that a more uniform, comparatively stress-free cure was attained.

  e. Mandrel Removal

Preheating the prepreg roving before winding has resulted in much more compact windings which have, in turn, made mandrel removal more difficult. Mandrel removal is more fully detailed in Section III,A,2.

Analysis conducted during mandrel design indicated that steel mandrels were desirable to withstand the highest anticipated compressive load due to filament tensioning and resin shrinkage. Since ease in mandrel removal is also dependent on the mandrel surface, all mandrels built for this program had a very slight taper (0.015-in. on diameter, per 30-in. length), a draw polish finish parallel to the longitudinal axis and a hard flash chrome finish. Mandrel removal was accomplished by standard arbor presses. Gaseous nitrogen was used as a cooling medium inside of the mandrels on occasion where part removal was difficult. Additional clearance between the part and the mandrel was obtained by mandrel thermal shrinkage.

The primary recommendations to effect efficient mandrel removal from the thick-walled parts are as follows:

  (1) The lowest tension possible for efficient cylinder fabrication, specifically on the inside plies.

  (2) An extremely finely finished mandrel with as large a taper as possible.

  (3) An adequate force to break the initial grip of the part to the mandrel and sufficient press stroke to push the mandrel all the way through the part.

III Design Analysis and Planning, (cont.)

F.   TEST METHODS

1.   Biaxial Hydrotest

Biaxial hydrotest has been the primary method of test for all cylinders on this program.

The test cylinders are mounted on end closure holding plates which are shown in Figure 3. These plates are stepped to provide a 0.400-in.- wide, minimum, support on the internal surface at each end of the cylinder.

A significant development relative to the testing of thick-walled cylinders was the clear evidence of the effects of end conditions and resulting lower stress levels apparant on several cylinders. Cylinders TW-18-1 and TW-19-1, for example, showed a clean, shear failure at approximately 45° from the part surface, as shown in Figure 4. This shear plane initiated at the intersection of the flat support surface and tapered sections of the internal support plates. Since the stress levels for these thick cylinders (0.601-in. thick for TW-18-1 and 0.747-in. for TW-19-1) were lower than several previously tested thinner cylinders (TW-15-1 and -2, and TW-13-2a), it appears that failure at stress levels considerably lower than ultimate material yield strength may be caused by the stepped steel end closures which give a "hard spot" type of internal support. This conclusion is based on consideration of the failure pattern and follows the analysis made by the David Taylor Model Basin which states "..... the stronger the frame, the weaker the vessel. This surprising result is explained by the fact that a light frame is less of a so-called 'hard spot' than a heavy frame, that is the light frame contracts more under external pressure thereby allowing a more uniform contraction of the shell and lower stresses (particularly the longitudinal bending stress) in the shell."[*]

To determine the effect of the solid end plate condition, tests were run on two identical 0.75-in. thick by 6.0-in.-ID by 5.0-in. long

---

[*]See Item 7 of the Bibliography.

III Design Analysis and Planning, F (cont.)

cylinders using different end conditions. The first cylinder, tested (TW-19-1) used the standard solid end plates and failed at 15,600 psi giving a maximum circumferential stress of 86,939 psi. The second cylinder tested, TW-19-4, used 0.44-in. wide by 0.44-in. thick filament-wound rings instead of end plates. TW-19-4 failed at 22,665 psi giving a maximum circumferential stress of 126,000 psi. This higher stress level represents an increase of approximately 30% over the cylinder tested with solid end plates and indicates that end conditions (the rigid end support plates) probably inhibited test values obtained on this program as well as on other deep submergence testing programs.

The effect of end conditions had been given much consideration based on the examination of many of the hydrotested cylinders. Conclusions regarding this condition were hard to reach because of the destruction caused by the implosive failure and the inelastic nature of the material. With improvements in test methods (such as filling the cylinders with water as a cushion) and with the thicker, shorter test cylinders, failures due to the end conditions became more suspect.

Significant strain data for instrumented cylinders was recorded on an oscillograph at specific increments during test. Strains were recorded from six circumferential gages 60° apart and two axial gages 180° apart at mid-length on the inside diameter of the part. Budd Metalfilm HE-181-E strain gages were used. All strain gages were water-proofed.

Pressurization was accomplished by a standard Sprague Pump System. The pressure vessels used for tests have been the Aerojet 17,500 psi chamber, shown in Figure 5, which can test parts up to 14.0-in.-dia and 35.0-in. long, and the 30,000 psi capacity creep chamber and pressurization system shown in Figures 6 and 7. The top head of the 17,500 psi chamber is shown above the end closure and cylinder assembly in Figure 3.

Test cylinders were filled with distilled water and vented during test, to reduce implosion and prevent complete destruction of the test specimen when collapse occurred. Filling the test specimens with water also protects the mounting shaft and end closure plates from excessive damage caused by the implosive force.

III Design Analysis and Planning, F (cont.)

2.   Data Reduction

Strain and pressure data obtained during hydrotest were converted into significant mechanical values using the following formulas, identified by $\triangle$, for reference in Section IV,A.

$\boxed{1}$ Maximum circumferential stress, inner surface $\sigma_{\phi i}$

$$\sigma_{\phi i} = -P \frac{2R_o^2}{R_o^2 - R_i^2}$$

$\boxed{2}$ Maximum circumferential stress, outer surface $\sigma_{\phi o}$

$$\sigma_{\phi o} = -P \frac{R_o^2 + R_i^2}{R_o^2 - R_i^2}$$

$\boxed{3}$ Axial (longitudinal) stress σ_{Xi}

$$\sigma_{Xi} = -P \frac{R_o^2}{R_o^2 - R_i^2}$$

$\boxed{4}$ Circumferential Modulus E_ϕ

$$E_\phi = \frac{\sigma_{\phi i2} (1 - \mu_1, \mu_2)}{\epsilon_{\phi i} + \mu_2 \epsilon_{Xi}}$$

$\boxed{5}$ Axial (longitudinal) modulus E_X

$$E_X = \frac{\sigma_{Xi2} (1 - \mu_1, \mu_2)}{\epsilon_{Xi} + \mu_1 \epsilon_{\phi i}}$$

$\boxed{6}$ Effective Modulus E_{eff}

$$E_{eff} = 2E_\phi \frac{K}{1 + K} , \quad K = \frac{E_X}{E_\phi}$$

III Design Analysis and Planning, F (cont.)

⟨7⟩ Critical instability pressure, P_c (Trilling Eq. 9)

$$P_c = \frac{2.42\ E_{eff}}{(1 - \mu^2)^{3/4}}\ \frac{(t/D)^{5/2}}{L/D - 0.45\ (t/D)^{1/2}}$$

μ assumed = 0.25

where

P_c = Critical instability pressure, psi

$-P$ = Pressure, psi

R_o = Radius, outer surface, in.

R_i = Radius, inner surface, in.

$\epsilon_{\phi i}$ = Midlength hoop strain, inner surface at specified pressure (approx 60% of $-P_c$), in./in.

ϵ_{xi} = Midlength axial strain, inner surface at specified pressure (approx 60% of P_c), in./in.

μ_1 = Hoop Poisson's ratio

μ_2 = Axial Poisson's ratio

$\sigma_{\phi i2}$ = Midlength hoop stress, inner surface midlength at specified pressure (approx 60% of P_c), psi

σ_{xi2} = Midlength axial stress, inner surface midlength at specified pressure (approx 60% of P_c), psi

t = Cylinder thickness, in.

D = Mean diameter, in.

L = Effective test length, in.

Circumferential modulus, axial modulus, and effective modulus are calculated using the stress, strain, and Poisson's ratios at approx 60% of ultimate failure stress. At this stress level, no major deviation or indication of instability is present, thus allowing calculation of true modulus values.

3. Test-Specimen Geometry

Specimen geometry (i.e., thickness and length) has been varied during this program, not only to determine the effect of length but also for

III Design Analysis and Planning, F (cont.)

economy. Cylinders having a geometry which predicted failure by instability and cylinders with a geometry predicting failure by yield were tested. These variations in length helped to attain stress levels closer to the ultimate yield strength of the material.

An investigation of the primary methods of failure (material yield and instability) indicated that test cylinders 6.0-in.-ID by 0.60-in. thick by 11.4-in. long would probably fail by material yield. Shortening the cylinder length therefore, and disregarding the effects of longitudinal bending stresses due to end conditions, should theoretically produce the same stress values as the 11.4 length 0.60-in. thick cylinder. Since this program was based on a comparison of stress values of representative concentric cylinders machined from thicker cylinders, specimen cost for thick cylinders would have been prohibitive if geometry were kept at the 11.4-in. test base length. This was especially true of large cylinders, like TW-20 which was fabricated to check scale effect.

G.   TOOLING AND TEST EQUIPMENT

1.   The following items of tooling were designed and fabricated for use on this program:

a.   A 6.0-in.-OD by 2.0-in. thick by 15.0-in. long aluminum mandrel (this mandrel was used for several initial test base cylinders). The use of high filament tensioning can tend to restrict mandrel expansion; the use of a high thermal expansion material, therefore, such as aluminum may not be desirable unless tensions are low enough to allow expansion without damage to the filaments.

b.   A 6.0-in.-dia by 15.0-in. long steel mandrel used for test cylinder winding. The lower thermal expansion of the steel, as compared with the aluminum, resulted in cylinders having less resin-crazing on the inner surface.

III Design Analysis and Planning, G (cont.)

        c.   A steel mandrel, 6.0-in.-dia by 30-in. long, was used for cylinder fabrication. This mandrel is long enough to facilitate the winding of two cylinders simultaneously. This length was required for the thicker test cylinders such as TW-18.

        d.   A 6.0-in.-dia by 45.0-long steel mandrel, which was required because of an expedited schedule and to fabricate longer cylinders from which could be machined shorter cylinders for several comparative tests.

        e.   A 12.0-in.-dia by 30.0-in. long steel mandrel, which was required for fabrication of test cylinders to check scale effect. This mandrel is shown with end dams attached in Figure 2.

        f.   A 24-in.-dia by 54.0-in. long mandrel, the use of which was planned for the fabrication of larger cylinders.

    2.   Test Equipment

        a.   Test Chamber

        Aerojet's 17,500-psi test chamber was modified to enable strain gage readings to be taken on both the inner and outer surfaces of the test specimens without the necessity of water-proofing of the strain gages. This feed-through is visible at the bottom of lower closure plate shown in Figure 3.

        New end-closure-plate fixtures, for holding and closing the ends of cylindrical specimens during creep and fatigue tests, and during short-term hydrotests, were fabricated. These fixtures will accommodate cylinders with diameters of from 6.0-in.-ID to 10.0-in.-OD (6.0-in.-ID by 2.0-in. thick wall). Feed-through seals of the fixtures allow strain gage leads to be carried to both the inner and outer surfaces of the test specimen. The rubber plug type of feed-through seal designed is similar to that used by the David Taylor Model Basin.

III Design Analysis and Planning, G (cont.)

        b.   Ring Compression Fixture

        This fixture was completed and satisfactorily tested. A leak developed in the hydraulic bag during calibration, and the bag is being repaired.

        c.   Creep and Fatigue Test Facility

        The first three units of this facility, utilizing 16-in.-dia projectiles (Mark 13 Mod 2) obtained from the Naval Weapons Depot, are now operational. The first creep chamber completed was used for hydro-testing of several cylinders (TW-18 and TW-19) and is now in use for creep testing TW-16-1. Two of these three initial units will be used for long-term creep tests; the third will be used for cyclic fatigue testing.

Note: All tooling, tool design, test equipment, and facilities used on this contract were supplied by the Aerojet-General Corporation, and are noted here for reference.

IV. CYLINDER FABRICATION AND TESTING

Cylinder fabrication and testing on this program started with 0.310-in.-thick by 6.0-in.-I.D. by 11.40-in.-long cylinders for establishing a test base. After determination that the fabrication methods and test methods were consistent, cylinders with increasing thickness were fabricated and tested. These thicker cylinders were constructed for use in determining any significant change in the physical or mechanical properties due to thickness. Cylinders with inside diameters of up to 18.0 in. were fabricated and tested to determine scale effect. Five 6.0-in.-ID by 11.4-in.-long cylinders with wall thickness from 0.500- to 0.720-in. were delivered to the David Taylor Model Basin.

A summary of all cylinders fabricated and tested is given in Table 1.

Significant details of construction and test results for all cylinders are as follows:

A. CYLINDER FABRICATION

1. TW-1

This cylinder was fabricated for verification of such details as parting agent, cure, mandrel removal and machining. Since this cylinder was fabricated before the reciept of HTS Roving, it was not tested.

(NOTE: Test results and significant data for cylinders No. TW-2 through TW-9 are given after TW-9, Item IV,A,10.)

2. TW-2

Specifications of this part are as follows: 0.314-in. thick 6.0-in.-I.D. by 11.400-in. long; 16 circumferential layers (32 plies); and 15 longitudinal layers (15 plies). The cylinder was fabricated using the DER 332/HHPA/BDMA Resin System, in-process impregnated HTS 20E Roving in the circumferential direction and laying the longitudinal layers in by hand utilizing Scotchply Minnesota Mining and Manufacturing 1009-26 preimpregnated tape. The circumferential filaments were wound with a tension pattern beginning with 12 pounds at the inner surface and gradually reducing in each successive layer to 8 pounds

IV Cylinder Fabrication and Testing, A (cont.)

at the outer surface. This tension pattern was based on the analysis presented in Appendix B. The part was wound on a thin-walled aluminum mandrel. This part had local delaminations on the inner surface which were believed to be caused by the high tension on the inner plies.

3. TW-3

Specifications for this part are identical to TW-2. The inner surface of this cylinder also showed local delaminations, again verifying, as with Cylinder TW-2, that tension on the inner plies was too high.

Photos of this cylinder before and after test are shown in Figure 8.

4. TW-4

Specifications for this cylinder were as follows: 0.312-in. thick; six circumferential layers (24 plies); five longitudinal layers (10 plies).

This was the first cylinder fabricated using E787 prepreg. A constant tension of 6-lb/20E roving was used for both the circumferential and longitudinal layers. Longitudinal plies were wound on end-over-end, parallel to the mandrel axis. A thin-walled aluminum mandrel was used. To avoid slippage of the longitudinal rovings, double back tape was wrapped around the mandrel circumference at each end, prior to winding each longitudinal layer. Fabrication of this cylinder indicated that winding the longitudinals was practical by the method noted. This method, however, was concluded to be not as good for the fabrication on the thicker, larger cylinders planned on this program. Winding the longitudinals on the thicker cylinders would have resulted in excessive buildup around the poles, wasted material, and as stated in the section on tensioning, would have resulted in detrimental residual stresses.

5. TW-5

Specifications for this cylinder were as follows: 0.357-in. thick: seven circumferential layers (28 plies), and six longitudinal layers (10 plies). A constant tension of 6-lb/20E roving was used for the circumferential layers. Longitudinal plies were laid in by hand, using unidirectional tape made from E787 prepreg (see Section III, E, 2, a). A thick-

IV Cylinder Fabrication and Testing, A (cont.)

walled aluminum mandrel was used. The ratio of filaments after machining was 2.8 circumferential layers to 1 longitudinal layer.

Visual inspection of the completed cylinder and 1/4-in. wide test rings cut from the cylinder, revealed the following conditions:

a.   Air entrapment and voids in the outer plies

b.   Small localized delaminations in the outer plies

c.   Some radial cracks or crazing of the inner plies.

6.   TW-6

Specifications for this cylinder were as follows: 0.380-in. thick, 7 cicumferential layers (28 plies), and 6 longitudinal layers (14 plies). The cylinder was wound on a thin-walled (7/8-in. thick) aluminum mandrel with a programed tension pattern of from 7 to 4-lb/20E Roving. No visible defects were observed in this cylinder.

7.   TW-7

Specifications for this cylinder were as follows: 0.359-in. thick, 7 circumferential layers (28 plies), and 6 longitudinal layers (14 plies). This cylinder was made on a 7/8-in.-thick aluminum mandrel with a programed tension pattern of 7 lb at the inner surface, decreasing to 4 lb at the outer surface.

Visual inspection of the cylinder after cure showed a small amount of telescoping of the outer circumferential plies. This telescoping of the outer plies resulted in a loss of tension, causing voids. A means of restraining the circumferential wraps from telescoping was accomplished on cylinders TW-8 and on.

The original wall thickness of this part was 0.458 in. The wall was machined to 0.359 in. to remove the local void areas which occurred at the outer layers.

IV Cylinder Fabrication and Testing, A (cont.)

8. TW-8

Specifications for this cylinder were as follows: 0.449-in. thick; 9 circumferential layers (36 plies); and 8 longitudinal layers (18 plies). The cylinder was wound with a programed tension identical to TW-7, with the following exceptions:

a. Longitudinal layers and circumferential windings were extended approximately 2 in. beyond the trim line of the part at each end of the mandrel to isolate any effects of telescoping from the finished part.

b. As a temporary expedient, shrink tape was wrapped around the cylinder circumference at the ends of the winding to provide some restraint against telescoping.

c. The cylinder was wound on a steel mandrel.

The TW-8 cylinder showed very little telescoping of the outer layers. No visible defects were notable in either the finished cylinder or test rings cut from it.

The following conclusions were drawn from cylinder TW-8: first, a positive means of eliminating telescoping of the circumferential plies is required to eliminate the voids due to the resulting loss of tension, and to maintain a programed tension pattern, and, second, winding on a steel mandrel apparently reduced crazing of the inner surface.

9. TW-9

Specifications for this cylinder were as follows: 0.350-in. thick; 7 circumferential layers (28 plies); and 6 longitudinal layers (14 plies). The cylinder was identical to TW-8, except that end plates (dams) were added to reduce telescoping and tension was programed from 8- to 4-lb/20E roving, from the inner to the outer layers.

Visual inspection of the machined specimen and the test rings indicated that there were no delaminations and that the inner surface was resin-starved.

IV Cylinder Fabrication and Testing, A (cont.)

Fabrication of cylinder TW-9 indicated that the use of end plates (dams) provided an adequate method of restraining the circumferential filaments from telescoping and causing voids and that the resin-starved condition on the inner surface was most likely caused by excessive tension on the inner plies, coupled with mandrel expansion during cure.

10. Test Results for Cylinders No. TW-2 through TW-9

Test cylinders TW-2 through TW-9 were mounted on end closure holding fixtures (Figure 3) which supported them in the pressure chamber (Figure 5). These cylinders were pressurized to failure using the following cycles:

a. Pressure was applied to 60% of predicted critical pressure at a rate of 500 psi per minute.

b. Above this pressure (60% of critical pressure) the loading rate progressed at 50 psi increments, the pressure being held for 2 min at each increment.

All cylinders showed the same type of longitudinal failure typical of a "buckling" or a "instability" analysis. Each increase in the thickness to diameter ratio was accompanied by a change in maximum circumferential stress levels attained as is shown in Figure 9. Data on tests TW-2 through TW-9 is presented in the following tabular display:

Cyl. No.	Thickness in.	ID in.	Overall Length in.	Density lb/in.^{3}	Weight Displacement	P_c psi	σ_{ϕ_i} psi Δ*	X_i psi
TW-2	0.314	5.997	11.400	0.0765	0.374	5,300	58,300	29,150
TW-3	0.310	5.997	11.401	0.076	0.374	5,350	59,000	29,500
TW-4	0.312	5.999	11.400	0.0757	0.369	5,050	55,550	27,775
TW-5	0.357	6.010	11.400	0.0753	0.409	6,000	59,687	29,843
TW-6	0.380	6.000	11.389	0.0756	0.435	7,650	72,037	36,019
TW-7	0.359	6.005	11.401	0.076	-	6,825	68,025	34,013
TW-9	0.350	5.999	11.407	0.0764	0.408	6,650	67,230	33,615

* See Section   for reference to formulas used.

IV Cylinder Fabrication and Testing, A (cont.)

11. TW-10

Specifications for this cylinder were 0.402-in. thick, 7 circumferential layers (28 plies), and 6 longitudinal layers (14 plies), giving a ratio of two circumferentials to one longitudinal. Two of the longitudinal plies were 3 plies thick, and four were 2 plies thick. Tension on the circumferentials was 5-lb/20E constant. This was the first test cylinder made on the 6.0-in.-dia. by 30.0-in. long steel mandrel with end dams.

The mandrel slid freely out of this cylinder, indicating that some mandrel expansion took place. This cylinder also showed crazing or resin cracking on the inner surface; this crazing is visible in Figure 10. It was concluded that crazing was caused by an insufficient or uneven resin cure. Thermocouples were placed close to the inner surface of succeeding cylinders to obtain more positive control of laminate temperature through the entire thickness.

This cylinder was machined into three shorter lengths and tested as follows: cylinders were mounted on end closure plates, and pressurized to 8000 psi at 500 psi/min. From 8000 psi to cylinder failure, loading was reduced to 50 psi increments held for two minutes.

Data on these three tests of the shorter lengths is tabulated below:

Cylinder Number	Thickness in.	ID in.	Overall Length in.	P_c psi	σ_{ϕ_i} psi	Density lb/in.^{3}	Weight/ Displacement
TW-10-1	0.402	6.000	11.4	8,700	78,087	0.076	0.454
TW-10-2	0.407	6.000	7.2	9,500	85,500	0.076	0.454
TW-10-3	0.402	6.000	4.13	9,800	88,200	0.076	0.454

This series of tests was run to determine for this thickness/diameter (t/d) relationship the effect test specimen length has on the attainment of maximum stress levels, and to investigate the possibility of using shorter cylinders during latter phases of the program. Results of the test indicated that shorter lengths would be advantageous for tests of later cylinders since progressively shorter cylinders achieved higher stress levels.

IV Cylinder Fabrication and Testing, A (cont.)

12.   TW-11

Specifications of this part were as follows: 0.750-in. thick; 15 circumferential layers (60 plies); and 14 longitudinal layers (30 plies). Winding tension was maintained at a constant 5.0 lb/20E roving on the circumferential layers. The standard cure was controlled by thermocouples wound into the part inner surface at cylinder mid-length. Figure 11 shows this part and mandrel.

Several significant areas of interest related to thick-walled cylinder fabrication became apparent during the fabrication of this part.

a.   Smoothness of circumferentials was hard to control because of twists, variations in the prepreg band width and thickness, and slight errors in the winding machine. The outer surface, therefore, became progressively more irregular with each ply. (A roller and use of heat to soften the resin was tried with considerable success on later cylinders to smooth the circumferential windings.)

b.   There was no craze-cracking on the inner surface indicating that the longer cure cycle, controlled by the deeply embedded thermocouples, was a decided improvement. Thermocouple wires are visible in Figure 11.

c.   Examination of the polished rings, shown in Figures 12 and 13, cut from sections of this cylinder showed some wrinkling of two plies near the outer surface. This wrinkling was probably due to lowered resin viscosity during cure which, with the filament tensioning, resulted in filament movement.

Cylinder No. TW-11 was machined into two cylinders, representative of the inner (TW 11-1) and outer (TW 11-2) surfaces, and rings for test as shown in Figure 14.

The hydrotest procedure for these two cylinders was as follows:

Cylinders were pressurized to 60% of their predicted failure pressures at 500 psi/min in 500 psi increments. Each increment was held for 1 minute. Strain readings were recorded at each increment.

IV Cylinder Fabrication and Testing, A (cont.)

From 6000 psi to test cylinder collapse, pressure was increased in 250 psi increments. Each increment was held 1 min.

Failure by instability is indicated by the strain-pressure curves shown in Figures 15 and 16. A summary of physical and mechanical values follows:

<u>Physical</u>

Cylinder No.	ID in.	Thickness in.	Overall Length in.	Weight lb	Density lb/in.	Weight/ Displacement
TW-11-1	6.000	0.444	11.405	7.692	0.075	0.489
TW-11-2	6.623	0.440	11.409	8.372	0.075	0.448

<u>Mechanical</u>

Cylinder No.	$E_{\phi i}$ X10^6 psi	E_{Xi} X10^6 psi	E_{eff} X10^6 psi	$P_c \triangle$ psi	P_c psi	$\sigma_{\phi i}$ psi	σ_{Xi} psi
TW-11-1	6.17	4.64	5.29	11,191	10,750	89,139	44,570
TW-11-2	5.79	4.41	5.00	9,079	8,500	76,908	38,454

A comparison of the test results of the two cylinders indicated that the inner surface cylinder (TW-11-1) exhibited higher mechanical values than the outer surface cylinder (TW-11-2). These lower results of the outer surface were probably caused by the wrinkling of the outer circumferential fibers as is shown in Figure 13. The test of these two cylinders also indicated that comparison of the inner and outer surfaces of cylinders would be simplified by a specimen geometry producing failures by yield.

13. <u>TW-12</u>

Specifications for this part were as follows: 0.380-in. thick by 6.0-in.-ID by 30.0-in. long, 8 circumferential layers (32 plies); and 7 longitudinal layers (16 plies).

This cylinder was wound utilizing a programed tension pattern designed so that thermal mandrel expansion would provide part of the final tension on the inner filaments. Five pounds tension 20E prepreg roving was selected

IV Cylinder Fabrication and Testing, A (cont.)

for the first layer. This tension had been used on previous cylinders with good results. Earlier attempts at incorporating a programed tension pattern into several cylinders used 12- or 8-lb tension on the inner plies, resulting in delaminations or resin-starved inner surfaces. The second circumferential layer was applied at 8.0-lb tension and each succeeding layer was decreased until 4.0-lb tension was attained at the outer surface.

During fabrication of this cylinder, a bump occurred due to a damaged cam on the winding machine which caused an instantaneous dwell at one point in the cylinder length. This cylinder was completed to allow a close evaluation of two cylinders, one containing an initial defect. Mandrel removal was somewhat more difficult than for the parts utilizing 5.0 lb constant tension, indicating, as predicted, that the higher tension restricted mandrel thermal expansion. The use of a low tension on the inner layer is a satisfactory method to obtain a programed tension pattern as no damage occurred on the inside surface.

This 30-in. long cylinder was machined into two 11.4-in. long cylinders and representative test rings. The cylinder containing the initial imperfection, caused by the nicked cam, was TW-12-2.

The hydrotest procedure for TW-12-1 was as follows:

The cylinder was pressurized to 6000 psig in 500 psi increments, for obtaining strain data. After venting to zero, the cylinder was again pressurized in 500 psi increments to 8000 psi, and strain readings were recorded at each increment. From 8000 psi to cylinder failure, increments were reduced to 200 psi. Duration at each increment was 1 min. Views of the cylinder after failure are presented in Figure 17.

Strain-pressure data presented in Figure 18 indicate that an "instability" failure occurred. Test results for these cylinders are given in the following tabulation:

IV Cylinder Fabrication and Testing, A (cont.)

Physical

Cylinder No.	ID in.	Thickness in.	Overall Length in.	Weight lb	Density $lb/in.^3$	Weight/ Displacement
TW-12-1	6.000	0.400	11.410	6.960	0.076	0.454
TW-12-2	6.000	0.400	11.402	6.985	0.076	0.454

Mechanical

Cylinder No.	$E_{\phi i}$ $X10^6$ psi	E_{Xi} $X10^6$ psi	E_{eff} $X10^6$ psi	P_c ⚠ psi	P_c psi	σ_{Oi} psi	σ_{Xi} psi
TW-12-1	6.30	4.93	5.53	9,064	9,225	83,320	41,600
TW-12-2	–*	–	–		7,950	71,804	35,902*

---

*No strain gages were installed on cylinder No. TW-12-2.

        TW-12-2 was tested, without strain gages, to determine any significant reduction in circumferential stress due to the wound-in initial defect.

        Examination of the test results for TW-12-1 shows an increase in modulus values when compared with several cylinders wound with constant tensions such as TW-11-1, TW-11-2, TW-15-1, and TW-15-2. A comparison of stress levels of TW-12-1 with TW-10-1 also shows higher values for TW-12-1. These test results indicate that programed tensioning should be an area for further analysis and model verification. The low results of cylinder No. TW-12-2 are conclusive evidence of the effect of initial imperfections.

     14.   TW-13

        Fabrication specifications for this part are the same as for TW-12. This 30-in. long cylinder was machined into shorter lengths which were subjected to various periods of exposure to 5000 psi pressure in simulated sea water. Results of these tests are given in the following tabulation:

IV Cylinder Fabrication and Testing, A (cont.)

Cylinder No.	ID in.	Thickness in.	Length in.	5,000 psi Exposure Period, hr	Weight Gain %	P_c psi	σ_{ϕ_i}
TW-13-1a	6.000	0.389	4.0	0	–	9,600	88,100
TW-13-1.	6.000	0.389	4.0	24	0	9,500	87,500
TW-13-1c	6.000	0.389	3.0	168	0	11,250	104,000
TW-13-2a	6.000	0.381	4.0	0	–	9,600	91,000
TW-13-2b	6.000	0.381	4.0	1 month	0	9,100	86,200
TW-13-2c	6.000	0.381	3.0	168	0	9,750	92,500

These tests demonstrated the following properties of filament-wound laminates due to exposure to 5000 psi up to one month.

a. Weight gain was so slight as to be immeasurable on a laboratory scale.

b. Reduction in collapse pressure between identical cylinders (e.g., between TW-13-2a and TW-13-2c, and TW-13-1a and TW-13-1b) shows a maximum 5% reduction in maximum circumferential stress levels at failure between the control cylinders and the cylinders exposed to 5000 psi sea water for time intervals of up to one month.

15. TW-14

Specifications for this part were as follows: 0.500-in. thick by 6.0-in. ID by 30-in. long; 10 circumferential layers (40 plies); and 9 longitudinal layers (20 plies). The circumferential plies were wound using 5.0-lb/20E roving constant tension.

This cylinder was machined into shorter cylinders for creep and fatigue testing as follows: Cylinder No TW-14-1a was instrumented with six circumferential and two longitudinal strain gages on the inner surface at cylinder mid-length. The cylinder was pressurized from 0 to 7160 psi in 500 psi increments. Strains were recorded at each increment. This 7160 psi pressure was sustained for 720 hours with no sign of failure.

TW-14-2a was subjected to cyclic loading of from 50 to 7160 psi at two cycles per minute. Failure occurred after 2571 cycles. Significant data

IV Cylinder Fabrication and Testing, A (cont.)

for these cylinders is given in the following tabulation.

Cylinder No.	Thickness in.	ID in.	Length in.	Test Type	P_c psi	$\sigma_{\phi i}$ psi
TW-14-1a	0.519	6.006	5.005	Creep	7,160	51,000
TW-14-2a	0.516	6.001	5.012	Fatigue	7,160*	51,000
TW-14-1b	0.528	6.002	5.015	Control	10 750	77,200

*Lower limit 50 psi.

16. TW-15

Specifications for this part were as follows: 1.250-in. thick; 25 circumferential layers (100 plies); and 24 longitudinal layers (50 plies). The circumferential plies were wound using 5.0-lb constant tension.

a. Winding

The cylinder was wound using a heat gun to continually heat the part surface in the area of the prepreg application. In addition, the roving was passed over a heated payoff roller to pre-soften and size the prepreg before it was wound onto the part surface. A Teflon-faced roller was used to smooth the circumferential plies before applying the longitudinals.

During the final stage of winding this part, local longitudinal wrinkles appeared in the circumferential plies. Apparently these wrinkles occurred between the hours of 12:00 PM and 8:00 AM while winding was not taking place, and may be attributed to shrinkage caused by both temperature and volumetric changes. A gradual redistribution of stresses may have been taking place in the part during this time. Upon warming the part, in preparation for the continuation of winding operations, the wrinkles disappeared. Winding was completed without further difficulty.

b. Machining

Observations during the machining of the OD and after parting of the test rings revealed the following conditions:

IV Cylinder Fabrication and Testing, A (cont.)

           (1)   The wall cross section was extremely dense and well-packed throughout. Polished rings out from the center and end sections show uniform and concentric layers without wrinkling. This uniform cross section, as shown in Figures 12 and 13 indicates that winding using a heat softened prepreg and applying heat and pressure roller to the part surface help to produce a densely packed cross section in which circumferential filament movement is minimized during cure.

           (2)   Some movement of the longitudinal plies was visible through the cured cylinder's outer surface.

           Cylinder No. TW-15 was machined into two cylinders, representative of the inner (TW-15-1) and outer (TW-15-2) surfaces, for testing.

        c.   Testing

           Both cylinders were hydrotested as follows:

           (1)   First Cycle: Cylinder was pressurized to 10,000 psi at 500 psi/min in 1000 psi increments. Strain gage data was recorded at each increment. Each increment was held 1 minute. Pressure was reduced to zero.

           (2)   Second Cycle: Cylinder was pressurized to failure as follows: Pressure was increased from 0 to 5000 psi at 500 psi per min from 5000 psi to 10,000 psi, in 1000 psi increments, and from 10,000 psi to cylinder failure in 200 psi increments. Strain data was recorded at each increment. Views of cylinder TW-15-2 before and after testing are shown in Figure 19.

           Significant test results for these cylinders are given in the following tabulation.

Physical

Cylinder No.	ID in.	Thickness in.	Length in.	Weight lb	Density lb/in.	Weight/ Displacement
TW-15-1	6.000	0.602	10.019	9.441	0.0757	0.625
TW-15-2	7.032	0.750	9.992	13.74	0.0750	0.650

IV Cylinder Fabrication and Testing, A (cont.)

Mechanical

Cylinder No.	$E_{\phi i}$ Δ $\times 10^6$ psi	E_{Xi} Δ $\times 10^6$ psi	E_{eff} Δ $\times 10^6$ psi	P_c psi	$\sigma_{\phi i}$ Δ psi	σ_{Xi} Δ psi
TW-15-1	5.95	4.50	5.13	14,000	91,476	45,738
TW-15-2	6.05	4.82	5.37	14,900	92,976	46,488

Both cylinders failed by material yield stress or by shear as shown by the strain pressures in curves in Figures 20 and 21. Other conclusions drawn from this cylinder indicated that: The application of heat during winding eliminated most of the fiber wrinkling experienced on TW-11. Winding the circumferentials in one direction only caused a visible angular displacement of the longitudinal elements during the cure cycle and resulted in an unbalanced stress pattern.

There was no decrease in the mechanical properties of these cylinders representative of the inner (TW-15-1) and outer (TW-15-2) surfaces of this 1.250-in.-thick cylinder.

This method of testing concentric cylinders representative of the inner and outer surfaces is a practical method of evaluation. This comparison would not be possible if full thickness cylinders were tested since the inner surface of thick cylinders is always more highly stressed than the outer surface during external pressurization.

17. TW-16

Specifications for this part were as follows: 0.750-in. thick by 6.0-in.-ID with 15 circumferential layers (60 plies) and 14 longitudinal layers (30 plies). This part was wound and cured in two steps. The first step involved applying 8 circumferential layers and 7 longitudinal layers; this was followed by curing, and the machining of the OD. The final stage was then wound onto this cylinder and a standard final cure was accomplished. This part has been machined into two 6.0-in.-ID by 11.4-in. long by 0.750-in. thick cylinders for test. Fabrication methods were the same as for TW-15. Creep tests are proceeding on this cylinder.

IV Cylinder Fabrication and Testing, A (cont.)

Longitudinal elements on this cylinder were also slightly displaced because of the unwinding action of the circumferential plies during cure. This "unwinding action" was concluded as being caused by winding the circumferentials in one direction only.

Cylinder TW-16-1 sustained pressures equivalent to compressive stress levels of 62,000 psi, and 71,000 psi for periods of 360 hours and 240 hours respectively. No significant creep rate was noted.

This cylinder is currently undergoing additional periods of pressurization on a company-funded program.

Cylinder No.	Thickness-in.	ID in.	Length in.	Test Pressure, psi	$\sigma \phi i$ psi	Duration Hours
TW-16-1	0.745	5.997	11.4	11,000	62,000	360
"	-	-	-	12,600	71,000	240
Test is continuing	-	-	-	-	-	-

18. TW-17

Specifications for this cylinder were as follows: 0.50-in. thick by 6.00-in.-ID, with 20 circumferential layers (40 plies), and 19 longitudinal layers (19 plies). Ratio of circumferentials to longitudinals was 2:1, fully dispersed. Each succeeding circumferential layer (2 plies) was reverse wound (helix was wound in the opposite direction) to attempt elimination of the displacement of longitudinal layers experienced on previous cylinders. Circumferentials were wound using 5.0-lb/20E prepreg constant tension. No indication of movement of the longitudinal plies was evident in the cured cylinder, indicating that reverse-wound cylinders have less movement during cure than cylinders wound by previous methods.

This cylinder was wound to determine the effect of ply dispersion on the properties of filament-wound reinforced plastic external pressure

IV Cylinder Fabrication and Testing, A (cont.)

vessels. A 5.0-in. length of this cylinder was hydrotested; and withstood 16,000 psi without failure. The test was suspended at this time because of a gage failure in the pressurization system. An 11.40-in. long cylinder (TW-17-1) was furnished to the David Taylor Model Basin for evaluation.

A summary of significant values relative to cylinder TW-17-2 follows:

ID in.	Thickness in.	Length in.	Density lb/in.^{3}	P_c* psi	$\sigma_{\phi i}$ psi	σ_{Xi} psi	Weight/ Displacement
6.001	0.526	5.00	0.076	16,000	115,725	57,865	0.567

19. TW-18

Specifications for this part were as follows: 1.250-in. thick by 6.0-in.-ID step-cured part. This cylinder was fabricated in two steps. The first step was 0.6-in. thick, and had 12 circumferential layers (48 plies), and 11 longitudinal layers (24 plies). The second step was 0.650-in. thick and had 13 circumferential layers (52 plies), and 12 longitudinal layers (26 plies). The standard cure was followed for each section except that the time at 325°F was reduced from 8 hours to 1 hour for the initial cure. Final cure was controlled by thermocouples wound into the first stage to guarantee an even cure. Each succeeding circumferential layer was reverse-wound. Five pounds constant tension was used throughout for the circumferential plies.

There was no movement of the longitudinal plies indicating that reverse winding to obtain a balanced winding is helpful. Figure 22 shows this cylinder before any machining. This cylinder was machined into thinner cylinders representative of the inner, outer, and step-cure line areas, as is shown in Figure 23.

---

*Test suspended before specimen failure because of broken gage.

IV Cylinder Fabrication and Testing, A (cont.)

The hydrotest procedure for Cylinder Nos. TW-18-1, TW-18-2, and TW-18-3 was as follows:

The cylinders were hydrotested in Aerojet's 30,000 psi test facility (utilizing 16-in. projectiles) shown in Figure No. 6. Cylinders were pressurized to failure as follows: from 0 to approx 60% of the predicted collapse pressure, the pressure was increased at 500 psi/min. From this pressure, the pressure was increased in 200 psi increments, and each increment held for two minutes until failure occurred.

An examination of TW-18-1 (inner surface cylinder) after test showed the same shear-type of failure at the ends as was shown for cylinder TW-19-1 in Figure 4.

Cylinder TW-18-2, the cylinder representing the outer surface of the original 1.25-in.-thick cylinder also showed the same type of failure as TW-18-1. TW-18-2 (outer surface) attained a higher stress level than did cylinder No. TW-18-1 (inner surface) indicating the attainment of a uniform construction and strength throughout the 1.25-in. thickness.

Cylinder No. TW-18-3, representative of the middle section of the original cylinder, and containing the step cure line, failed at a lower stress than TW-18-1 and TW-18-2. This cylinder also failed in shear indicating the effects of end conditions.

Significant data for these three cylinders is as follows:

Cylinder No.	ID in.	Thickness in.	Length in.	Density lb/in.^{3}	P_c psi	$\sigma_{\phi i}$ psi	σ_{Xi} psi	Weight/Displacement
TW-18-1	6.000	0.601	5.000	0.075	13,400	87,598	43,799	0.625
TW-18-2	7.223	0.700	4.988	0.065	13,750	92,173	46,086	0.628
TW-18-3	6.625	0.587	5.000	0.065	11,750	83,305	41,653	0.587

IV Cylinder Fabrication and Testing, A (cont.)

20. Cylinder TW-19

Specifications for this part were as follows: 15 circumferential layers (60 plies), and 14 longitudinal layers (28 plies) equivalent to the thickness of 30 circumferential plies.

This 0.75-in. thick cylinder was cut into four 5.0-inch lengths for creep, fatigue and standard hydrotests.

TW-19-1 cylinder was hydrotested in the projectile chamber and failed at 15,600 psi giving a maximum circumferential stress of 86,939 psi. This cylinder after hydrotest is shown in Figure 4, which clearly pictures the shear type of failure which has been experienced on several cylinders.

To determine if the rigid end plates instigated this failure, a duplicate cylinder, TW-19-4, was tested using 0.44-in.-wide by 0.44-in.-thick circumferential wound fiberglass rings at both ends, in place of the rigid end plates. This Cylinder, (TW-19-4) failed at 22,665 psi giving a maximum circumferential stress level of 126,076, an increase of 30% over the cylinder tested with rigid end plates. No sign of a shear type of failure was evident in this cylinder.

Significant test results of these two cylinders are as follows:

Cylinder No.	ID in.	Thickness in.	Length in.	Density lb/in.^{3}	P_c psi	$\sigma_{\phi i}$ psi	σ_{Xi} psi	Weight/Displacement
TW-19-1	6.006	0.747	4.988	0.076	15,600	86,939	43,469	0.74
TW-19-4	6.002	0.749	5.006	0.076	22,665	126,078	63,039	0.74

Cylinder TW-19-2 was instrumented with six circumferential and two longitudinal strain gages on the inner surface at cylinder mid-length. The cylinder was pressurized from 0 to 9250 psi, a compressive stress of 52,000 psi, in 500 psi increments. Strains were recorded at each increment. This compressive stress was sustained for 336 hours with no significant change in strain data. This creep test was maintained for 336 hours. Cylinder TW-19-3 was subjected to cyclic loading of from 50 psi to 9250 psi (a compressive stress of 52,000 psi) at a

IV Cylinder Fabrication and Testing, A (cont.)

rate of two cycles per minute. This cylinder was tested for 10,000 cycles' with no indication of failure.

Cylinder No.	Thickness, in.	ID in.	Length in.	Test Pressure, psi	$\sigma_{\phi i}$ psi	Test Type	Duration
TW-19-2	.748	6.005	4.996	9250	52,000	Creep	336 hours[*]
TW-19-3	.751	5.999	4.996	9250	52,000	Cyclic	10,000 cycles[**]

21. TW-20

Specifications for this cylinder were as follows:

4.00-in. thick by 12.0-in.-ID by 30.0-in. long. This cylinder was wound in four 1.0-in. thick steps, each step being cured and machined smooth and concentric to the axial centerline before the succeeding step was wound on. The first three steps were cured by the standard method specified in Section III,D,2,d except that time at $325°F$ was reduced from 8 hours to 4 hours for Step I, 3 hours for Step II, 2 hours for Step III and 8 hours for Step IV. Approximately 0.016-in. was removed during each machining operation. Each 1.0-in.-thick step consisted of 20 hoop layers (80 plies) and 19 longitudinal layers (slightly thicker and equivalent to 10 hoop layers). The ratio of circumferentials to longitudinals was 2:1. A tension of 4.0-lb/20E Prepreg was used on the circumferential windings to guarantee mandrel removal. A photo taken during winding of the circumferential layers is shown in Figure 2.

Fabrication of this 4.0-in. thick, 12.0-in.-ID cylinder was completed without any major problem. Normal difficulties expected during fabrication of any large, developmental part, included such problems as handling because of the combined weight of the part and mandrel of approximately 1000 lb, and scheduling for machining on a large lathe, as required by the four-step winding.

---

[*] Lower pressure limit = 50 psi.

[**] No sign of failure.

IV Cylinder Fabrication and Testing, A (cont.)

Selection of the four-step winding was based on the success of the two previous step-fabricated and cured parts; TW-16 (0.75-in. thick) and TW-18 (1.25-in. thick). Also, since this cylinder required approximately 500 lb of material and considerable fabrication time, a step-cure approach was determined to be the surest method of guaranteeing the successful fabrication of a high-quality cylinder. A closer control of in-process aging (time at room temperature) for the prepreg roving was also maintained by utilizing the step-cure method. Aging of resin and prepreg material is an important parameter of material strength being investigated on another program at Aerojet. Bulk-winding time might be sufficiently long to cause aging detrimental to adequate cure and subsequent loss of strength.

Mandrel removal was accomplished with little difficulty indicating that a tension of 4.0-lb/20E prepreg was a valid selection. The only thing that kept part removal from being a very simple operation was the non-availability of the press which was planned to be used and which had sufficient daylight and stroke to push the mandrel completely out of the part. Cylinder TW-20 after removal from the mandrel, is shown in Figure 24.

This cylinder was then machined into three concentric 10.0-in. long cylinders representative of the inner 0.700-in. thick section (TW-20-2), the middle 0.802-in. thick section (TW-20-3) and the outer 0.949-in. thick section (TW-20-4). This machining was accomplished by first using an air-motor driven end mill in the tool post of a lathe to machine into the cylinder approximately 3-in. from each end, by then drilling a series of holes through the remaining 4.0-in., and by next band-sawing the material remaining between the holes into separate cylinders. These three cylinders were then remachined on the inner and outer surfaces to obtain the required part dimensions. Thicknesses of these cylinders were based on the cylinder diameters and on the 11,000 psi capacity of the large test pressure vessel of the Southwest Research Institute: Southwest contracted to perform the hydrotesting of these parts. These three concentric cylinders are shown in Figure 1.

IV Cylinder Fabrication and Testing, A (cont.)

Several 4-in. thick rings, 3/8-in. wide were cut off of the remaining cylinder by using an air-motor driven 12-in.-dia diamond wheel mounted on a tool post with the cylinder mounted in a lathe. After cut-off, the rings were polished to permit close observation of layer straightness and thickness. One of the polished rings is shown in Figure 25. A ring section is shown in Figure 26. Visual examination verified the uniformity of construction throughout the entire 4.0-in. cross-section. All layers were free of wrinkles indicating that 4.0-lb/20E Roving tension is sufficient to produce straight filaments, where proper processing methods are used. No cure lines due to the step cure were discernible. Slightly thinner plies due to machining can be observed at each 1-in. step, as shown in Figure 26.

Testing of these cylinders was sub-contracted to Southwest Research Institute, San Antonio, Texas. The hydrotest end condition specified by Aerojet was a solid bulkhead inside the cylinder having the same cross-section used in tests of smaller cylinders. Southwest substituted end rings in place of the solid bulkheads in order to reduce the high bending stress adjacent to these areas. Although this was a valid approach, the judicial selection of ring material and sizes could have resulted in more significant test results.

Each of these three concentric cylinders (TW-20-2, -3 and -4) were instrumented with 6 hoop strain gages and two longitudinal strain gages at the centerline on both the inner and outer surfaces. The test procedure for each of the three cylinders was as follows:

Pressure was increased from 0 to 5000 psi in 500 psi increments. From 5000 psi to cylinder failure, pressure was increased in 50 psi increments, each increment was held for one minute.

A summary of the data follows:

IV Cylinder Fabrication and Testing, A (cont.)

PHYSICAL

Cylinder No.	Thickness No.	ID in.	Length in.	Weight lb	Density lb/in.^{3}	Weight Displacement
TW-20-2	0.700	11.994	9.984	21.118	0.078	0.445
TW-20-3	0.802	15.171	10.010	30.035	0.076	0.375
TW-20-4	0.949	18.411	9.984	43.420	0.075	0.362

MECHANICAL

Cylinder No.	$E_{\phi i}$ X10^6 psi	E_{xi} X10^6 psi	E_{eff} X10^6 psi	P_c psi	$\sigma_{\phi i}$ psi	σ_{xi} psi
TW-20-2	5.38	4.38	4.82	9500	95,900	47,950
TW-20-3	5.60	5.08	5.32	7600	83,470	41,735
TW-20-4	6.30	-*	-*	7200	80,740	40,370

*Erratic strain data.

Cylinder No. TW-20-2 failed at a pressure of 9500 psi with a maximum circumferential stress of 95,900 psi. This cylinder was tested using 0.75 in. wide by 0.75 in. thick mild steel end rings. Failure was probably due to buckling caused by the low yield strength (30,000 psi) of the steel end ring. Strain data obtained indicate a buckling (or three-lobe) collapse mode. A failure pressure associated with a bulkling mode was not attained however, because of instability of the end rings. Also, failure could have been caused by shear adjacent to the end rings.

Cylinder No. TW-20-3 failed at a pressure of 6200 psi with a maximum circumferential stress of 83,470 psi. This failure pressure was con- siderably lower than for TW-20-2 and was due to end support rings of insufficient strength. End rings of the same cross section as were used on TW-20-2 were utilized for TW-20-3. Since TW-20-3 was larger than cylinder TW-20-2, the end

IV Cylinder Fabrication and Testing, A (cont.)

rings were correspondingly weaker. With the proper end rings, it is believed that TW-20-3 would have sustained approximately the same circumferential stress as TW-20-2.

Based on the results of Cylinders No. TW-20-2 and TW-20-3, the end rings for Cylinder No. TW-20-4 were designed such that theoretically, the rings would not fail nor would the cylinder fail by inter bay buckling until the hoop stress reached a value of 100,000 psi. The external pressure corresponding to this hoop stress is 9000 psi. Additional strain gages were placed on the rings and on the shell close to the rings to monitor the longitudinal strains in these areas. During the initial pressurization of this model, the pressure could not be maintained above 3400 psi and the model was removed for inspection. The examination disclosed that the end closure plate at the top of the model had deformed. This deformation produced large longitudinal stresses at the top edges of the model causing a local failure of the material. The model was machined to remove the damaged material. This machining shortened the model length to 7.5 in.

During the second pressurization, the maximum stress in the shell occurred adjacent to the end stiffening ring. Its magnitude, at an external pressure of 7200 psi, was approximately 128,000 psi. The failure of this model was due to high longitudinal stress and shear stresses adjacent to the end ring before a mode of failure associated with 100,000 psi circumferential stress at mid bay could occur.

No positive correlation can be drawn from the test results of these three concentric cylinders (TW-20-2, TW-20-3 and TW-20-4) because of the different modes of failure (i.e., inter-bay buckling on TW-20-2, premature end ring failure of TW-20-3 and a shear type failure of TW-20-4.

Since a duplicate 4.0-in. thick by 12.0-in.-ID by 10.0-in. long cylinder was available from the same winding, it was decided to run another series of hydroburst tests.

IV Cylinder Fabrication and Testing, A (cont.)

The design of the models for the second test series was based on obtaining identical thickness-to-diameter and length-to-diameter relationships for both the cylinders and the end stiffening rings to obtain identical modes of failure. The model design was also based on obtaining a circumferential stress of 100,000 psi at mid-bay at a pressure of 9800 psi. The analysis used for design is given by a numerical example which applies also to selection of stiffening rings for the other models.

Previous results indicated that flat solid plates should not be used for tests of cylinders having geometries similar to those discussed here because of the high bending stresses which occur. Therefore, the end rings of the hydrotest closures were designed to minimize the bending stresses in the shell, adjacent to the rings. The design of end rings requires a cross section which will maintain circularity of the cylinder at the stiffening ring, and offer the minimum of restraint to radial motion of the cylinder. To permit a design in which minimum bending or shear occurs in the shell at the stiffening rings, the end rings should be made of the same material as the shell. However, time and funding did not permit the fabrication of rings of the required size of filament-wound fiber-glass construction. Aluminum (7079 T-6) was selected therefore, as the material of construction. The method of ring size selection follows:

(The numerical example uses the stiffening rings selected for Model TW-20-5.)

a. Step 1

A shell thickness of 0.65 which would produce a circumferential stress of 100,000 psi at a pressure of 9800 psi is chosen.

$$\sigma = \frac{Pr}{t}$$

$$P = \frac{100,000(0.65)}{6.65} = 9800 \text{ psi}$$

IV Cylinder Fabrication and Testing, A (cont.)

        b.   Step 2

The critical buckling pressure (Pcr/SH) of the shell was next determined to check that the shell will not buckle before a circumferential stress of 100,000 psi was obtained. The modulus of elasticity for this numerical example was assumed to be 4.2×10^6.

$$Pcr/SH = \frac{2.42\ E_{eff}}{(1-\mu^2)^{3/4}} \quad \frac{(t/D)^{5/2}}{L/D - 0.45(t/D)^{1/2}} = 15,000\ psi$$

$$Pcr/SH = 15,000\ psi > P$$

Subsequent calculations, therefore, were made for P = 9800 psi

        c.   Step 3

The assumed stiffener is:

        width (b) = 0.4-in.
        depth (d) = 1.2-in.
        $E_{st} = 10 \times 10^6$ psi (aluminum)

        d.   Step 4

The shear in the shell adjacent to the stiffeners was determined by the following formulas, from item No. 11 of the bibliography,

$$V = 0.66K\ P\sqrt{rh} \tag{1}$$

    V = Shear in the shell

where:

    P = Hydrostatic pressure

    r = Shell radius

    h = Shell thickness

    K = Relative stiffness factor

The derivation of K is given in item No. 11 of the bibliography.

IV Cylinder Fabrication and Testing, A (cont.)

Its value is

$$K = \frac{1}{1 + 1.555 \; \dfrac{r_{st}^2}{A_{st}} \sqrt{\left(\dfrac{h}{r}\right)^3}} \qquad (2)$$

where

$$A_{st} = 2 \; bd \; \frac{E_{st}}{E_{sh}}$$

where

-
b   = width of end stiffener

d   = depth of end stiffener

E_{st} = modulus of elasticity of the stiffener material

E_{sh} = modulus of elasticity of the shell material. (Assumed as 4.2×10^6 psi)

$$A_{st} = 2(0.4)(1.2) \; \frac{10 \times 10^6}{4.2 \times 10^6} = 2.85 \; \text{in.}^2$$

Using Equation (2)

$$K = \frac{1}{1 + 1.555 \; \sqrt{\left(\dfrac{0.65}{6.32}\right)^3} \cdot \dfrac{(5.4)^2}{2.285}} = .606$$

and, using Equation (1),

$$V = 0.66 \; (0.606) \; 9800 \; \sqrt{6.32(0.65)} = 8000 \; \text{pli}$$

IV Cylinder Fabrication and Testing, A (cont.)

       e.   Step 5

Knowing V, the stress in the stiffener was determined by

$$\sigma_{st} = \frac{Vri}{bd} = \frac{8000\ (6)}{(0.4)(1.2)} = 100,000\ psi$$

During testing of similar models, the strains recorded in the stiffener did not exceed 2/3 of the expected strains. The expected stress in the stiffener, at an external pressure of 9800 psi, was about 65,000 psi, which is close to the proportional limit of the aluminum selected for the stiffener.

       f.   Step 6

The critical buckling pressure of the stiffener is now calculated and checked to determine that $P_{cr/st} > V$

The critical buckling pressure of the stiffener is given by Reference 12 of the bibliography as:

$$P_{cr/st} = \frac{3\ E_{st}\ I_{st}}{r_{st}^{3}}$$

where

I_{st} = Moment of inertia of stiffening ring

r_{st} = Radius of stiffener

$$P_{cr/st} = \frac{3 \times 10 \times 10^{6}\ (0.4)(1.2)^{3}}{12(5.4)^{3}}$$

       g.   Step 7

Next the shear stresses and bending stresses in the shell at the stiffeners are determined. The shear stress is:

$$\sigma_{sh} = 1.5\ \frac{V}{h} = 1.5\ \frac{(8000)}{0.65} = 18,500\ psi$$

IV Cylinder Fabrication and Testing, A (cont.)

$$\sigma_{sh} = 18,500 \text{ psi}$$

The bending moment in the shell at the stiffener is given in item No. 11 of the bibliography as

$$M = 0.257 \text{ KPrh}$$

$$M = 0.257 \ (0.606)(9800)(6.32)(0.65) = 6270 \text{ lb-in.}$$

The bending stress in the shell at the stiffener is given by bibliography item No. 12 and is determined by

$$\sigma_b = \frac{6m}{h^2} = \frac{6(6270)}{(0.65)^2} = 89,600$$

The total longitudinal stress therefore is

$$89,600 + 50,000 = 139,600 \text{ psi}$$

Since allowable shear stresses and longitudinal stresses are not presently well defined, Step 7 cannot be carried out.

These cylinders (TW-20-5, TW-20-6, and TW-20-7) were tested by the same procedures used for Cylinders No. TW-20-2, TW-20-3 and TW-20-4. Additional strain gages were placed on the end stiffening rings in order to record that failure of the rings did not occur before mid-bay dircumferential compressive failure occurred. Longitudinal strain gages were placed on the shell adjacent to the stiffening rings to record longitudinal strain. In this manner, the tests could be stopped, and the end rings modified, if the longitudinal strains became too large. Six hoop strain gages and two longitudinal strain gages were installed at the center of the cylinders on both the inner and outer surfaces.

All cylinders were pressurized from 0 to 5000 psi, in 500 psi increments. From 5000 psi to cylinder failure, the pressure was increased in 50 psi increments, and each increment held for one minute.

Test results and significant data are as follows:

IV Cylinder Fabrication and Testing, A (cont.)

	Cylinder				Stiffening Ring*	
Model No.	Thickness in.	ID in.	Length in.	Width in.	Thick in.	Material
TW-20-5	0.650	12.000	6.65	0.40	1.20	Al 7079 T-6
TW-20-6	0.790	14.800	8.20	0.495	1.48	"
TW-20-7	0.980	18.181	10.00	0.60	1.80	"

*All stiffening rings had a 5° taper for one-half the width of the ring

Cylinder No.	$E_{\phi i}$ X10^6 psi	E_{xi} X10^6 psi	E_{eff} X10^6 psi	P_c psi	$\sigma_{\phi i}$ psi	σ_{xi} psi
TW-20-5	4.90	4.94	4.92	8200	88,200	44,100
TW-20-6	4.76	5.56	5.13	6500	54,462	27,231
TW-20-7	4.83	5.56	5.16	6400	69,126	34,563

Cylinders No. TW-20-6 and TW-20-7 failed by shear at the end rings as indicated by the appearance of clean 45° failure planes. Cylinder TW-20-5 probably failed by shear; as there was no indication of a buckling mode evident in the strain data, and since the circumferential stress at failure for TW-20-5 was lower than obtained from Cylinder No. TW-20-2.

These shear failures indicate that: the end rings were sufficiently strong to resist buckling or yield up to the failure pressure; and that the rings were too rigid to allow adequate radial shell displacement. The use of aluminum, (modulus of 10×10^6 psi) for the end rings is believed to be the principal cause of the shear failures. A contributing cause may have been the small bearing area left on the rings after the 5° relief was added.

It is believed that shear failures can be eliminated by the following: by a judicial selection of model geometry; by the use of a ring material which is the same as the shell; and by increasing the strength of the shell at the end ring areas. Selection of an optimum model length would

IV Cylinder Fabrication and Testing, A (cont.)

minimize bending and shear forces at the rings. The use of a material for the
rings which is similar to the shell material is recommended as a means of
approaching an optimum condition. The use of a similar material would allow the
selection of a ring cross-section which will offer the minimum of restraint
to radial motion of the shell. It is also recommended that the strength of the
shell material should be increased at the points of high stress near the end
stiffening rings.

Calculation of moduli from the strain data show a close
correlation to the smaller 6-in.-dia cylinders.

Scale effect, on a gross basis, is probably not a major
parameter. Firm proof requires additional improvements in test methods and
end support conditions and in the design, fabrication and testing of additional
cylinders.

22. TW-21

Specifications for this part were as follows: 0.50-in. thick
by 6.0-in.-ID by 30-in. long; 10 circumferential layers (40 plies); and
9 longitudinal layers (equivalent to 20 plies). This cylinder was machined into
two 11.40-in. long cylinders (TW-21-1 and TW-21-2) which were shipped to the
David Taylor Model Basin.

23. TW-22

Specifications for this part were as follows: 0.74-in. thick
by 6.0-in.-ID by 30.0-in. long; 14 circumferential layers (28 plies); and
13 longitudinal layers (equivalent to 14 plies). This cylinder was machined into
two 11.4-in. long cylinders (TW-22-1 and TW-22-2) which were shipped to the
David Taylor Model Basin.

24. Conclusions

a. Thicknesses greater than the presently wound 1-1/4-in.
one-step winding appear feasible if precise control is maintained of filament
placement.

IV cylinder Fabrication and Testing, A (cont.)

b. Test results indicate that the mechanical properties of cylinders with wall thicknesses up to 4.0-in. thick remains constant throughout the entire thickness. This conclusion is based on the test results of representative thinner cylinders machined from the thicker cylinders.

c. Programed tensioning of the circumferential windings has resulted in higher mechanical values, but, because of the insufficient number of tests conducted to date, no positive conclusion can be stated.

d. Maximum dispersion of all longitudinal and circumferential plies resulted in cylinders having a significant increase in stress levels. Fabrication cost of maximum dispersion cylinders is much greater than for the standard 4:2 dispersion cylinders, however, because handling of thinner layers is more difficult and the number of layers is doubled. A feasible solution would be the use of a maximum dispersion on the inner surface (the area of highest stress) and the use of thicker layers toward the outer surface or by modifying the winding equipment to economically wind a maximum dispersion pattern.

e. Test cylinder L/D (length/diameter) ratio was reduced from the standard 11.4-in. length for 6.0-ID cylinders to an L/D of less than 1.0 to simplify the evaluation of the laminate by obtaining a yield failure, and to maintain the costs of the thicker and larger diameter cylinders within the working budget.

f. The testing of concentric cylinders that have been machined from representative sections of thicker cylinders has proved to be a practical method of evaluation. The comparison of mechanical values representative of the inner and outer sections would not be possible if full thickness cylinders were tested, since the inner surface of thick cylinders is always more highly stressed than the outer surface during external pressurization. The testing of thinner representative cylinders also allows testing to be performed at a lower pressure and under conditions more representative of actual design concepts.

IV Cylinder Fabrication and Testing, A (cont.)

g.   Step cures are extremely interesting from both a quality-control and a fabrication standpoint. By this method, one step can be wound, inspected and reworked if necessary by machining, before winding the next step. This method should also allow the use of thinner mandrels as the cured first stage becomes a mandrel for the second stage. When prepreg is used, step curing is also advantageous in order to cure the part within the tolerance of resin advancement (time of prepreg at room temperature).

h.   Radial craze-cracking appeared on the inside diameter of several early cylinders. It is probable that an uneven cure due to a variation in temperature gradient throughout the composite cross-section were the contributing factors. Thermocouples were placed close to the inner surface on later cylinders to obtain an even cure resulting in cylinders having no craze-cracking on the inner surface.

i.   A means of positively sizing the prepreg before application to the cylinder is required to maintain consistently smooth windings without gaps or build-ups which in turn contribute to straightness of longitudinal plies.

j.   "Telescoping" of the outer layers results in loss of tension, and subsequent voids. The addition of dams virtually eliminated the telescoping.

k.   Reverse winding each successive circumferential layer results in a balanced winding pattern with no filament cross overs as the longitudinal layer forms a separating element. Reverse winding results in considerably less movement of the longitudinal plies because of lowered resin viscosity during cure.

l.   Cylinders fabricated using unidirectional tape for the longitudinal layers are more consistent, have fewer gaps, and are easier to fabricate than those having wound-on longitudinal layers. Tape has the added advantage of being an easier means of varying the dispersion of plies than are wound-on lungitudinals, which can substantially increase composite stress levels.

IV Cylinder Fabrication and Testing (cont.)

B.   MECHANICAL TESTING OF RINGS AND RING SEGMENTS

Rings or ring segments from all test cylinders fabricated during
this program were mechanically tested for axial shear as shown in Figure 27;
horizontal shear, as shown in Figure 28; and for compressive modulus. These tests
were conducted to verify the fabrication processes and to determine any possible
correlation between specific mechanical (uniaxial) test results and biaxial
cylinder hydrotest results. The ring bending test was used to determine the
unidirectional compressive modulus.

It was planned that values for the unidirectional compressive
yield stress would be obtained on the Aerojet ring compression fixture. This
fixture was "proofed" on several rings and worked satisfactorily. A leak
developed in the hydraulic bag during calibration, however, necessitating
fabrication of a new bag which could not be delivered prior to the completion of
the program.

Mechanical and gravimetric test results for rings and segments
tested on this program are summarized in the following tabulation:

IV Cylinder Fabrication and Testing, B (cont.)

Cylinder No.	t Thickness in.	b Width in.	Horizontal Shear σ psi[*]	Axial Shear Stress σ psi[**]	Compressive Modulus X10^6 psi[***]	Resin %
TW-2	0.314	0.500	6,320	5,035	-	17.55
TW-3	0.310	0.500	6,330	5,333	-	17.93
TW-4	0.312	0.250	7,950	6,237	-	20.97
TW-5	0.357	0.250	9,352	7,115	-	21.47
TW-6	0.380	0.250	8,819	7,194	-	20.31
TW-7	0.359	0.250	7,746	7,072	-	21.23
TW-8	0.447	0.250	8,382	7,099	-	20.10
TW-9	0.350	0.250	10,304	7,757	-	19.45
TW-10	0.402	0.251	9,770	7,356	2.9	19.78
TW-11-1	0.443	0.253	10,412	7,206	2.8	21.04
TW-11-2	0.437	0.255	-	-	2.7	21.04
TW-12	0.404	0.248	9,458	7,038	2.9	19.16
TW-13	0.381	0.253	10,103	8,904	3.3	19.6
TW-14	0.496	0.249	11,458	7,654	3.1	20.5
TW-15-1	0.601	0.252	10,793	7,869	3.1	20.7
TW-15-2	0.750	0.252	-	-	3.1	20.7
TW-16-1	0.497	0.252	-	6,135	3.4	21.0
TW-16-2	0.501	0.251	-	-	4.2	21.05

[*]Horizontal interlaminar shear stress $= \frac{3}{4} \frac{PU}{bt}$

[**]Axial interlaminar shear stress $= Pu/D_s b$

[***]Compressive modulus $= Ec = \frac{1.786 \ r^3 \ avg}{bt^3} \cdot \frac{P}{\Delta}$

where

Pu = ultimate pressure at failure, lb

P = pressure, lb

b = width, in., t = thickness, in.

D_s = diameter of sheared off ring, in.

r avg = average of inner and outer radius, in.

Δ = ring deflection at a specific pressure, in.

IV Cylinder Fabrication and Testing, B (cont.)

Cylinder No.	t Thickness in.	b Width in.	Horizontal Shear o psi*	Axial Shear Stress o psi**	Compressive Modulus X10⁶ psi***	Resin %
TW-17	0.526	0.249	7,543	6,744	3.2	20.77
TW-18-1	0.603	0.251	9,605	7,401	3.1	21.10
TW-18-2	0.601	0.243	9,878	-	3.25	21.10
TW-19	0.748	0.252	11,333	6,987	3.15	20.2
TW-21	0.515	0.252	10,779	5,558	3.2	20.9
TW-22	0.719	0.239	11,386	6,327	3.2	20.5

Following are conclusions concerning mechanical tests on rings and specimens.

1. Values from mechanical tests show consistent results for horizontal shear, axial shear, and compressive modulus. The test values indicate improvements instigated in test cylinder fabrication during the program.

2. Resin percentage was held extremely constant, furnishing an excellent base for comparison for future cylinders with other resin percentages.

3. Since the axial interlaminar shear test is conducted on a full ring (instead of on a ring segment as is the horizontal shear test), it may be a more accurate indication of resin shear strength.

4. All test results substantiate the selection of U. S. Polymeric E787 prepreg as an adequate material of construction for the initial phases of study.

5. No correlation of data can be made between the mechanical tests and the hydrostatic-biaxial tests due to the changes in test cylinder thickness throughout the program.

V.   PHOTOMICROGRAPHIC ANALYSIS

Photomicrographic analysis was utilized to investigate the composite micro-scopic structure. This method of analysis has been used to take a close look at some of the more obvious construction deviations. Photomicrographs included in this report, therefore, cannot be construed as typical of the entire cylinder but rather as localized conditions which may indicate trends for improvement areas.

Photomicrographs were taken of the inner and outer layers of rings from test cylinders to determine any physical change. A well-fabricated cylinder will have straight uniform layers, even resin dispersion, very few voids in any area, and an overall uniform appearance.

Figures 29 through 36 show some good examples of the type of minor deviations which have appeared in the cylinders fabricated during this program. A bried description is included with each figure.

The following conclusions based on an analysis of these photomicrographs show that:

A.   Delaminations of the inner circumferential plies are most likely due to inadequate resin strength. The strain in the inner circumferential layer due to pretensioning, mandrel expansion, and resin shrinkage, may produce loads against the unstrained longitudinal elements, which are beyond the capability of the matrix.

B.   Outer plies show more voids and resin pockets than do inner plies, This is evidence that tension in the outer plies or overwrap pressure was not maintained during cure. Methods of maintaining pressure such as dams and shrink tape were incorporated during the program.

C.   Prepreg roving shows "layering" not seen in in-process impregnated wound cylinders. Preheating the prepreg material to precisely control resin flow at the time of winding has resulted in less "layering."

V Photomicrographic Analysis (cont.)

D.   Ability of the winding machine to accurately place the roving band is necessary to avoid resin pockets and the resulting stress risers which contribute to structural failure.

E.   Density of the composites has improved since dams were added to mandrels to eliminate movement of circumferential filaments. This is apparent by examination of Figure 32 (showing a microscopic section of TW-8, which was built without dams) and of Figures 33, 34, 35, and 36 (microscopic sections of cylinders that had dams).

F.   A definite resin layer appears adjacent to the inner surface of the longitudinal layer. This has been concluded as being due to the method of fabricating the tape.

G.   Photomicrographic analysis is a definite asset in recording and improving significant fabrication details.

VI.   RECOMMENDATIONS FOR FUTURE WORK

A.   The present program should be extended to allow the attainment of the higher material ultimate compressive yield strength properties which this program has indicated are possible. Specifically, test methods and model designs (including the selection of optimum stiffener material and sizes) should be improved so that true compressive failures (not shear-failures) may be obtained. The basis for an analytical investigation of the determination of optimized test model conditions (including end stiffening rings) has been established by the present program. This theoretical analysis should in turn, be verified by model fabrication and test.

B.   Programed tension patterns to achieve a uniform stress distribution across the cross-section of externally pressurized filament-wound cylinders should be more closely evaluated.

A limited number of tests on the present program showed that it is difficult but desirable to incorporate a programed tension pattern into a wound composite structure in order to increase mechanical values.

C.   The effects of resin content, ply dispersion and dispersion patterns should be investigated further.

These parameters should be fully evaluated by the design, fabrication and testing of models representative of actual operating conditions. Short-term and long-term hydrotests and cyclic loading tests at stress levels of, say, 50, 65 and 80% should be conducted.

D.   The effects of scale should be further confirmed by the design, fabrication, and testing of representative cylinders; specifically recommended are cylinders 12.0-. 24.0-, and 48.0-in. dia.

E.   The present contract for the study of thick-walled vessels should be extended so that design analyses to optimize various promising methods of construction applicable to thick-wall hull structures can be conducted. These analyses should include modular or building block approaches, combinations of materials employing the advantages of filament-wound plastics and high strength metals, and structures which would utilize recommendations and advancements from deep submergence programs and material sources.

BIBLIOGRAPHY

1.   Fried, N., Survey of Methods of Test for Parallel Filament Reinforced Plastics, Tech. Project 6189, Naval Material Laboratory, Brooklyn 1, New York.

2.   Fried, N., and Winans, R. R., The Compressive Strength of Parallel Filament Reinforced Plastics, Naval Material Laboratory, Brooklyn 1, New York.

3.   Elkin, R. A., Compressive Testing of NOL Rings, Narmco Research and Development, A Division of Telecomputing.

4.   Roark, Formulas for Stress and Strain, McGraw-Hill, New York, 1954.

5.   Pulos, J., Reinforced Plastics for Hydrospace Use, Report No. 1504, David Taylor Model Basin.

6.   Zak, Dr. A. R., Scale Effect - Thick Cylindrical Laminates, Technical Memorandum No. 322-61-6, Structural Materials Division, Aerojet-General Corporation.

7.   Trilling, C., The Influence of Stiffening Rings on the Strength of Thin Cylindrical Shells Under External Pressure, U.S. Experimental Model Basin, Report No. 396, 1935.

8.   Ballow, Lt. L. D., USN, Thesis Elastic Instability of Relatively Thick Circular Cylindrical Shells Subjected to Hydrostatic Pressure, The Luckenbach Graduate School Webb Institute of Naval Architecture.

9.   Windenburg, D. F. and Trilling, C., Collapse by Instability of Thin Cylindrical Shells Under External Pressure, U. S. Experimental Model Basin, Report No. 385, 1934.

10.   Timoshenko, S., Theory of Plates and Shells, McGraw-Hill, New York and London, 1940.

11.   De Hart, R. C. and Basdikas, N. L., Yield Collapse of Stiffened Circular Cylindrical Shells, Southwest Research Institute, Nonr Contract No. 2650, Project NR 064-435.

12.   Timoshenko, S., Theory of Elastic Stability, New York and London, Mc Graw-Hill, 1936.

TABLE 1

SUMMARY OF CYLINDER FABRICATION AND TESTING

| Cylinder No.*	Thickness in.	ID in.	Length in.	P_c psi	$\sigma_{\phi i}$ [1] psi	E_{eff} [6] X10^6 psi	Weight/Displacement	Remarks
1	0.310	6.000	11.400	-	-	-	-	To establish fabrication processes.
2	0.314	5.997	11.400	5,300	58,300	-	0.373	12 to 8-lb tens. Local ID delams.
3	0.310	6.000	11.400	5,350	59,000	-	0.370	12 to 8-lb tens. Local ID delams.
4	0.312	5.999	11.400	5,050	55,550	-	0.368	6-lb tens. Wound longitudinals. No defects.
5	0.357	6.010	11.400	6,000	59,687	-	0.409	6-lb tens.-ID crazing.
6	0.380	5.999	11.389	7,650	72,037	-	0.435	8 to 4-lb tens., No visible defects.
7	0.359	6.005	11.401	6,825	68,025	-	0.409	7 to 5-lb tens.-ID crazing, circ. telesc.
8	0.447	5.998	11.405	Not Tested			-	7 to 5-lb tens. - Shrink Tape - telescoping
9	0.350	5.999	11.407	6,650	67,230	-	0.408	8 to 4-lb tens. Dams added to mandrel. Dry ID.
10-1	0.402	6.000	11.407	8,700	78,087	-	0.454	5-lb const. tension.
10-2	0.402	6.000	7.00	9,500	85,500	-	0.454	Slight ID crazing (1st Shear).
10-3	0.402	6.000	4.00	9,800	88,200	-	0.454	Slight ID crazing.
11-1	0.444	6.000	11.405	10,750	89,139	5.29	0.489	5-lb const. tension.
11-2	0.440	6.623	11.409	8,500	76,908	5.00	0.448	Thermocouples close to ID. No visible defects.
12-1	0.400	6.000	11.410	9,225	83,320	5.53	0.454	Programed tension (5 lb/8 lb to 5 lb) No defects.
12-2	0.400	6.000	11.402	7,950	71,804	-	0.456	
13-1A	0.389	6.000	4.000	9,600	88,100	-	0.442	Control hydrotest (same as 12).

* Dow DER 332 HHPA/BDMA - Scotchply 1009 26% resin used for Cylinders 1, 2, and 3.
U.S. Polymeric E787/HTS 20-E prepreg 20% resin used for Cylinders 4 through 22.

Table 1
Sheet 1 of 4

TABLE 1 (cont.)

Cylinder No.*	Thickness in.	ID in.	Length in.	P_c psi	$\sigma_{\phi i}$ [1] psi	E_{eff} [6] X10^6 psi	Weight/Displacement	Remarks
13-1B	0.389	6.000	4.000	9,500	87,500	-	0.442	24-Hour exposure to 5000 psi sea water, no weight gain.
13-1C	0.389	6.000	3.000	11,250	104,000	-	0.442	168-Hour exposure to 5000 psi sea water, no weight gain.
13-2A	0.381	6.000	4.00	9,600	91,000	-	0.442	Control hydrotest.
13-2B	0.381	6.000	4.00	9,100	86,300	-	0.442	One-month exposure to 5000-psi sea water, no weight gain.
13-2C	0.381	6.000	3.00	9,750	92,500	-	0.442	168-Hour exposure to 5000-psi sea water, no weight gain.
14-1A	0.519	6.005	5.005	7,160	52,450			(Creep test suspended after 720 hr with no sign of failure.) (5-lb const.)
14-2A	0.516	6.001	5.012	7,160	52,450			Cyclic fatigue test - failure after 2571 cycles.
14-1B	0.528	6.002	5.015	10,750	77,655	-	0.568	Control hydrotest
15-1	0.602	6.000	10.019	14,000	91,476	5.13	0.625	1.25-in.-thick bulk cured cyl; 5-lb const. tension, 15-1 and 15-2.
15-2	0.750	7.032	9.992	14,900	92,976	5.37	0.650	
16-1	0.745	5.997	11.4	12,600	71,000			(Creep test - 720 hr with no sign of failure) Step-cured cyl., 5-lb const. tension.
17-1	0.526	6.000	11.40	14,200	102,600	4.98	0.567	2 to 1 ply dispersion, 5-lb const. tension, reverse wound circs. DTMB Delivery No. 1
17-2	0.526	6.001	5.000	16,000	115,725	-	0.567	2 to 1 dispersion, 5-lb tension
18-1	0.601	6.000	5.000	13,400	87,598	-	0.625	1.25-in.-thick step cylinder; inner surface.

*Dow DER 332 HHPA/BDMA - Scotchply 1009 26% resin used for Cylinders 1, 2, and 3.
U.S. Polymeric E787/HTS 20-E prepreg 20% resin used for Cylinders 4 through 22.

Table 1
Sheet 2 of 4

TABLE 1 (cont.)

Cylinder No.*	Thickness in.	ID in.	Length in.	P_c psi	$\sigma_{\phi i}$ △1 psi	E_{eff} △6 X10⁶ psi	Weight/ Displacement	Remarks
18-2	0.700	7.223	4.988	13,750	92,173	-	0.74	Outer surface.
18-3	0.597	6.605	5.000	11,750	83,200	-	0.587	Middle surface with cure line.
19-1	0.747	6.006	4.988	15,600	86,939	-	0.738	45° failure at ends.
19-2	0.748	6.005	4.996	9,250	52,000			Creep test - suspended after 336 hr.
19-3	0.751	5.999	4.996	9,250	52,000			Failure test - suspended after 10,000 cycles.
19-4	0.749	6.002	5.002	22,665	126,000	-	0.739	Ends stiffened with filament wound rings.
20-1	4.000	11.995	-	-	-	-	-	Machined into TW-20-2, -3, -4, -5, -6, -7 - four-step winding and cure. 4-lb tension.
20-2	0.700	11.995	9.984	9,500	95,900	4.82	0.405	Inner surface - buckling due to end rings.
20-3	0.802	15.171	10.010	7,600	83,470	5.32	0.373	Middle surface with cure line buckling due to end rings.
20-4	0.949	18.410	9.993	7,200	80,740	-	0.362	Outer surface - shear failure.
20-5	0.650	12.000	6.650	8,200	88,201	4.92	-	Inner surface - shear failure.
20-6	0.790	14.800	8.200	6,500	70,801	5.13	-	Middle surface with cure line - shear failure
20-7	0.980	18.181	10.000	6,400	69,126	5.16	-	Outer surface - shear failure.
21-1	0.521	6.002	11.383	13,700	100,200	4.86	0.560	DTMB Delivery No. 2, 4:2 dispersion, 5-lb tension.
21-2	0.518	6.006	11.400	13,600	99,800	4.92	0.550	DTMB Delivery No. 3, 4:2 dispersion, 5-lb tension.

* Dow DER 332 HHPA/BIMA - Scotchply 1009 26% resin used for Cylinders 1, 2, and 3.
U.S. Polymeric E787/HTS 20-E prepreg 20% resin used for Cylinders 4 through 22.

Table 1
Sheet 3 of 4

TABLE 1 (cont.)

Cylinder No.*	Thickness in.	ID in.	Length in.	P_c psi	$\%\phi_i$ △1 psi	E_{eff} △6 X10⁶ psi	Weight/ Displacement	Results
22-1	0.716	5.999	11.395	20,700	118,700	4.83	0.710	DTMB Delivery No. 4, 4:2 dispersion, 5-lb tension.
22-2	0.712	6.002	10.408	19,700	114,000	4.77	0.710	DTMB Delivery No. 5, 4:2 dispersion, 5-lb tension.

*Dow DER 332 HHPA/BDMA - Scotchply 1009 26% resin used for Cylinders 1, 2, and 3.
U.S. Polymeric E787/HTS 20-E prepreg 20% resin used for Cylinders 4 through 22.

Table 1
Sheet 4 of 4

Concentric Cylinders Machined from 4.0-in. Thick x 12.0 I.D. Cylinder

Figure 1
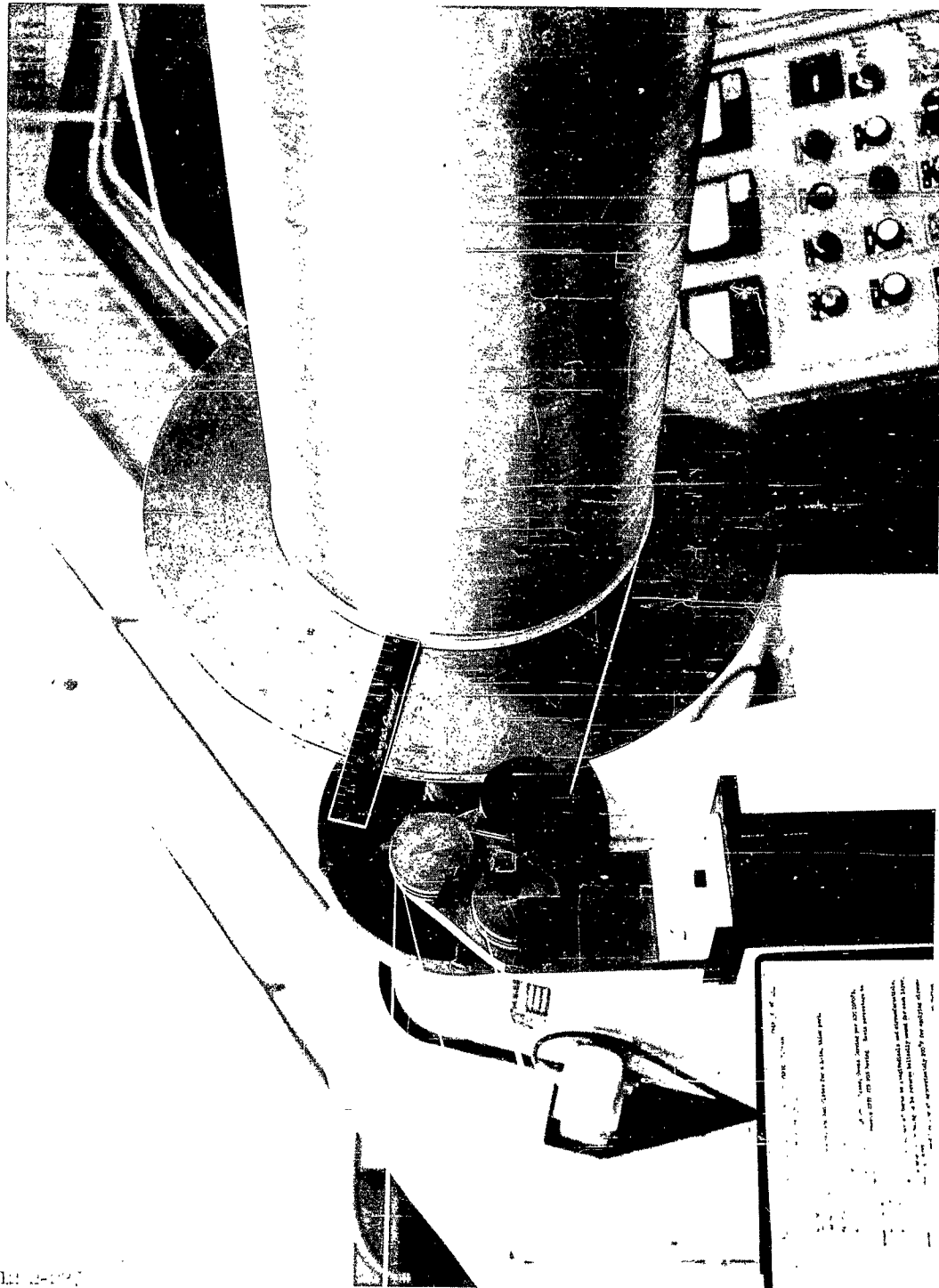
Winding of Circumferentials on 12.0-in. Dia. Mandrel

Figure 2
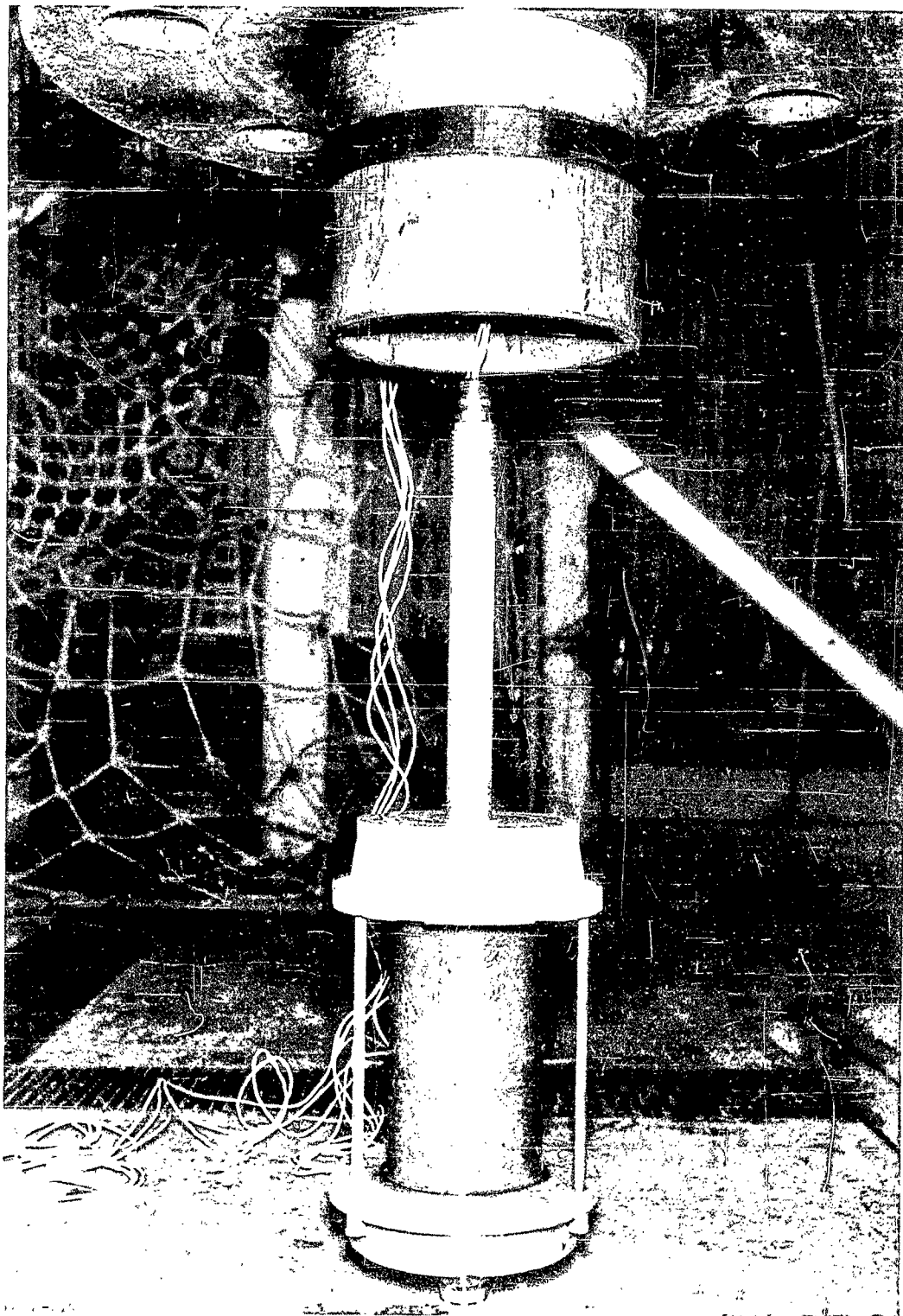
6.0-in. ID Cylinder Mounted on Test Fixture

Figure 3

263-984

TW 19-1 Showing the Type of Failute Which has Occured at
the ends of Several Cylinders. The Ring has been
Turned over to Provide a Better View of the
Failure Angle, Indicating a Shear Failure.

Shear Failure of TW 19-1 Test Cylinder
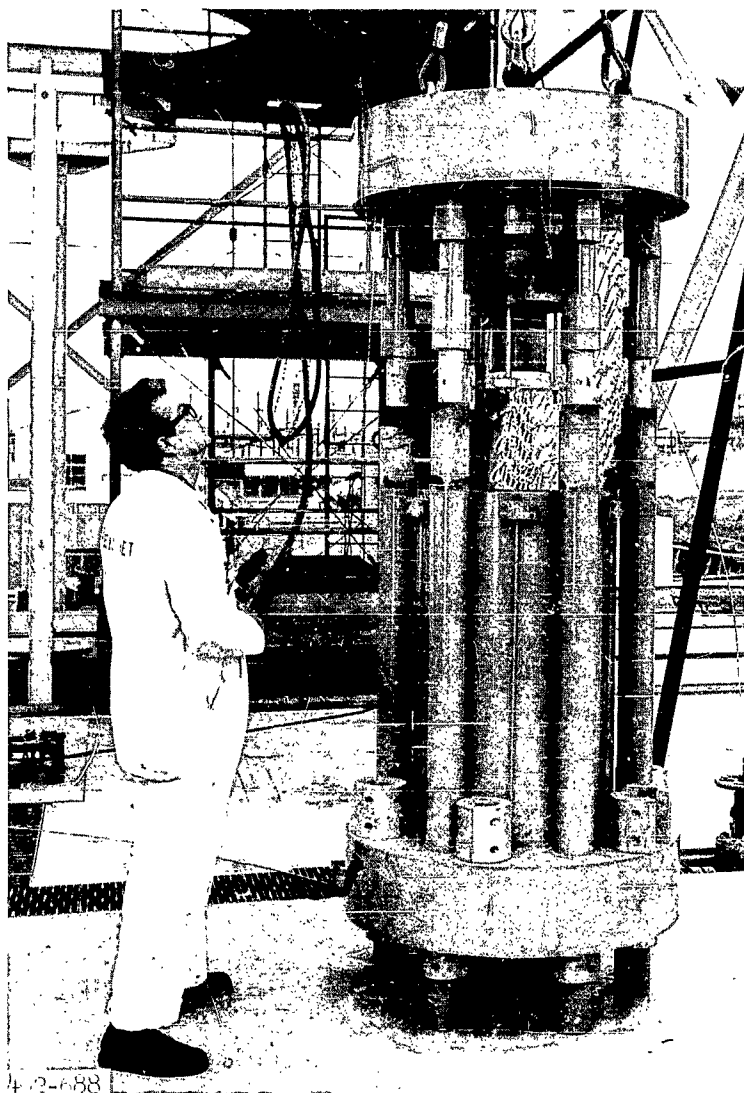
Figure 4

Installation of Test Cylinder into 17,500-psi Pressure Vessel

Figure 5
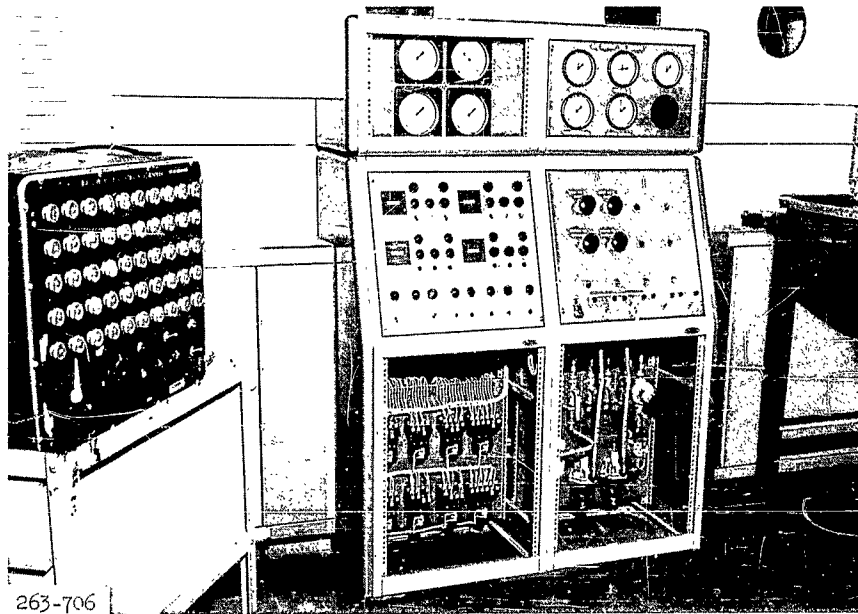
263-706

Creep and Fatigue Pressurization Control Console
and 50 Channel Strain Scanner for
30,000 psi Creep and Fatigue Facility
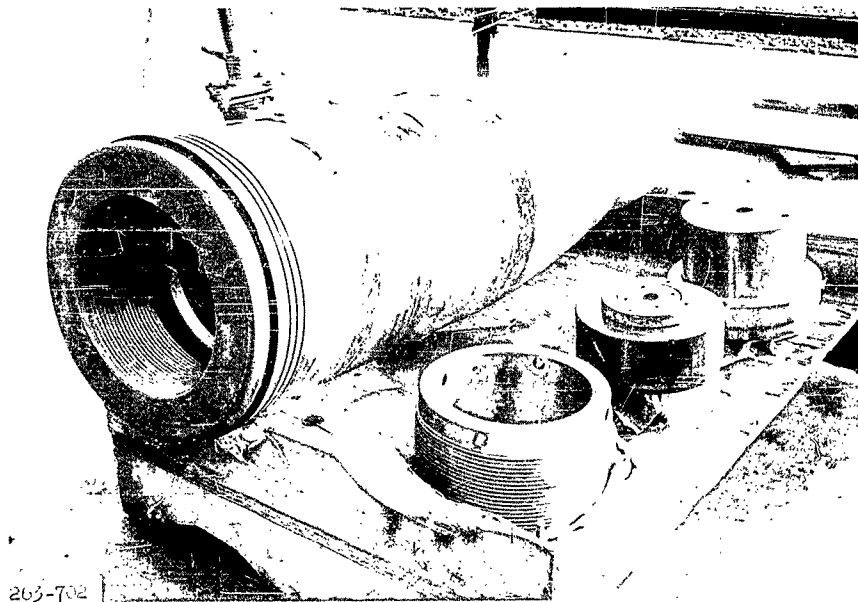
263-702

One of the Projectile Pressure Chambers
Utilized on Creep and Fatigue Facility

30,000 psi Pressure Chamber
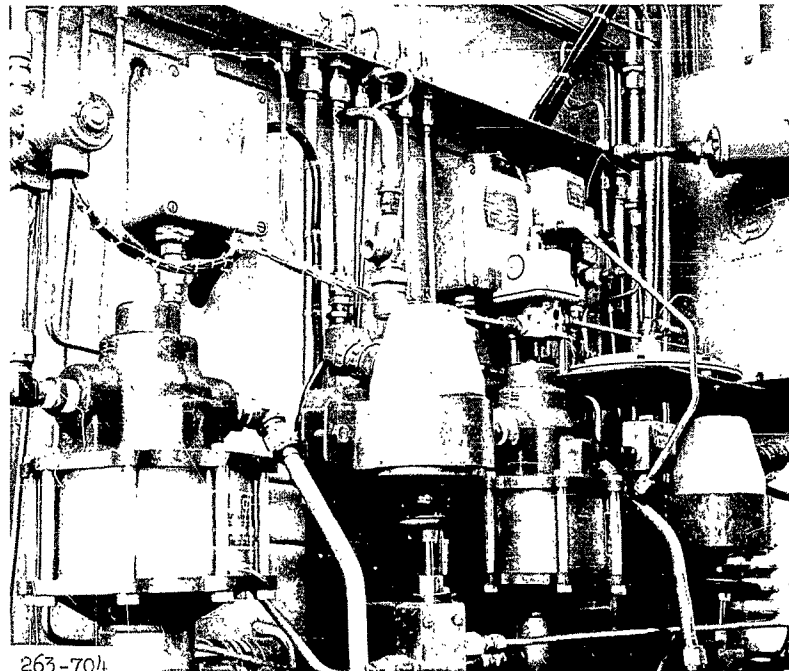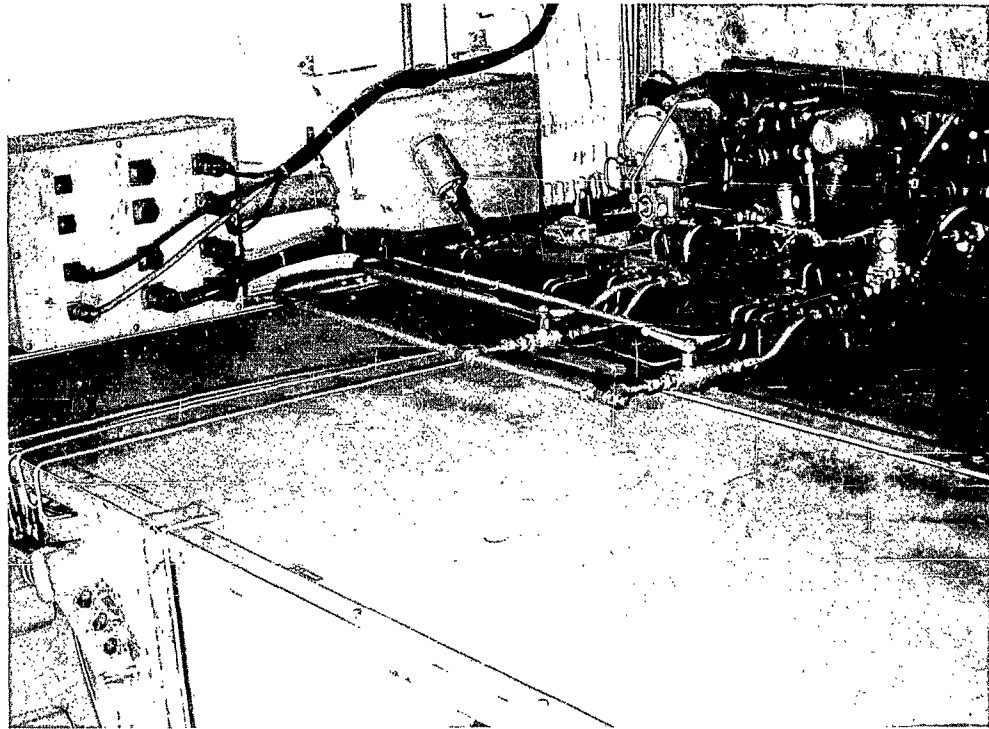
Figure 6

263-704

Part of the Creep and Fatigue Pressurization System

Creep Pressurization Console

Figure 7

662-1017

762-301
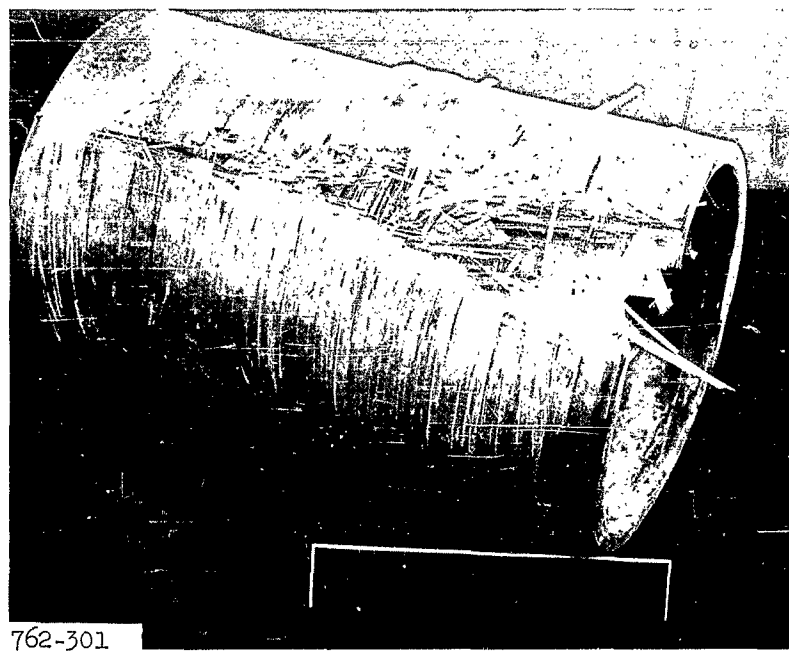
TW-3 Showing Test Cylinder Before and After Hydrotest

Figure 8
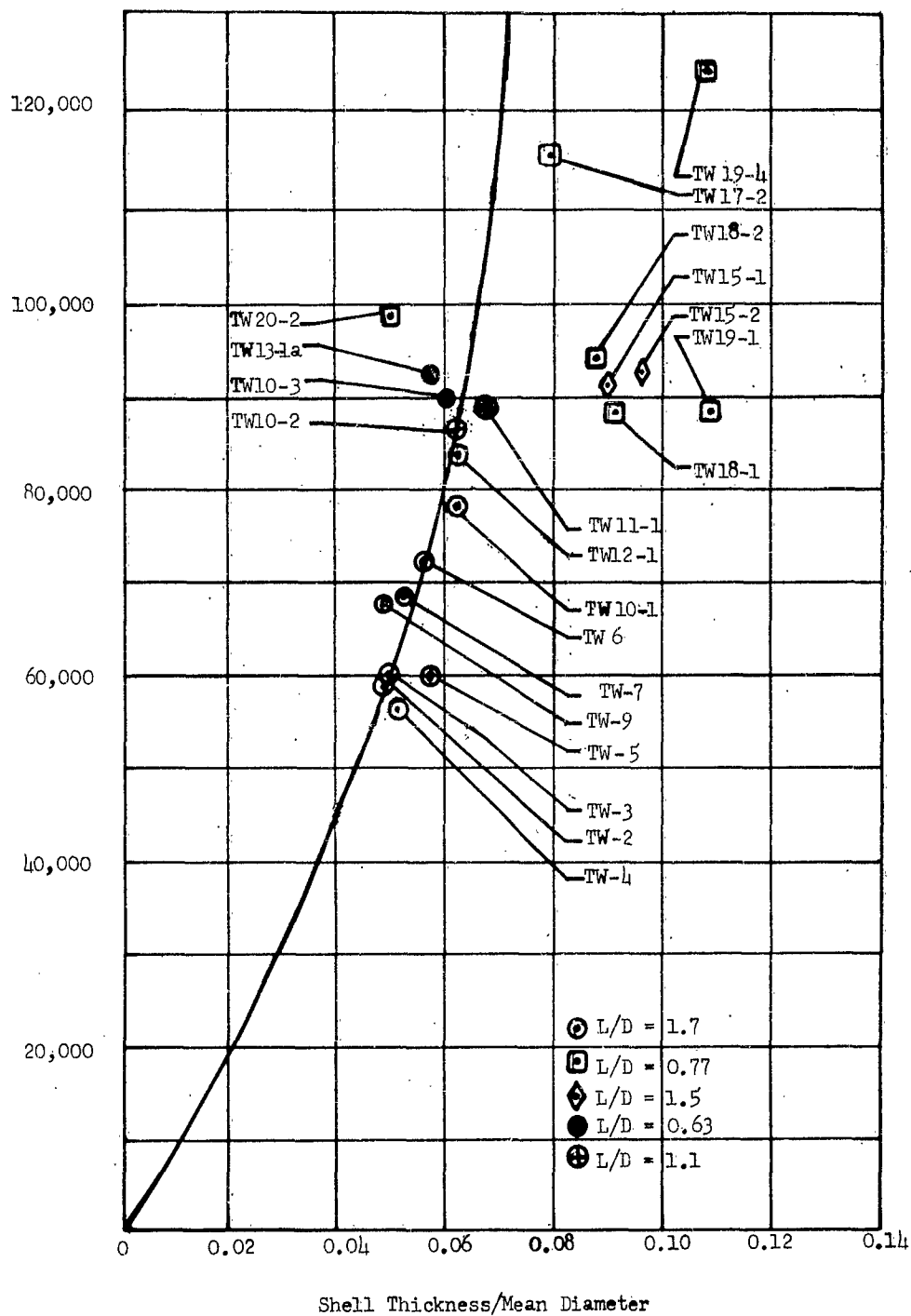
Curve - Stress @ Collapse for Unstiffened Cylinders

Figure 9

TW-10-1 Showing Typical Hydrotest Failure

Figure 10
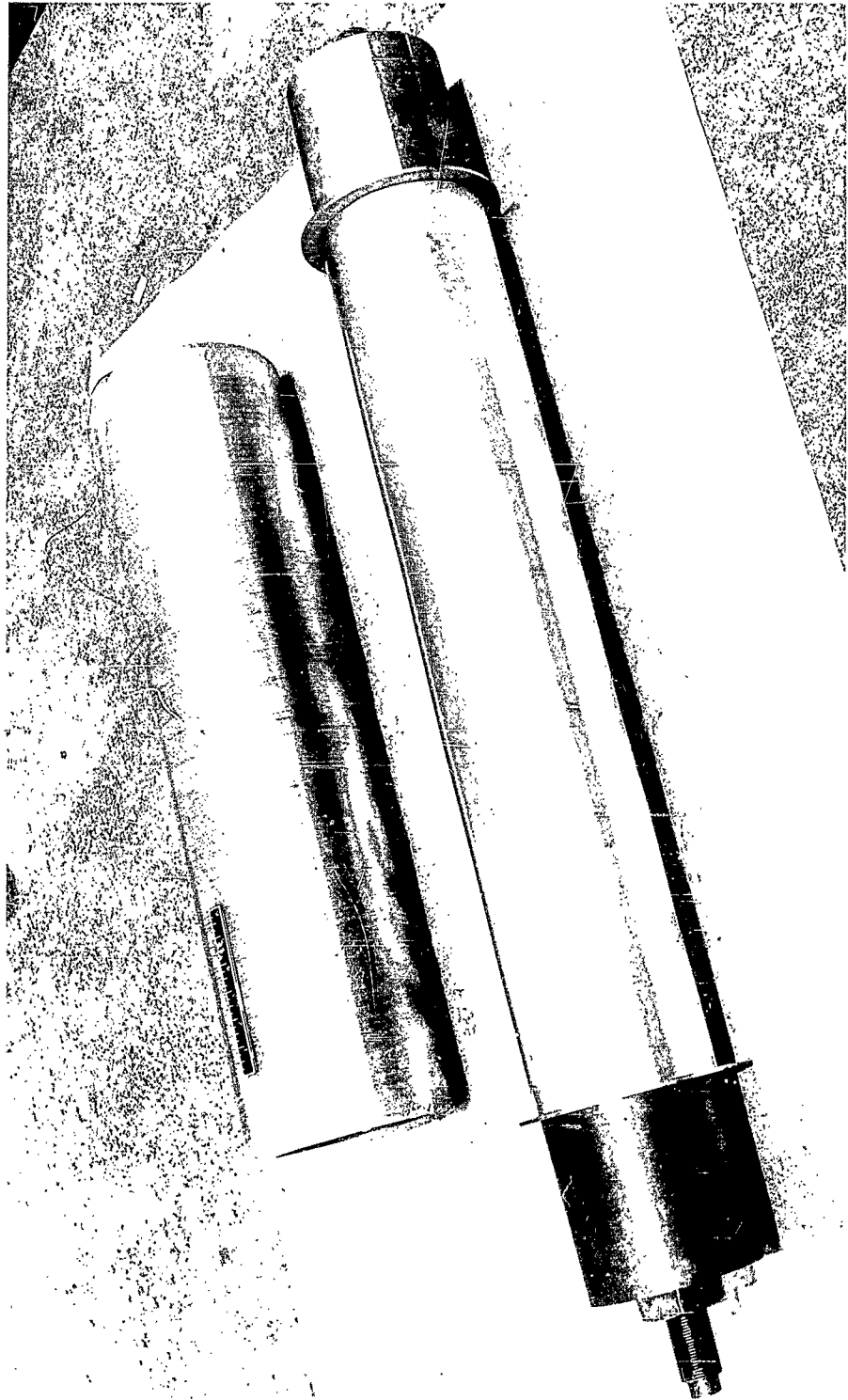
TW-11 Cylinder and 6.0-in.-Dia. Steel Mandrel

2-110
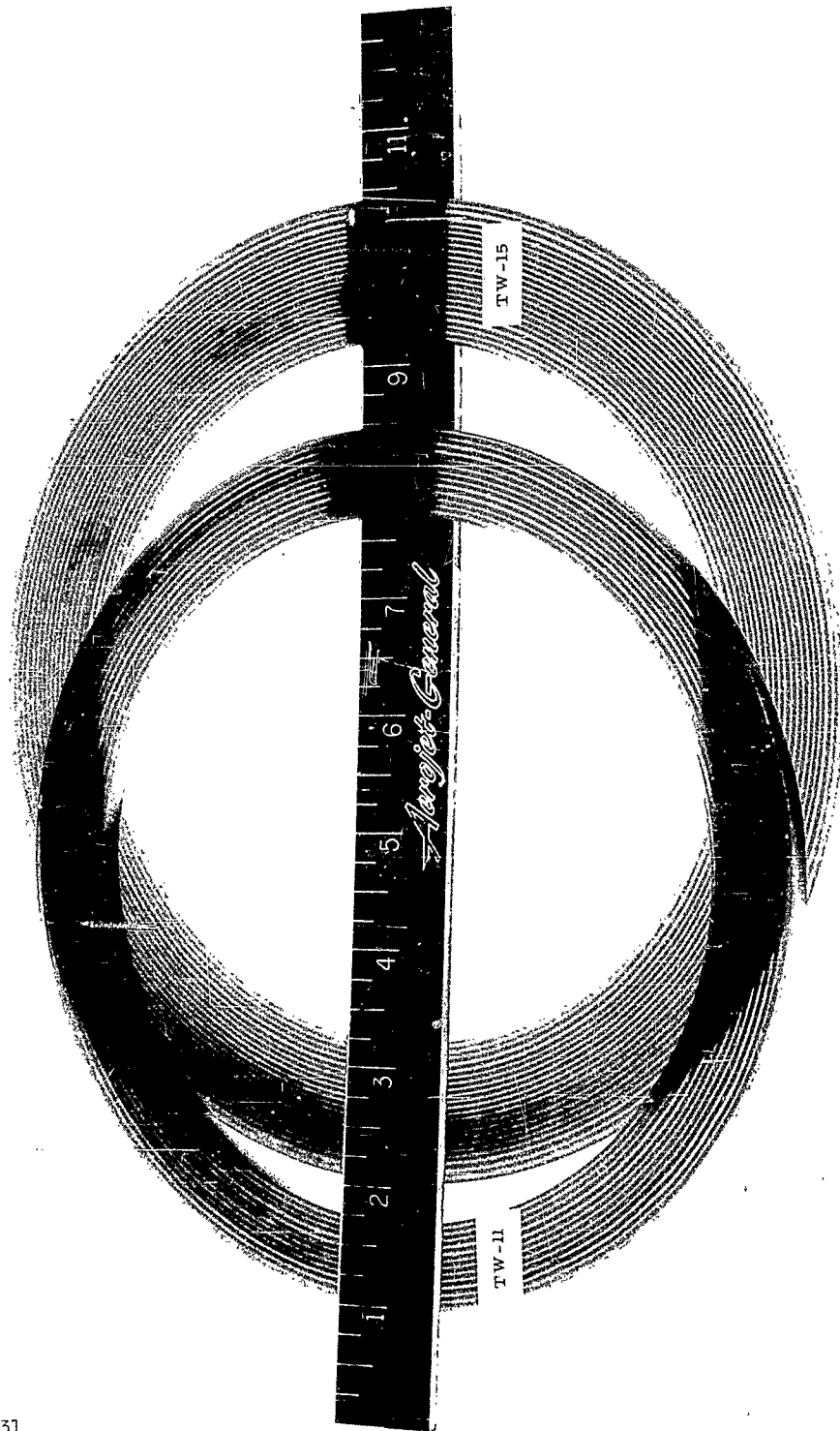
Figure 11

Polished Rings From Cylinders TW-11 and TW-15

1lo2-831

Figure 12
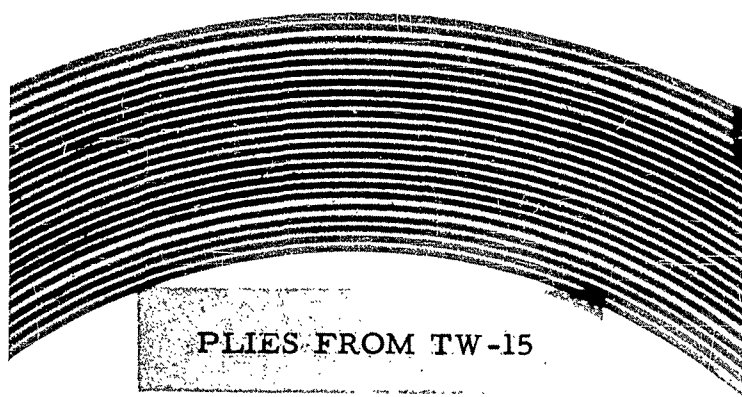
PLIES FROM TW-15

TW-15
Shows Consistently Straight Circumferential Filaments &
Uniform Longitudinal Filaments
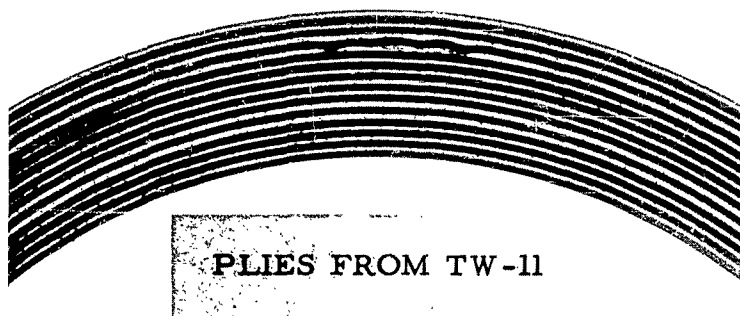
PLIES FROM TW-11

TW-11
  Notice the Wavy Condition in the Outer Plies Indicating
  a Loss of Tension & Fiber Movement.

Plies from Cylinders TW-11 and TW-15

Figure 13
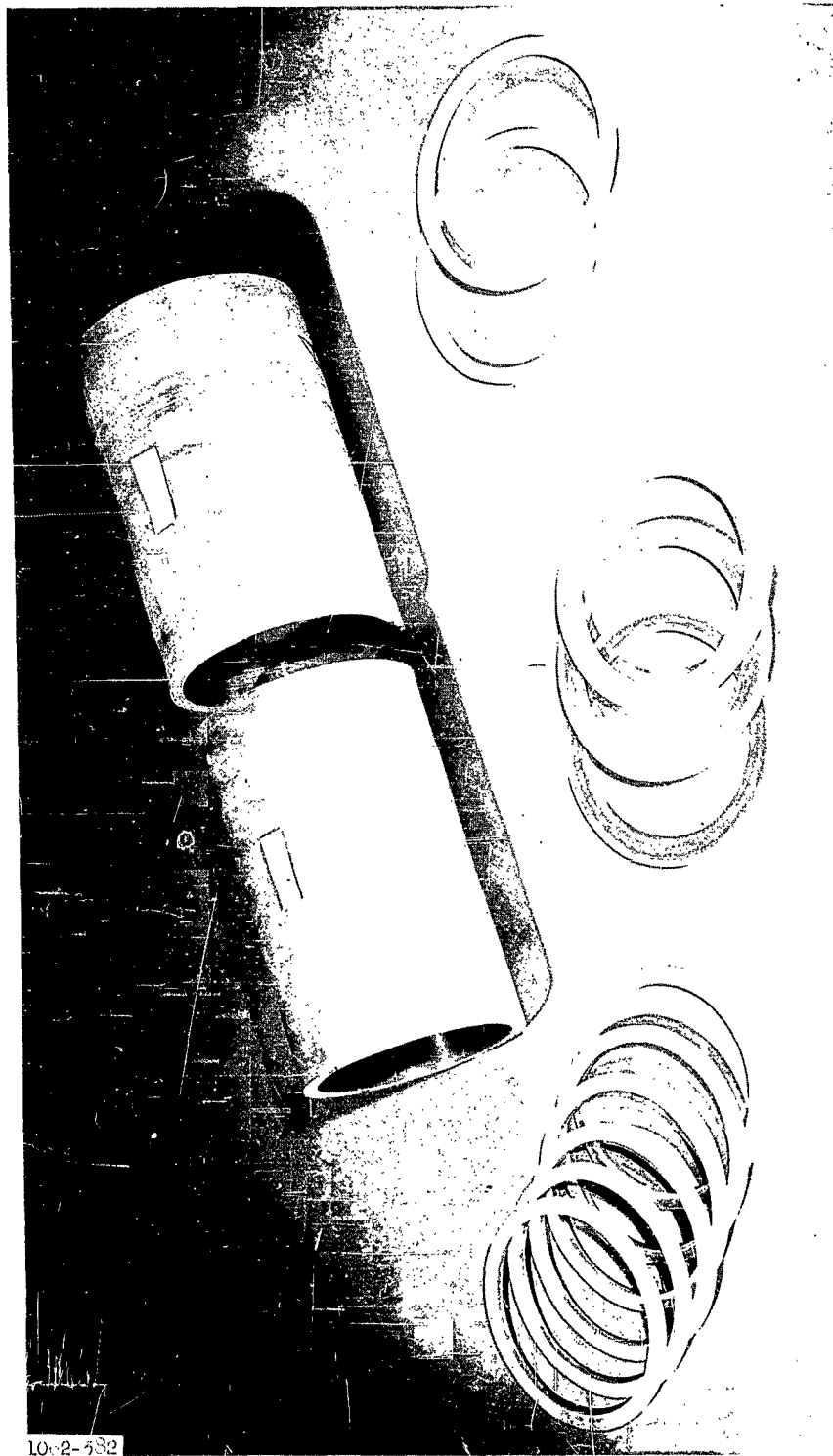
Figure 14

Test Cylinders and Test Rings Cut From TW-11

TW-11-1 CIRCUMFERENTIAL &
LONGITUDINAL GAGES
AT CENTER OF CYLINDER

Figure 15

TV-11-2 CIRCUMFERENTIAL &
LONGITUDINAL GAGES
AT CENTER OF CYLINDER
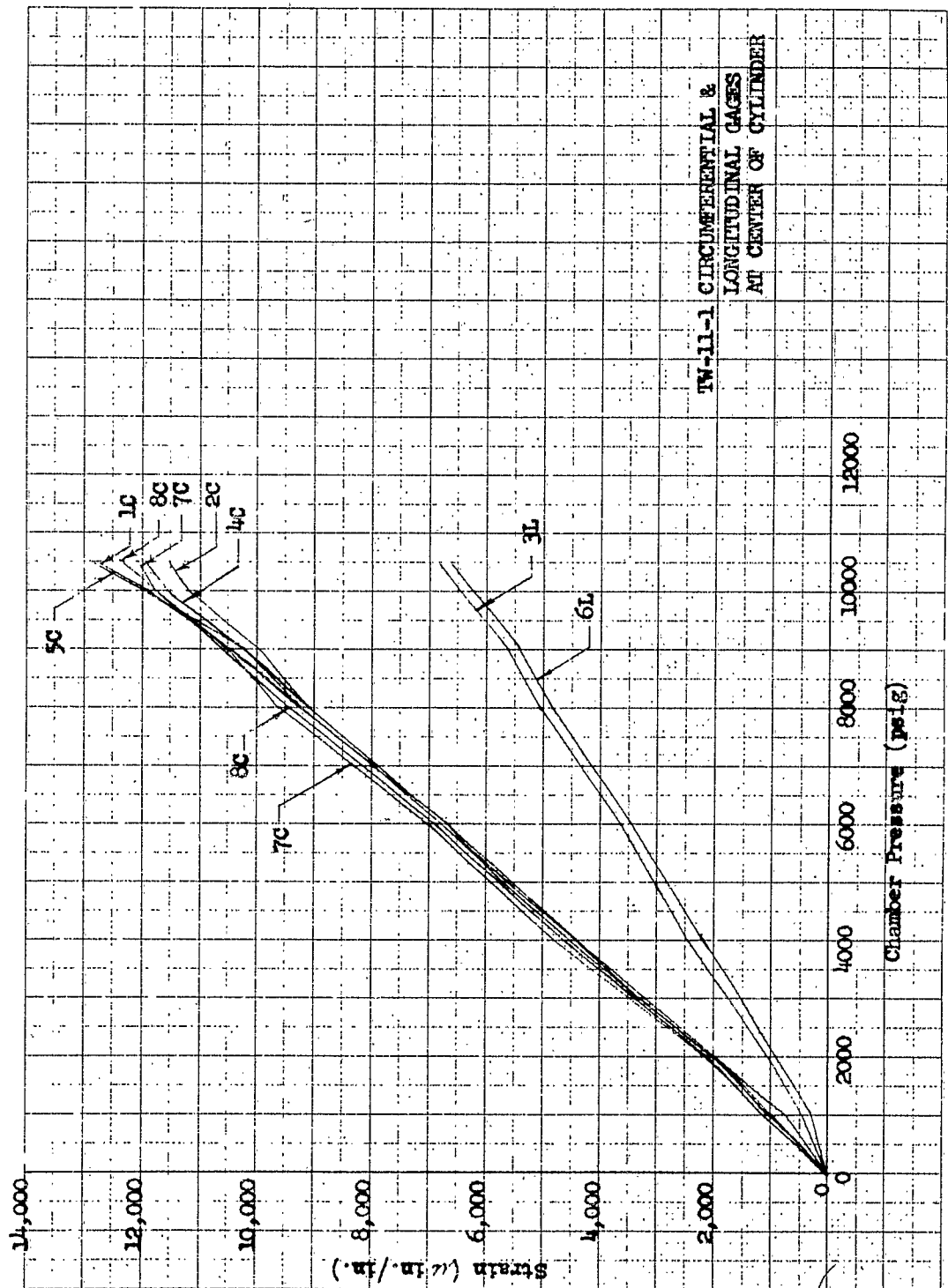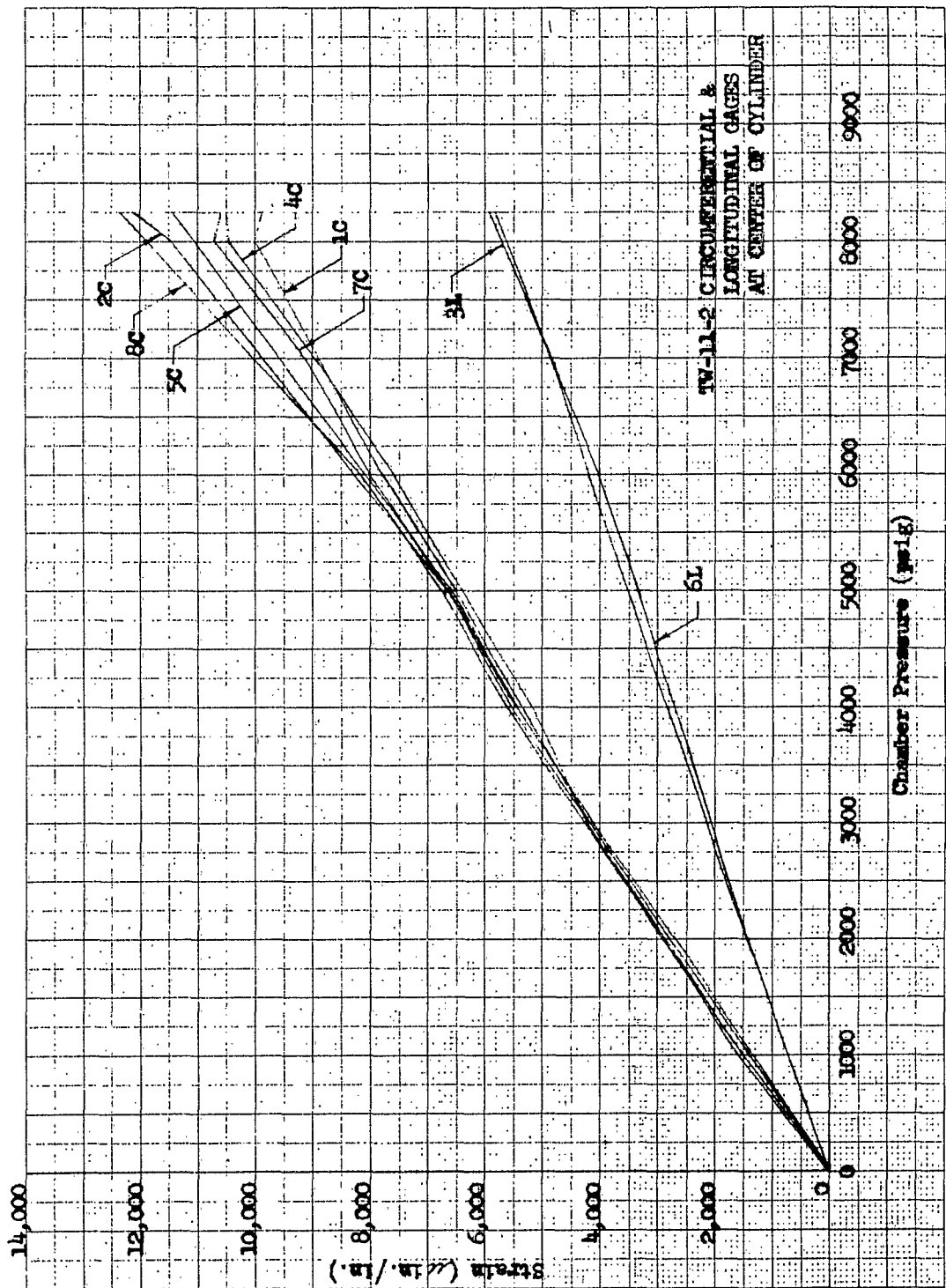
Figure 16

Figure 17

TW12-1 Cylinder, Outer & Inner Views After Hydrotest

TW-12-1 CIRCUMFERENTIAL &
LONGITUDINAL GAGES
AT CENTER OF CYLINDER
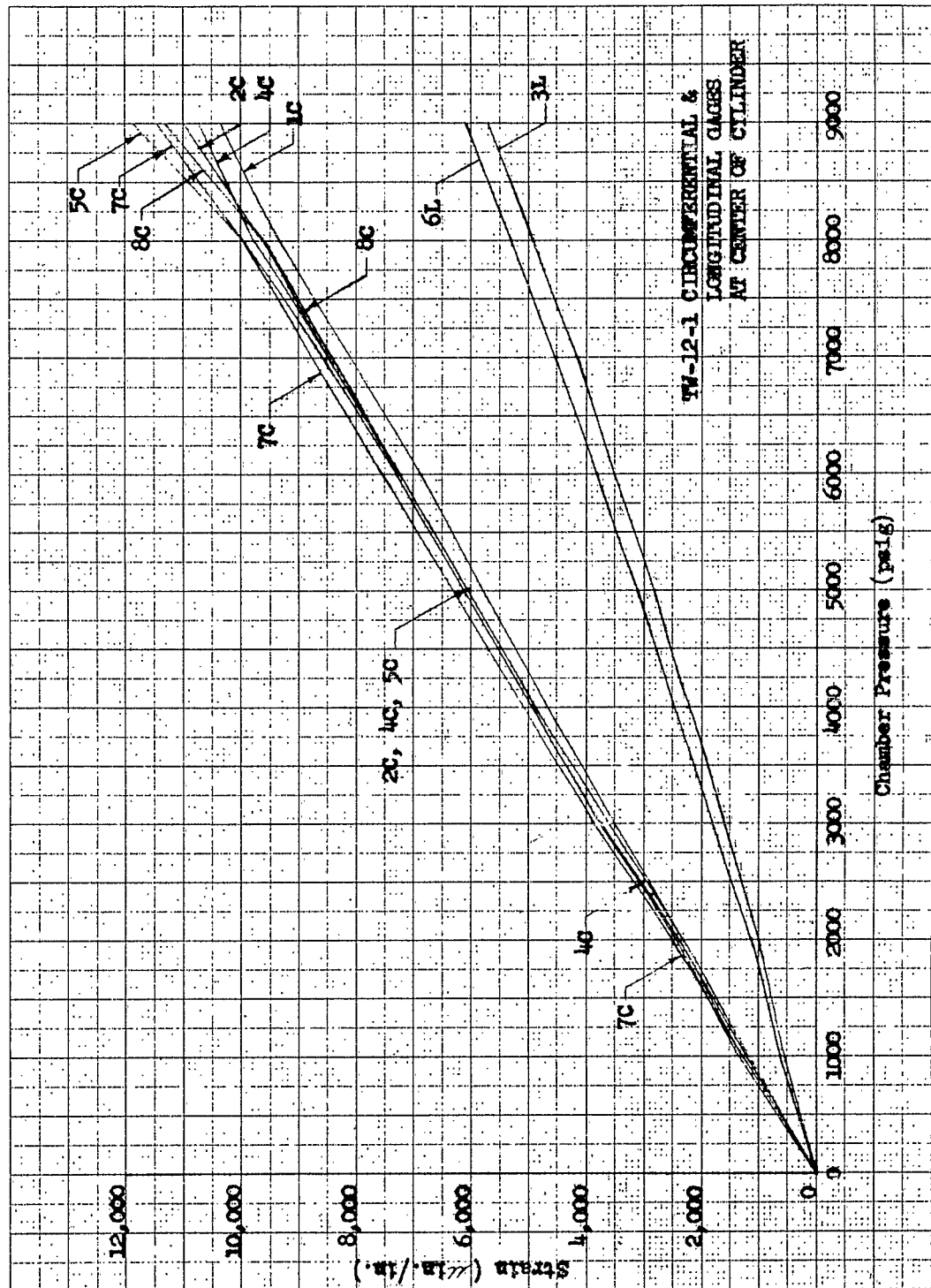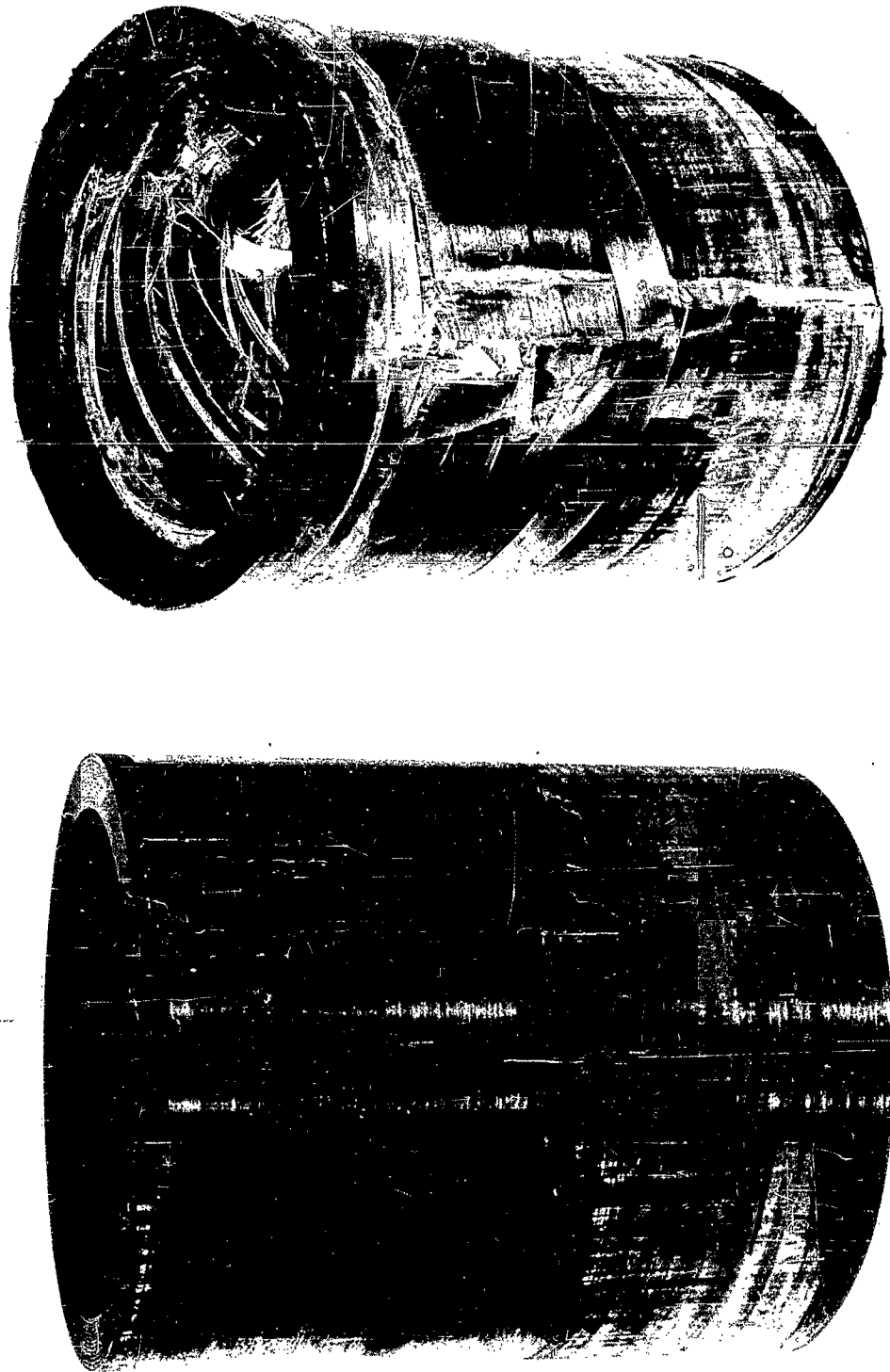
Figure 18

Figure 19

TW15-2, Before and After Hydrotest

Figure 20

TW-15-2 CIRCUMFERENTIAL & LONGITUDINAL GAGES AT CENTER OF CYLINDER
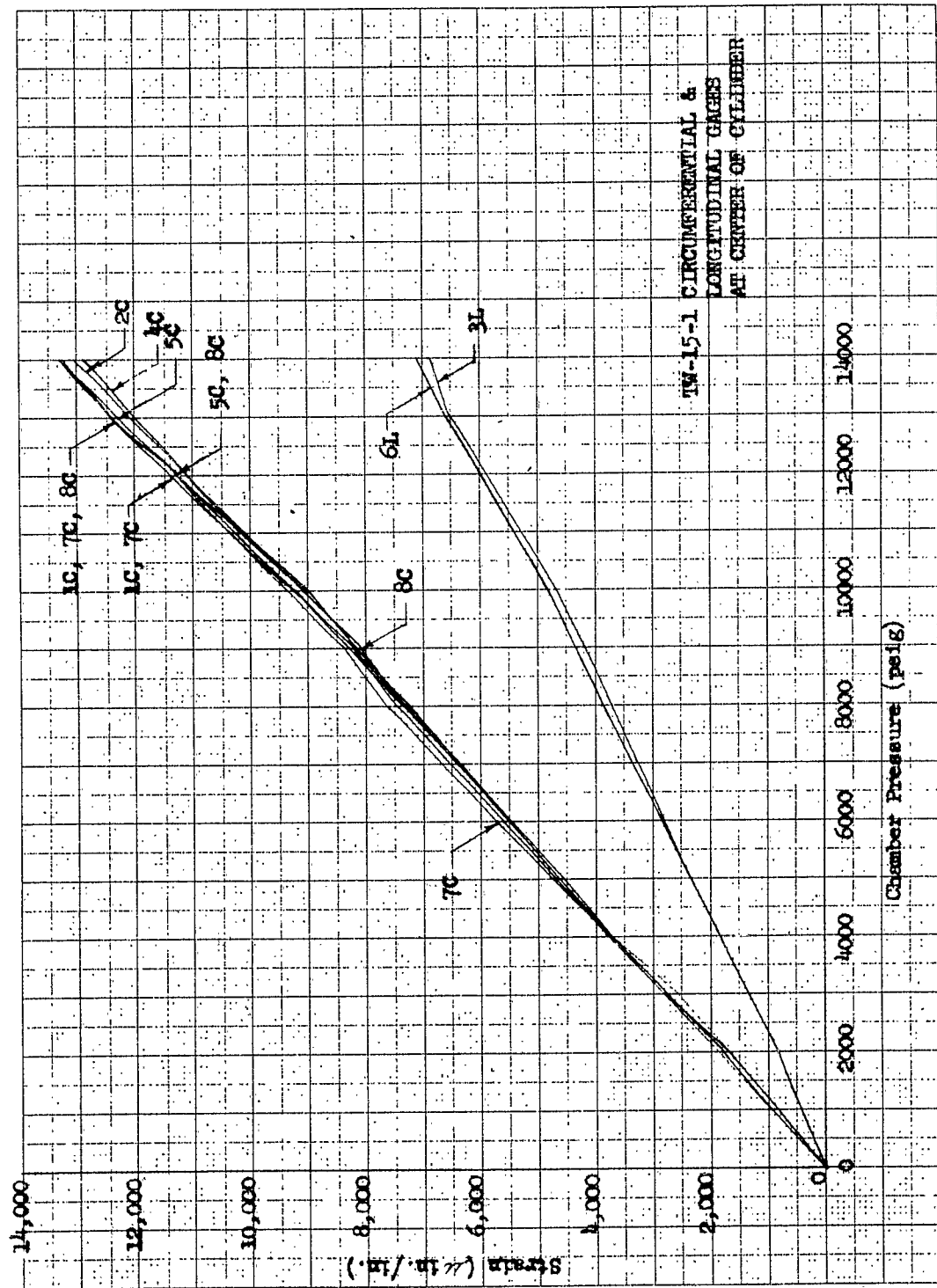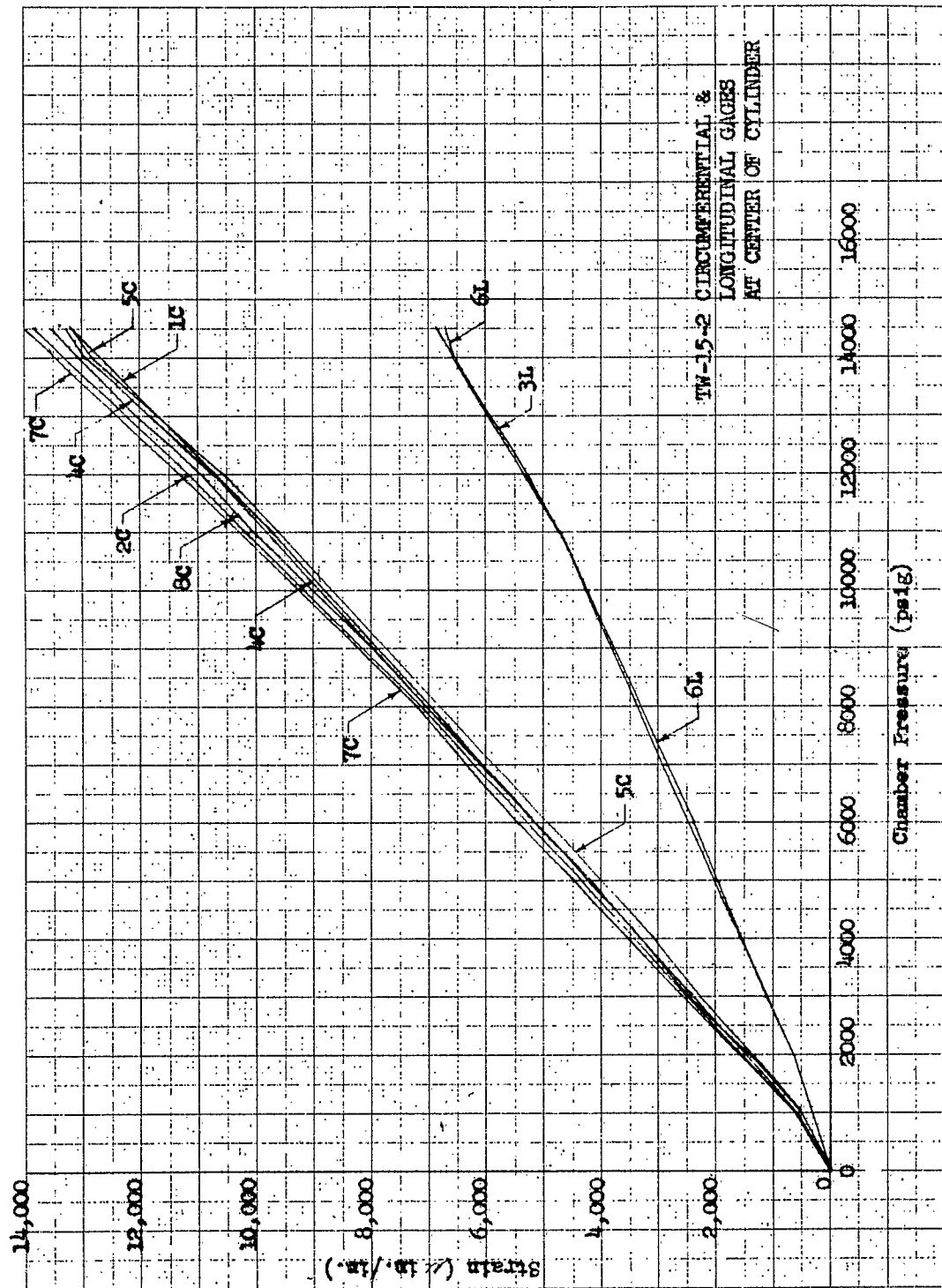
Figure 21

TW-18, 1.250-in. Thick X 6.0-in. ID Cylinder

Figure 22
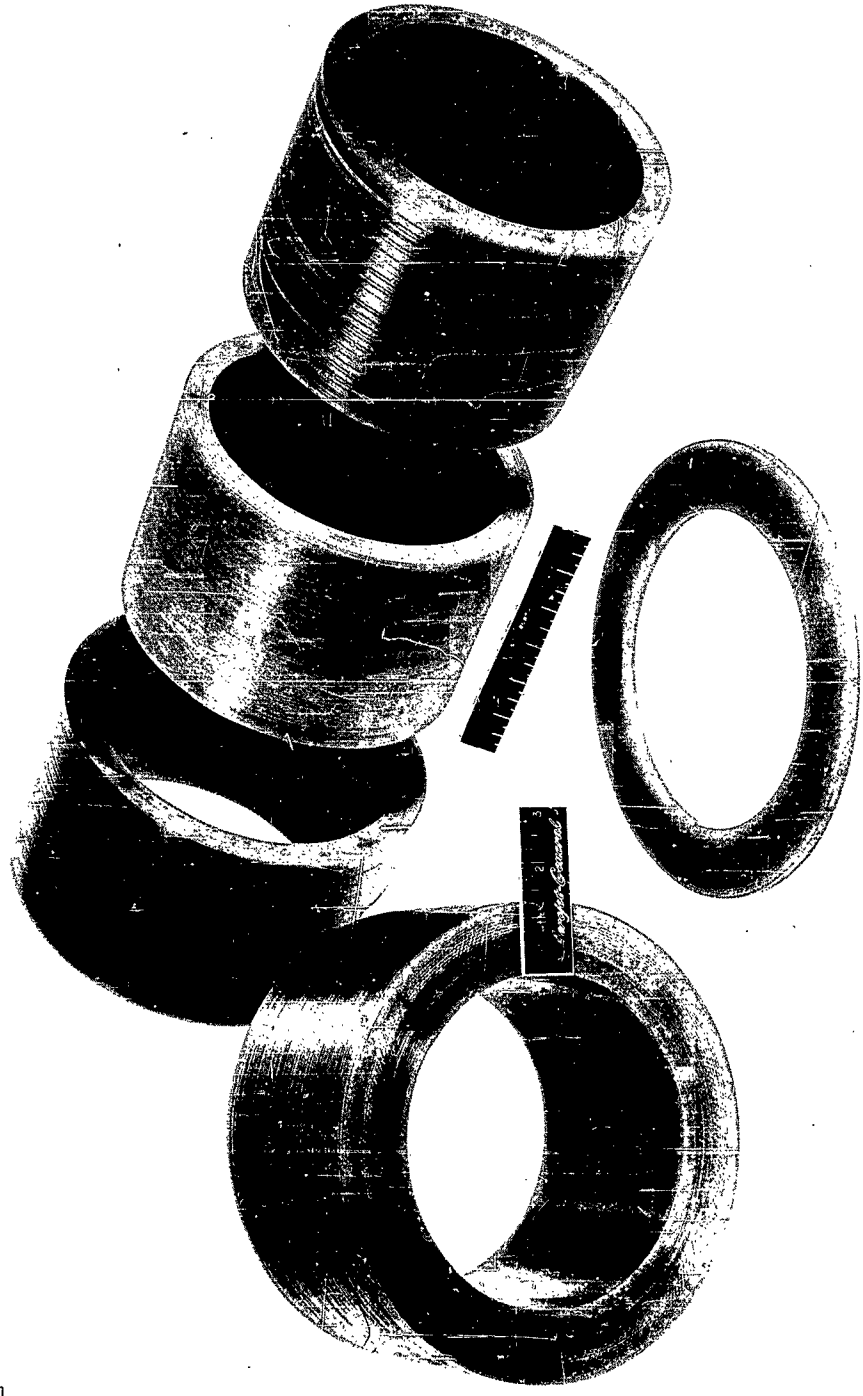
163-1471

Figure 23

TW 18-1, TW 18-2, TW 18-3 Concentric Cylinders
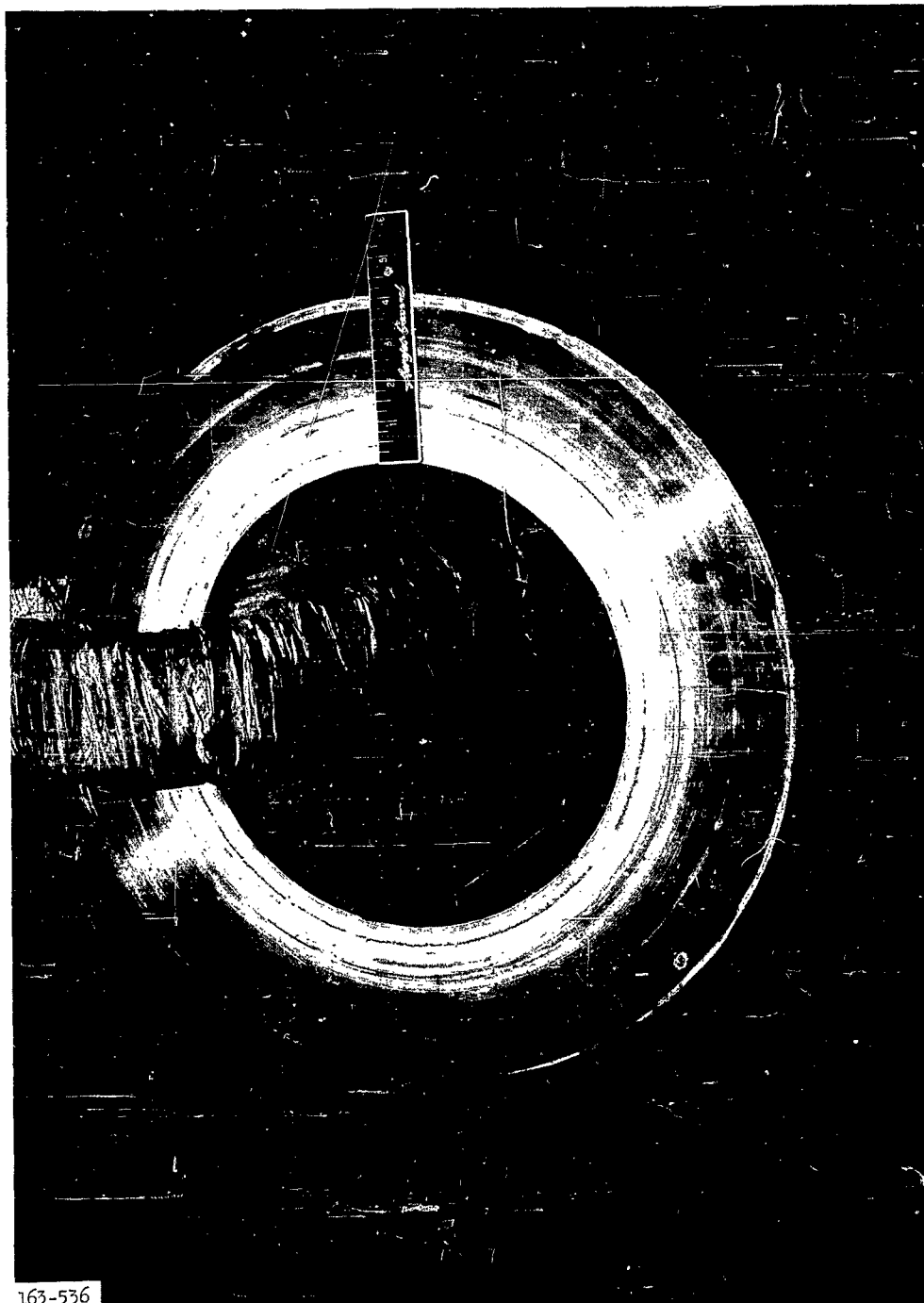
163-536

TW 20 After Removal from Mandrel

Figure 24
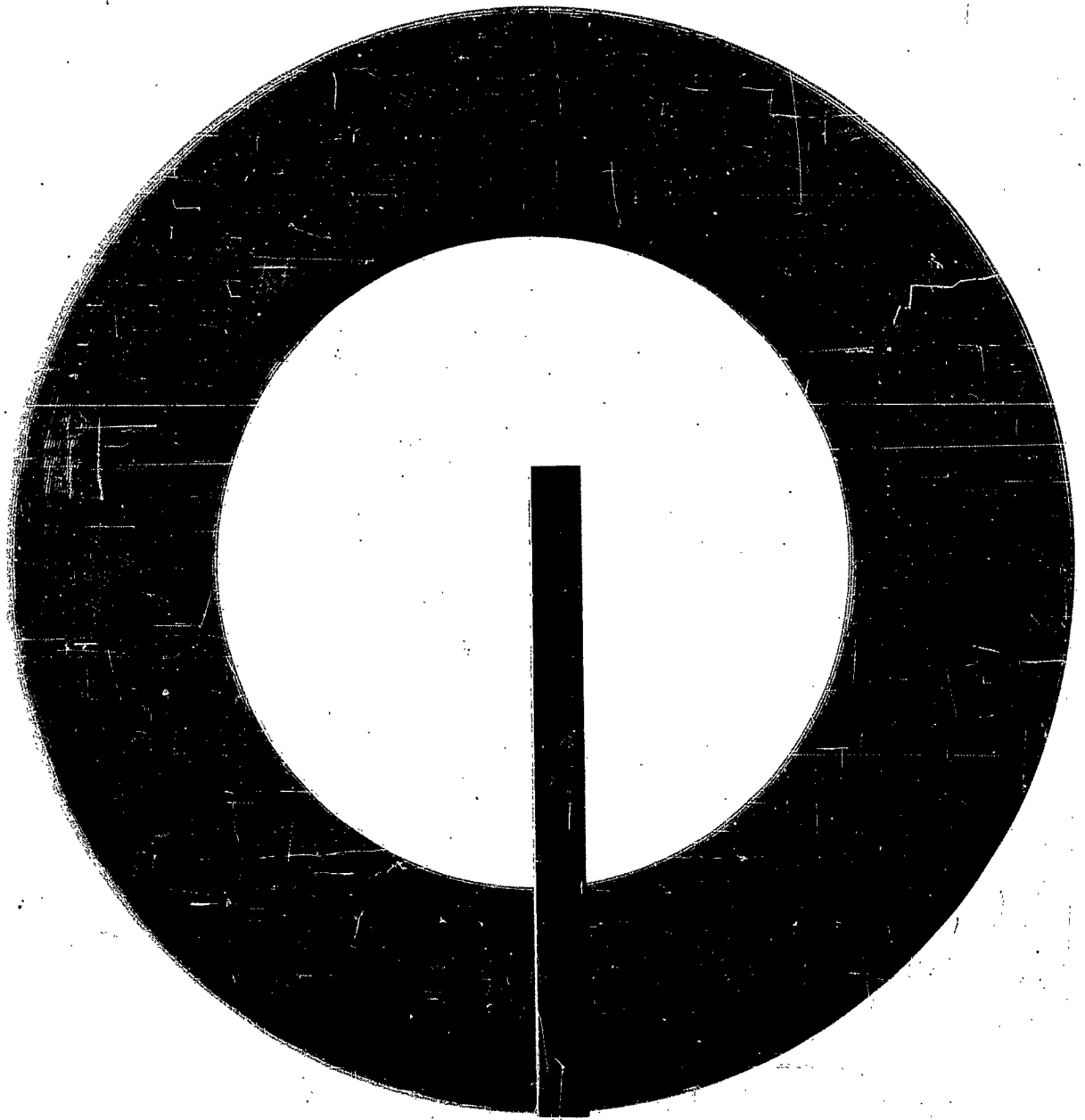
163-1509

Polished Ring from Cylinder No. TW-20
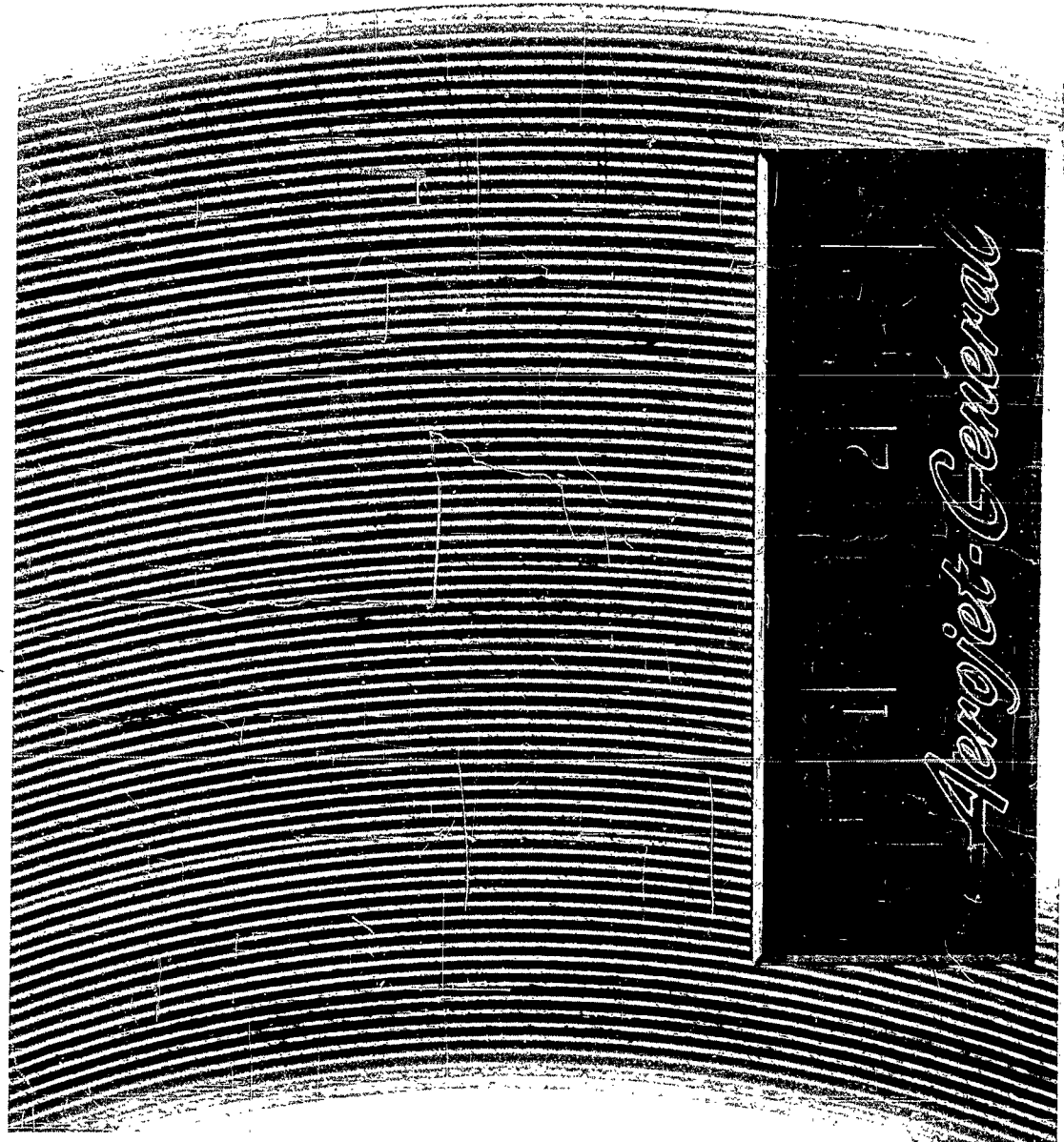
Figure 25

Section of Ring from Cylinder No. TW-20

163-1510

Figure 26

462-264

462-262
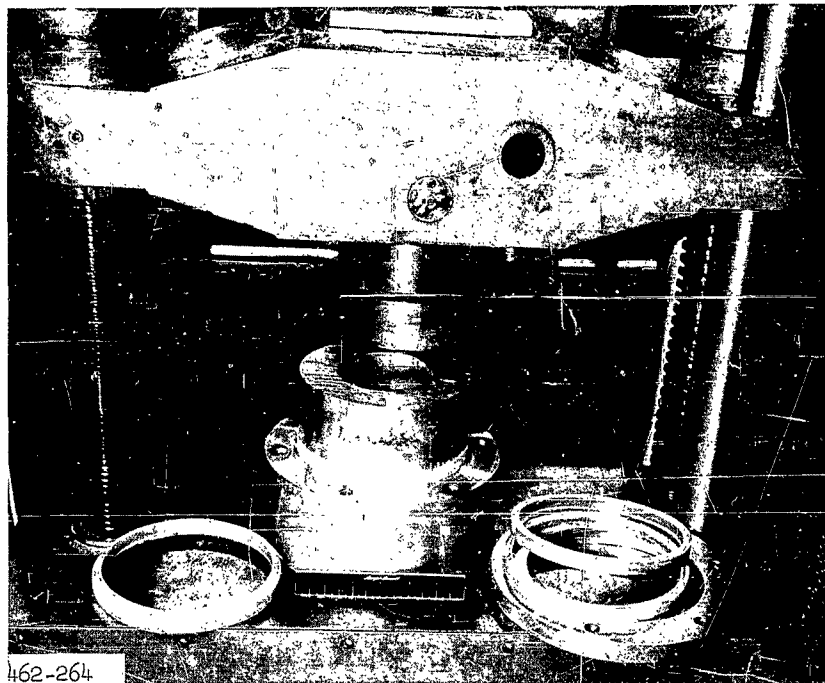
Axial Shear Fixture

Figure 27

Note:

1. Test Specimen cut from Ring off of Test Cylinders
2. Rate of Cross-Head Motion: 0.05 in./min.
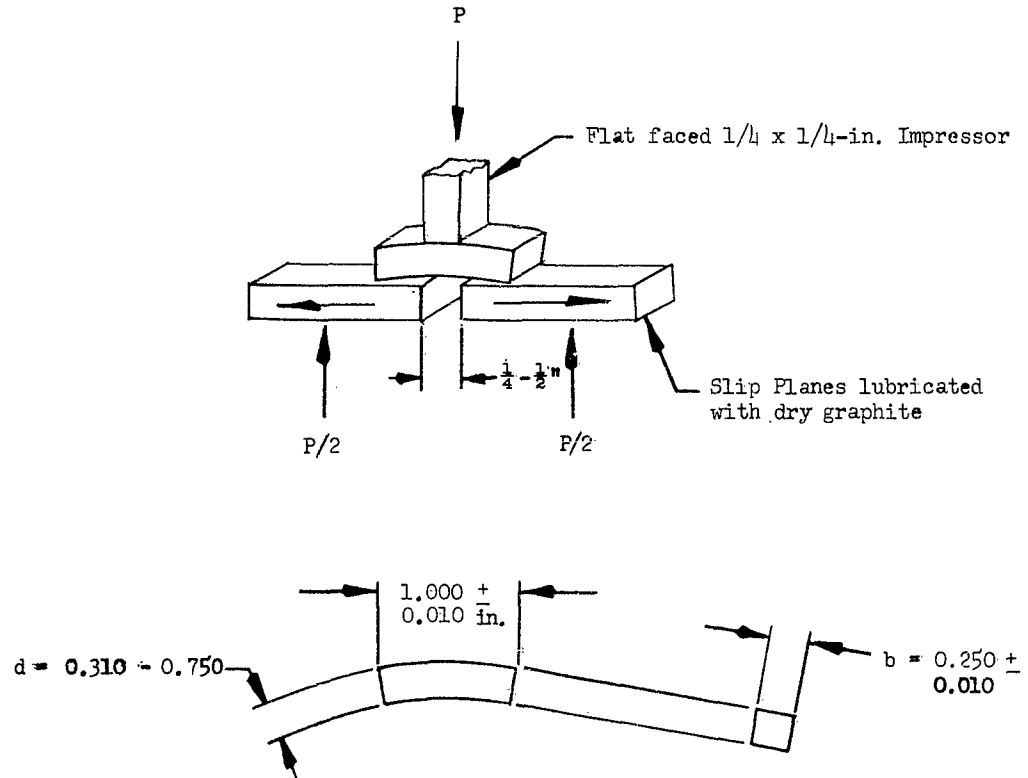
Horizontal Shear Test Method

Figure 28
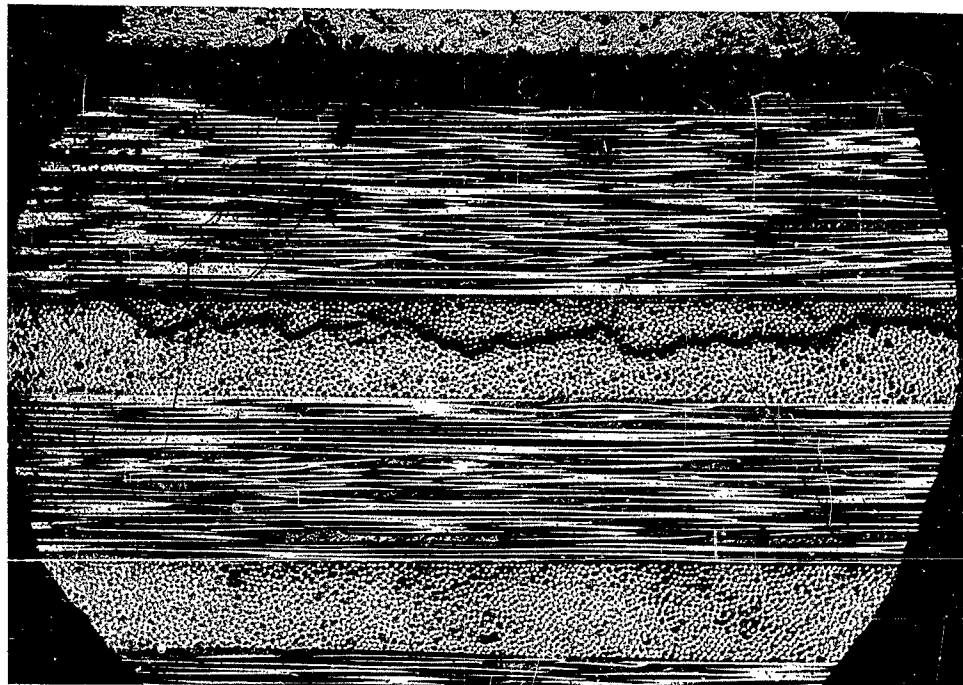
Circ.

Long.

Circ.

Long.

TW-2 Inner Layers. View Looking at ends of Longitudinal Filaments.
A Good Example of Delamination in the First Longitudinal.
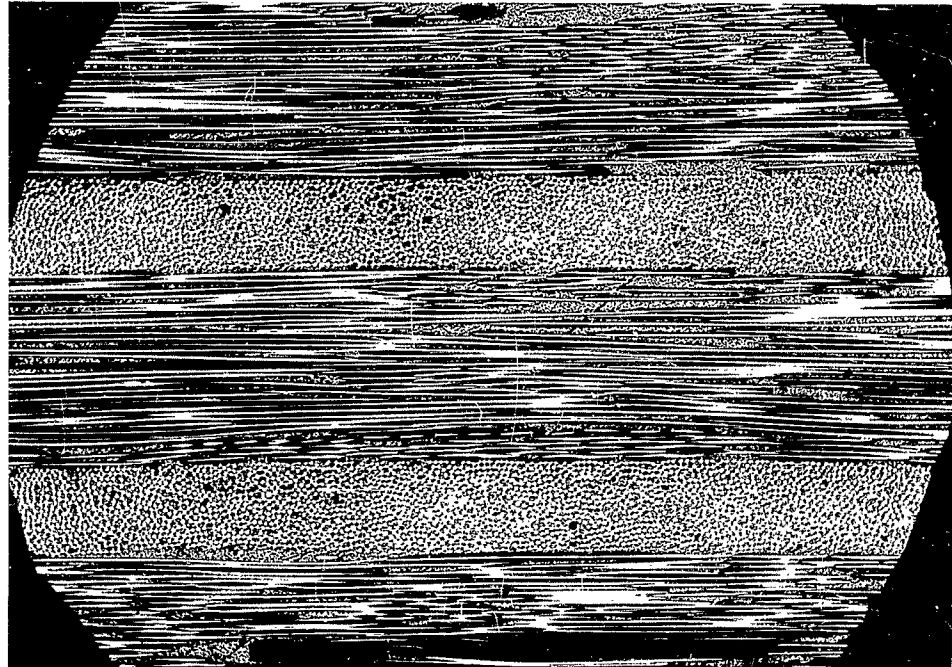
Circ.

Long.

Circ.

Long.

TW-2 Outer Layers. View Looking at Ends of Longitudinal Filaments.
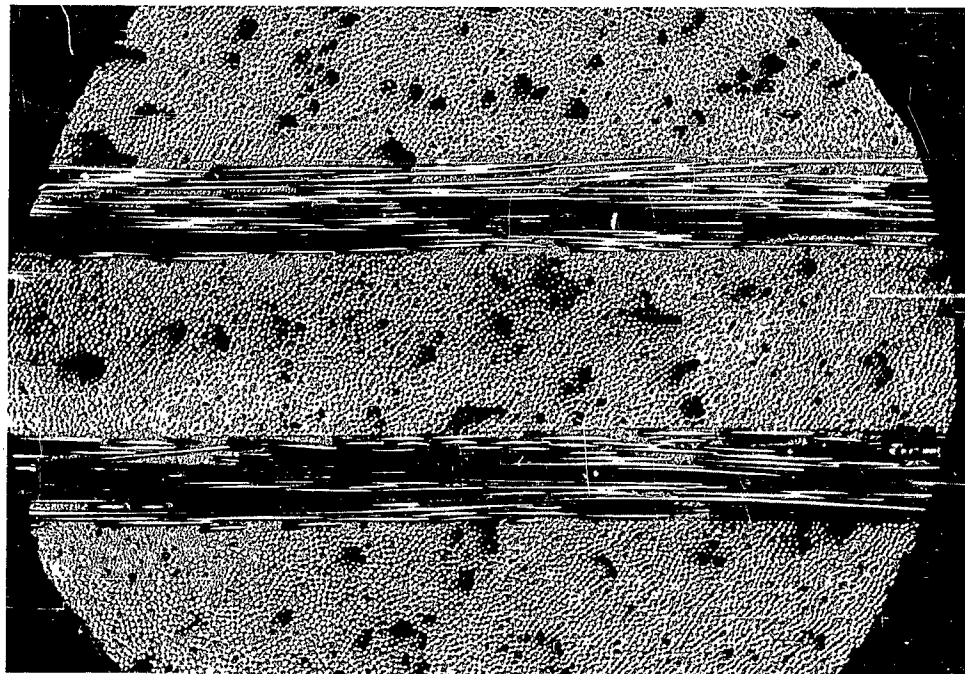A Well Packed, Void Free Structure in Evident. (100X)

TW-2 Photomicrographs

Figure 29
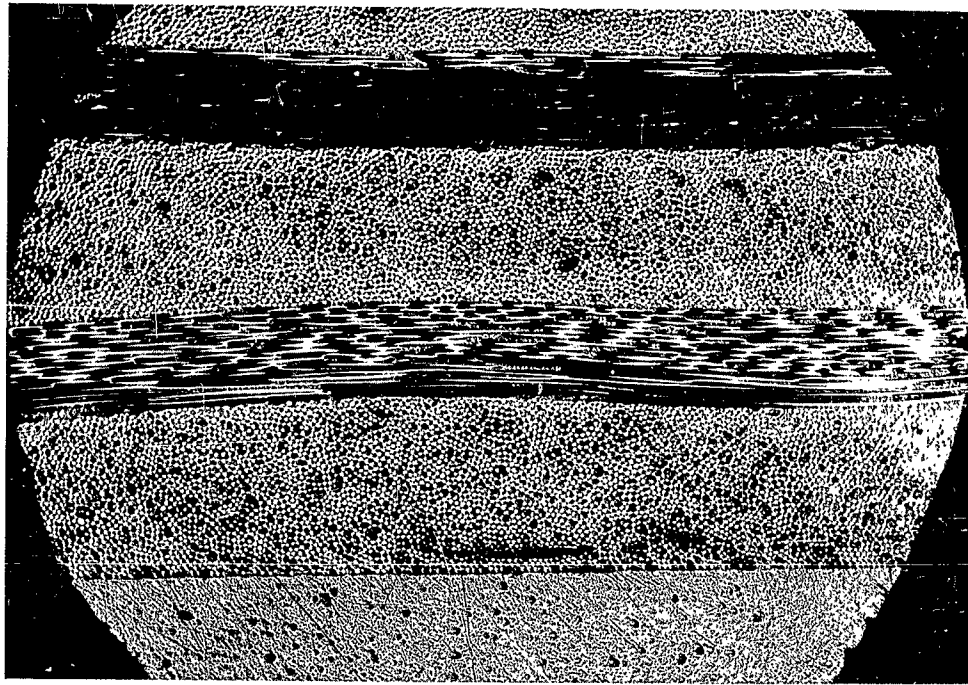
TW-3 Inner Layers, View Looking at Ends of Circumferential Filaments   (100X)
Good Packing of the Filaments with a Minnimum of Voids or
Resin Pockets is Shown
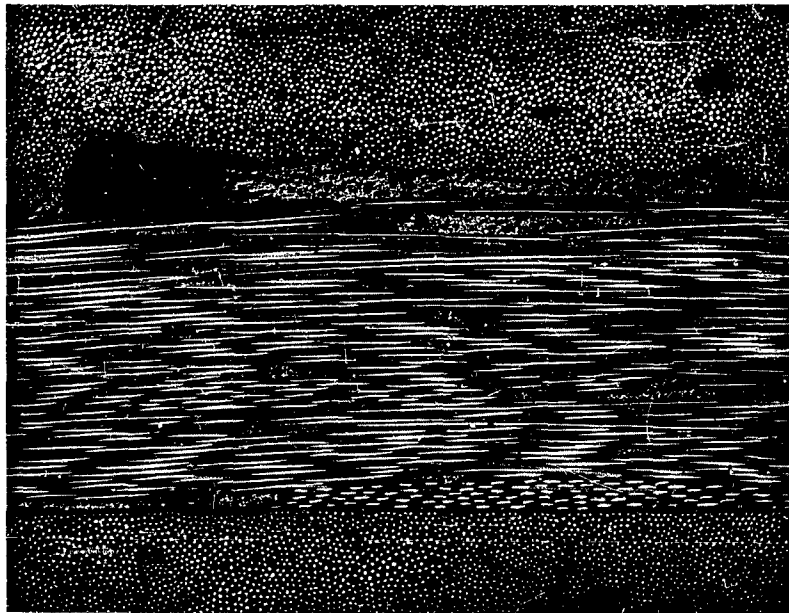

TW-3 Outer Layers, View Looking at Ends of Circumferential Filaments   (100X)
Note the Large Quantity of Voids and Resin Pockets.
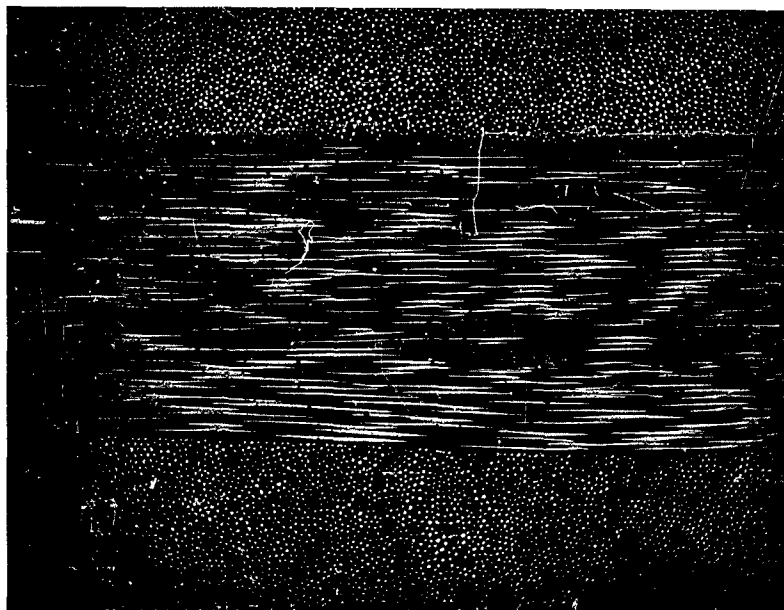
TW-3 Photomicrographs

Figure 30

Circ.

Long.

Circ.

TW-6 Outer Layers.   View Looking at Ends of Circumferential Filaments
Several Voids are Apparent, Indicating too low a Tension as a Result
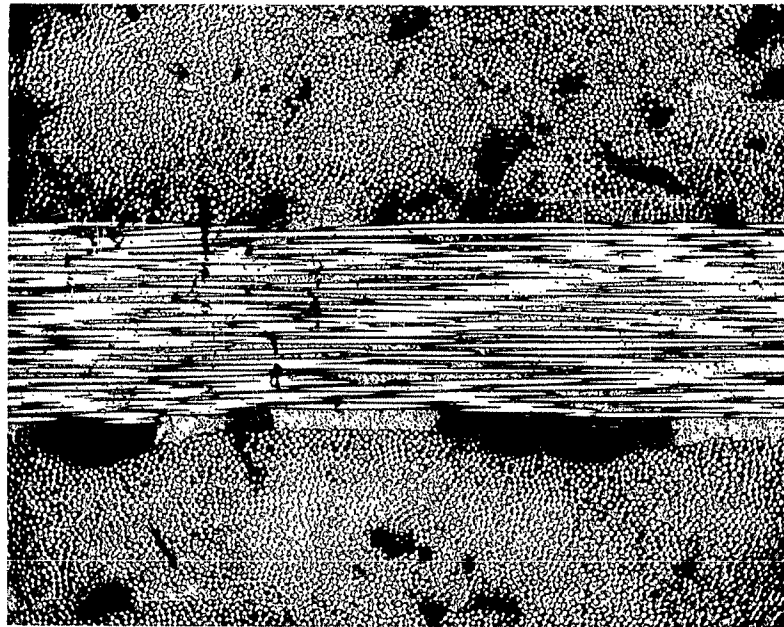of Telescoping.

Circ.

Long.

Circ.

TW-6 Inner Layers.   View Looking at Ends of Circumferential Filaments   (100X)
Good Packing is Evident in the Circumferentials with some Universally
Dispersed Resin Pockets in the Longitudinals
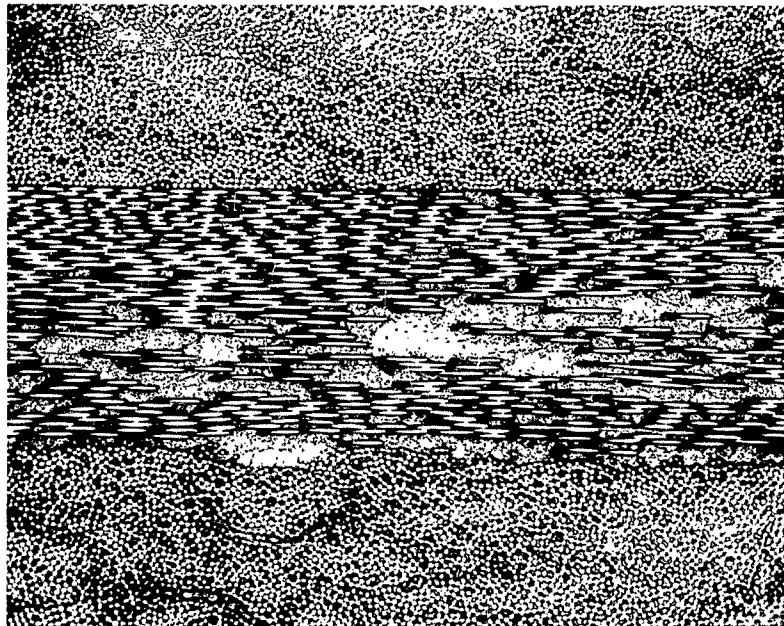
TW-6 Photomicrographs

Figure 31

Circ.

Long.

Circ.

(3) Outer Plies

Circ.

Long.

Circ.

(3) Inner Plies

TW-8 View Looking at Ends of Circumferential Filaments. Example
of Insufficient Pressure During Cure and Voids in the Outer
Plies Caused by Loss of Tension.

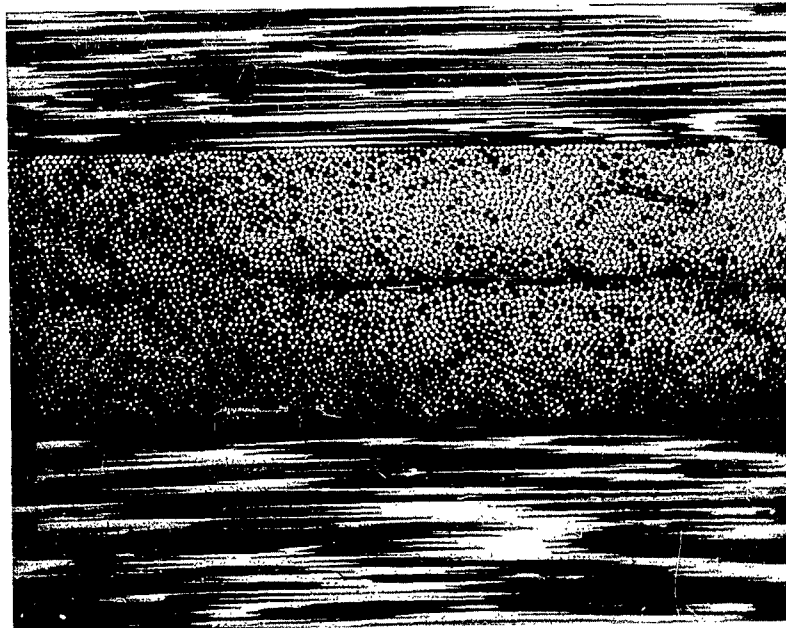TW-8 Photomicrographs

Figure 32

Circ.
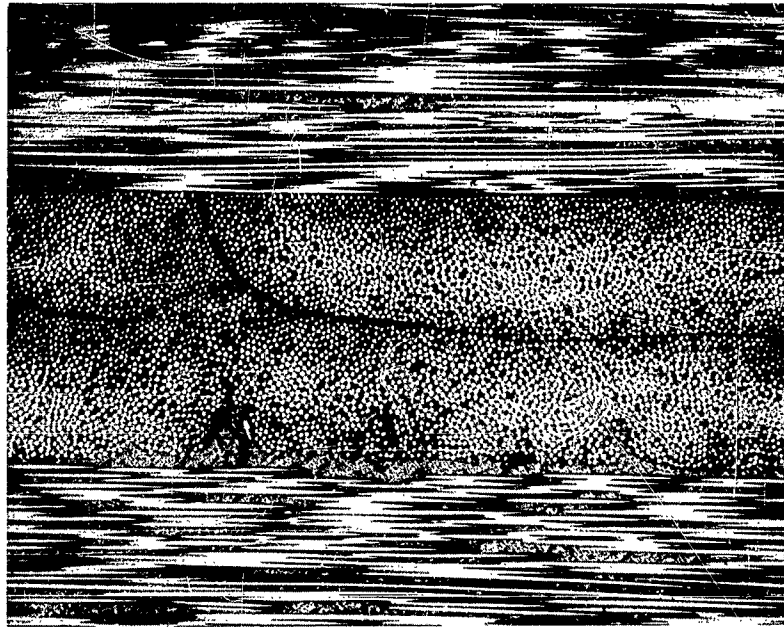
Long.

Circ.

(3) Outer Layers

Circ.

Long

Circ.

(3) Inner Layers

TW-9 Looking at ends of Longitudinal Filaments (100X).
A Good Example of Dense Windings with Some Indication of Resin
Planes Between Plies. The Wide Grey Area is Resin.

TW-9 Photomicrographs

Figure 33

Circ.

.Long

Circ.

(3) Outer Plies

Circ.

Long.

Circ.

(3) Inner Plies

TW-12 Looking at Ends of Longitudinal Filaments (100X).
Resin Layer Between Inner Surface of Longitudinal and Circ.
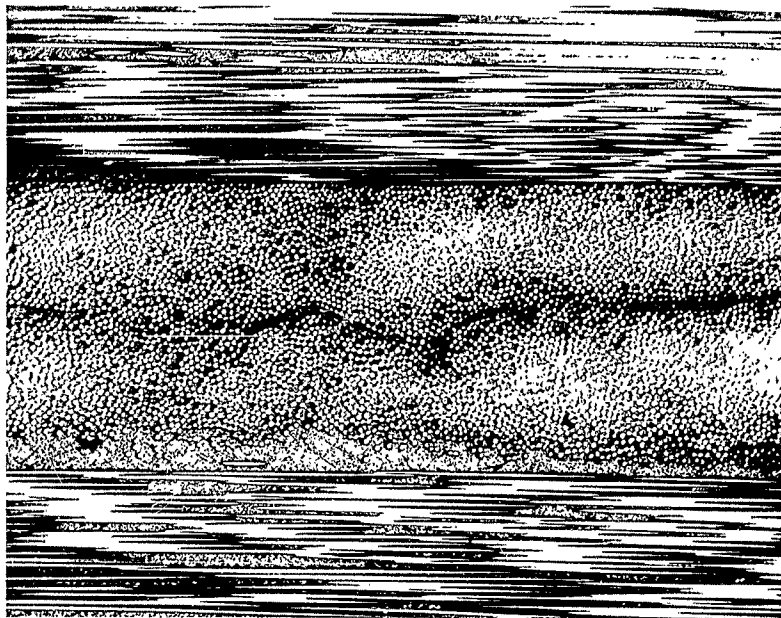This is Inherent in the Method of Fabricating Unidirectional Tape.

TW-12 Photomicrographs

Figure 34
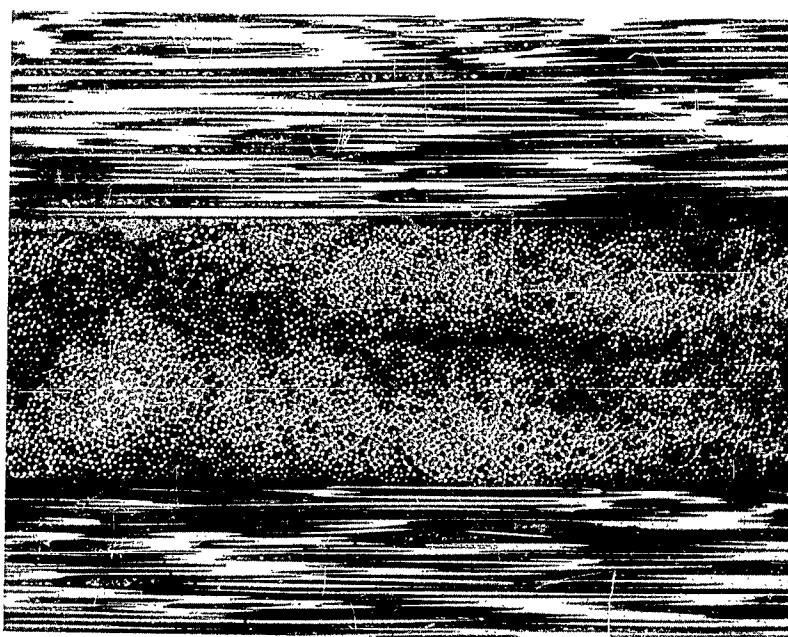
Circ.

Long.

Circ.

(3) Outer Plies
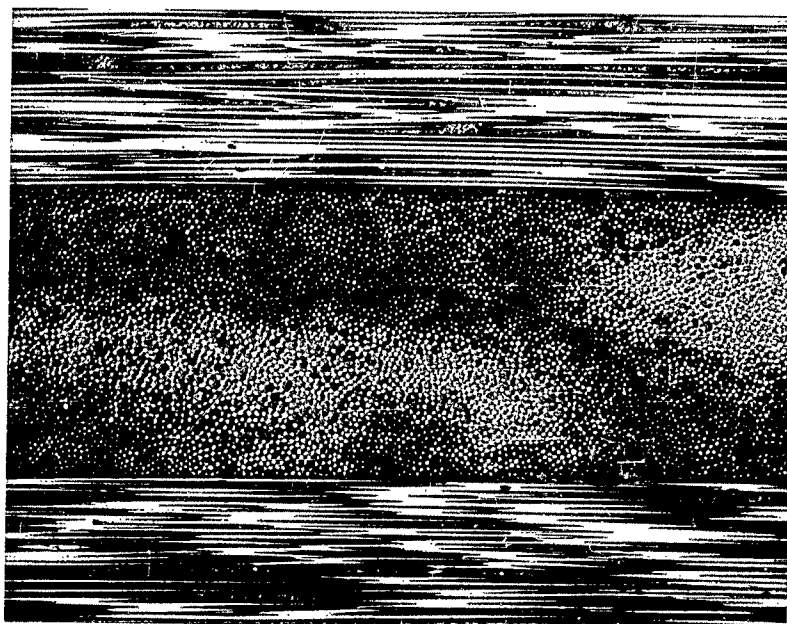
Circ.

Circ.

Long.

Circ.

(3) Inner Plies

TW-13 Looking at Ends of Longitudinal Filaments.
An Excellent Example of Uniform Construction with Good
Longitudinals and Few Resin-Rich Areas.

TW-13 Photomicrographs

Figure 35
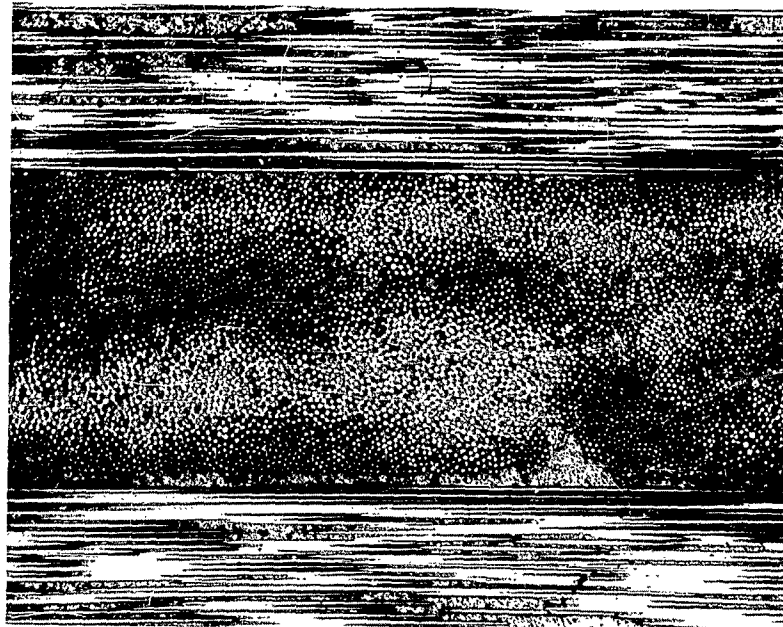
Circ.

Long.

Circ.

Looking at ends of Longitudinal Filaments
Showing Good Longitudinal Layer

Circ.

.Long.

Circ.

TW 15-1 Looking at Ends of Circumferential Filaments
Showing Generally Good Circumferential Filaments

TW-15 Photomicrographs

Figure 36

APPENDIX A

CIRCUMFERENTIAL FILAMENT-TENSIONING AND STRESS DISTRIBUTION

When a pressure vessel is subjected to high external pressures, various stresses are introduced into the structure. It is theoretically possible to build a fiber-reinforced plastic external-pressure vessel in which the combinations of stresses arising from external pressure, winding tension, and cure temperature can be bala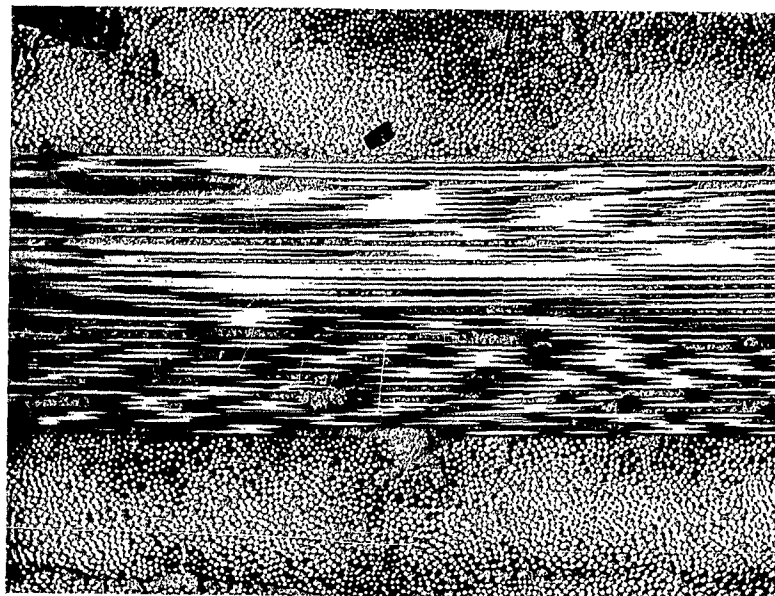nced to give an optimum stress pattern throughout the cross section of the vessel, provided the external pressure is known. The stress distribution for such a vessel is considered optimum when each layer of the anisotropic structure, such as a filament-wound cylinder, is equally stressed under a given external pressure.

In this case, the cylinders being considered are thick-walled and composed of many layers of glass filament with a resin matrix. Normally, for any external pressure vessel, the inner surface has a higher compressive stress than the outer surface at the time the vessel is subjected to external pressure. Winding-tension and cure stresses, however, produce a combination of compressive and tensile stresses across a cross section of the cylinder wall when they are considered by themselves. Since the cure stresses can be predicted but not controlled, and winding tensions can theoretically be controlled, there is a winding-tension pattern which will give a uniform stress in each layer of glass roving when combined with a known external pressure and predetermined cure stress.

The problem of analyzing and equalizing stresses in these vessels can be divided, therefore, into three basic categories - external pressure stresses (circumferential and radial), thermal stresses (cure), and winding tensions.

1. **External Pressure Stresses - Circumferential**

Circumferential stresses resulting from a known constant pressure (internal or external) may be calculated for a composite cylinder consisting of any number of laminations and any known material or combination of different materials, by the method of extensional stiffness distribution. The pressure in any lamination or ring is a product of the total pressure on the cylinder and the extensional stiffness of the ring in question, divided by the summation or total stiffness of the cylinder.

For a ring of unit width

$$\text{Extensional stiffness} = K = \frac{Et}{r^2} \tag{1}$$

where E = modulus of elasticity of ring material, t = cross-sectional ring thickness, and r = radius to middle surface of ring.

For n concentric rings, the total stiffness of a cylinder is

$$\sum K = K_1 + K_2 + K_3 + \ldots \ldots \ldots K_n \tag{2}$$

The pressure in the first ring is

$$P_1 = \frac{PK_1}{\sum K}$$

where P = total pressure in lb/sq in., or, in the nth ring,

$$P_n = \frac{PK_n}{\sum K} \tag{3}$$

The stress in each ring is the average stress across the thickness of the ring.

$$\sigma_1 = \frac{P_1 r_1}{t_1}$$

or, in the nth ring,

$$\sigma_n = \frac{P_n r_n}{t_n} \tag{4}$$

Stress in the nth ring can be calculated in terms of total
pressure, P, by combining Equations (3) and (4):

$$\sigma_n = \frac{PK_n r_n}{t_n \sum K} \tag{5}$$

From Equation (1) $\quad K_n = \dfrac{E t_n}{r_n^2}$

then $\qquad \sigma_n = \dfrac{PE}{r_n \sum K}$ (6)

For greater accuracy, rings may be subdivided into sub-
thicknesses and radii corresponding to their middle surfaces. Division of rings
beyond each layer of filament, however, would be of little value, since tension
control is limited to each lamination or ply.

2.   Thermal Stress Analysis

When a multilayered composite cylinder is subjected to
temperature differentials throughout the total thickness of the cylinder, or
when the cylinder is composed of laminate materials with different coefficients
of thermal expansion, with all layers raised to a constant differential temperature
with respect to the temperature at time of fabrication, then stress results
in each layer as a consequence of these energy changes. Since these energy
changes are internal, some of the layers must be in compression and others in
tension to maintain equilibrium within the structure of the cylinder.

In determining stresses resulting from thermal expansion, a
relaxation method is used. This method is similar to that cited for the deter-
mination of stress resulting from pressures as applied to internal or external
pressure vessels.

For any composite cylinder composed of n laminations, the
algebraic summation of the pressures caused by thermal stress across the wall
thickness of the cylinder must equal zero to maintain equilibrium.

A reference point may be assumed, which can most conveniently be selected as the temperature at the time of cylinder fabrication. Take any given ring within the cylinder raised or lowered to a new temperature and allow this ring to expand or contract unrestricted by adjacent rings. This dimensional change is noted. A pressure is then applied uniformly around the ring in order to contract or expand the ring radially to bring the ring back to the original dimension that existed at the assumed reference point prior to the temperature change; this thermal stress pressure is noted. The same procedure is used for each ring within the cylinder, and the thermal stress pressures are added together algebraically. Since the summation of the pressures must be zero for equilibrium, the summation is changed in sign and redistributed in accordance with the distribution of pressures by the stiffness method cited. This redistribution is then added to the initial pressures algebraically; the system is then balanced for equilibrium.

Formula for initial pressures by equating deflection:

$$\frac{Pr^2}{Et} + r\alpha\Delta t = 0$$

$$P = -\frac{Et\alpha\Delta t}{r} \tag{7}$$

when

P = pressure - lb/sq in.

E = modulus of elasticity - lb/sq in.

t = thickness - in.

α = coefficient of expansion - in./$^{\circ}$F

Δt = temperature differential - $^{\circ}$F

r = mean radius of lamination - in.

3.   Winding Tension Analysis

The effects of winding tension may be analyzed by the stiffness distribution method cited. A point of reference is made for zero radial displacement of filaments and mandrel, or at the point where there is no pressure upon the winding mandrel or filament layers due to tension in the glass roving.

A-4

Pressures are determined for each layer of glass roving or for multiple layers of roving using a constant tension setting. If variable tensioning or step tensioning is used throughout the buildup of the cylinder wall, then the pressure is determined for each step. The algebraic summation of these pressures is not in equilibrium and must be balanced by the stiffness distribution method to bring the structure and mandrel in equilibrium. If the mandrel is removed, the structure will change its stress distribution and another distribution must be made. The only change in the analysis is that the reference point must be changed when the redistribution is made in the filament structure using those pressures for the redistribution.
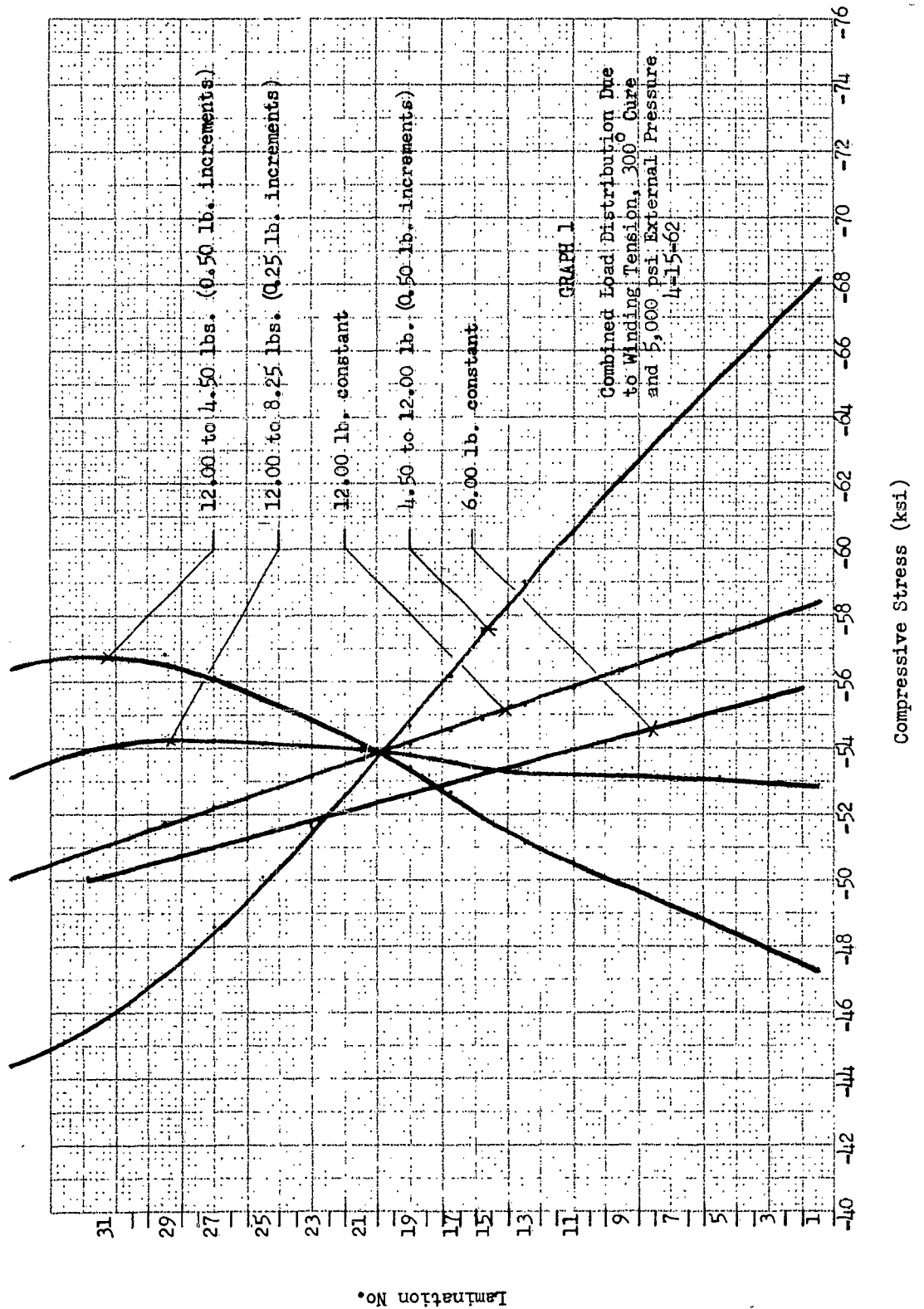
Step curing of filament structures for winding tension may be made in the same manner - the point at reference will change with each step cure. A redistribution will take place with removal of the mandrel.

4.   Summary

An approximate method is given to determine the effects of external pressure, thermal stresses, and winding tension. The solution for any given composite cylinder is a trial-and-error process. A fairly close final solution can be attained after two or three trials.

If the mandrel is a thick-walled homogeneous cylinder, the Lamé theory may be coupled with this theory for more exact analysis. The Lamé deflection equation for a thick-walled externally pressurized cylinder is used. A unit pressure is assumed, and the reciprocal of the deflection equation gives the stiffness of the mandrel, which is additive to the other stiffnesses.

Plotted curves showing the stress distribution throughout the cross section of a 0.310-in. thick by 6.0-in.-dia cylinder subjected to 5,000 psi pressurization is shown in Figure A-1. These curves were used for the determination of theoretically optimum filament tensioning programs for the initial 0.310-in. thick by 6.0-in.-ID test base cylinders, which were fabricated on a thick wall study program (NObs 86406, W.O. 0623-01).

GRAPH 1

Combined Load Distribution Due to Winding Tension, 300° Cure and 5,000 psi External Pressure
4-15-62

12.00 to 4.50 lbs. (0.50 lb. increments)

12.00 to 8.25 lbs. (0.25 lb. increments)

12.00 lb. constant

4.50 to 12.00 lb. (0.50 lb. increments)

6.00 lb. constant

Compressive Stress (ksi)

Lamination No.

Figure A-1

APPENDIX B

SCALE EFFECTS - THICK CYLINDRICAL LAMINATES

SCALE EFFECT - THICK CYLINDRICAL LAMINATES

A.   INTRODUCTION

Different size models of an elastic body which have all their correspond-
ing dimensions reduced, or increased, in the same ratio from some fixed standard
model are referred to here as being linearly scaled. It is the purpose of this
report to investigate on a rigorous theoretical basis if such linear scaling of
thick cylindrical laminated tubes will produce changes in the stress distribution
when the tubes are subjected to external pressures. Included also is the effect
of linearly scaling the elastic coefficients of the laminates.

The general governing equations are written, and then the displacements
and coordinates are non-dimensionalized with respect to an arbitrarily chosen
characteristic length. The elastic coefficients are also non-dimensionalized
with respect to a characteristic coefficient. The actual stresses are retained
in the formulation. Therefore, if this non-dimensionalizing procedure eliminates
the dependence of all governing equations on the actual size of the model, then,
obviously, the stress distribution obtained from the solution of these equations,
will also be independent on the size. Similar conclusions hold for the depend-
ence of the stress distribution on the actual value of the elastic constants.
However, in most cases, the models would be made from the same material and
therefore the scaling of the elastic constants would not be a factor to be con-
sidered.

B.   CONCLUSION

Theoretically, scaling does not upset the stress distribution, and the
buckling load, when buckling occurs, will be only a function of non-dimensional
length and coefficients.

C.   SOME PRACTICAL ASPECTS

On the practical side there will be a limit beyond which any further scaling down of the models will begin to produce different stress distribution for the same surface stresses. The following two considerations illustrate how this could happen.[*] First, consider two laminations, as shown in Figure 2 below:
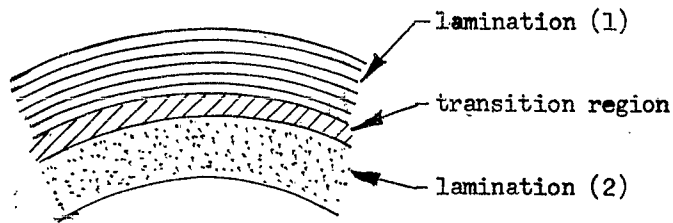
Figure 2

During the manufacture of laminated structures there will be a region between the laminates which cannot be considered to belong to either of laminations; this we will label the transition region. In any theoretical analysis it is usually assumed that this region is so thin that it is in fact a line discontinuity, and this is a good actual approximation for a wide range of sizes of the laminates. However, as the laminates are scaled down the transition region will not, in general, be scaled down in the same ratio since really there is no control over its width and it is only a function of the manufacturing process. In fact, it is likely that the width of the transition region will remain

---

[*] Fortunately, these two effects are not of importance for the present state of the art and current manufacturing techniques.

reasonably constant. Suppose now that the dimensions of the model are scaled down further and we now have the situation shown below in Figure 3.
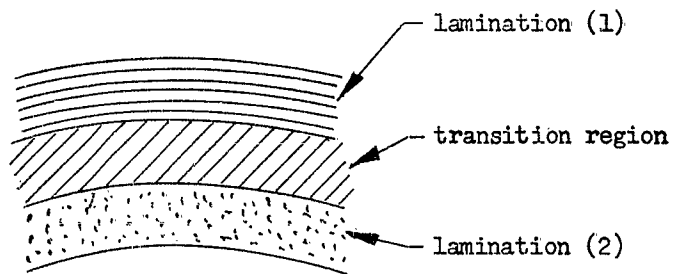
Figure 3

It is obvious that due to the increased relative dimension of the transition region, the two models are now not linear scales of each other, and, therefore, for the same applied surface stresses the two models will have different stress distribution.

The second effect that can produce different stress distribution as the model is scaled down, is the following. The laminates can be considered as homogenous orthotropic material if there are a large number of fibers in the cross-section of the lamination. However, let us suppose that during scaling the fiber size remains constant and therefore when the model has been reduced to some small size the cross-section may have a relatively small number of fibers and may look something like Figure 4.

fibers

resin
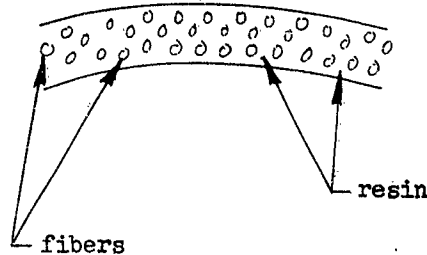
Figure 4

It is obvious that the cross-section is now no longer homogenous and therefore the scaling will again change the stress distribution; in fact, it will be impossible to define an effective modulus since the averaging process will break down.

At first it seems that the effects which will upset the scaling of laminated models are things which cannot be readily estimated. However, this is not always the case. One way of estimating the limit beyond which scaling will begin to change the stress distribution is to manufacture a range of different sizes of similar laminated models and load them with equal surface stresses or pressures. Concentrated loads can be used but it must be remembered that these must be varied as the square of the characteristic length of each model. Some suitable displacements or strains can be measured for each model and the ratio of these displacements to the characteristic length of the model plotted against the characteristic length. The plot will have the form shown in Figure 5.

$$\frac{\text{displacement}}{\text{length}} = \frac{d}{L}$$

scaling not good

scaling can be used

limiting value of scaling

L = characteristic length
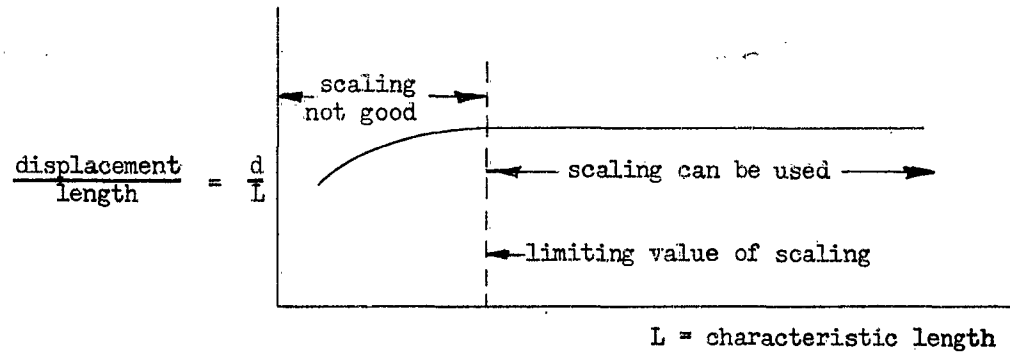
Figure 5

In the region where the curve is straight the scaling will not produce a change in the stress distribution. The region where the curve begins to deviate from the straight line the scaling begins to change the stress distribution.

What type of experiments could be carried out to produce such results would depend on the ease of manufacture of the models, and the choice of loading would depend on available equipment. For example, a square laminated plate, clamped on its edges, could be used and be loaded with a concentrated load in the center; the displacement measured could be the lateral displacement of the center point. Alternately, if a circular cylinder could be used and loaded with internal pressure, the increase in the diameter could be measured. And, of course, there are many other possible arrangements of this experiment which could be set up.

D. **PROOF THAT STRESS IS INDEPENDENT OF MODEL SIZE**

1. Equilibrium Equations for an Element (see Love[*], p. 90)

(see p. 12 for List of Symbols)

$$\frac{\partial \sigma r}{\partial r} + \frac{1}{r}\frac{\partial \sigma r\theta}{\partial \theta} + \frac{\partial \sigma rz}{\partial z} + \frac{\sigma r - \sigma \theta}{r} = 0$$
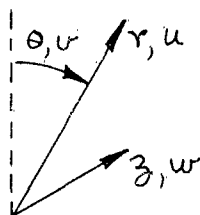
$$\frac{\partial \sigma r\theta}{\partial r} + \frac{1}{r}\frac{\partial \sigma \theta}{\partial \theta} + \frac{\partial \sigma \theta z}{\partial z} + \frac{2\sigma r\theta}{r} = 0$$

$$\frac{\partial \sigma rz}{\partial r} + \frac{1}{r}\frac{\partial \sigma \theta z}{\partial \theta} + \frac{\partial \sigma z}{\partial z} + \frac{\sigma rz}{r} = 0 \qquad (1)$$
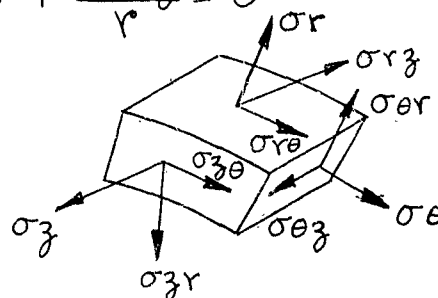
Cylindrical Coordinates   Element of the Shell

2. Strain Displacement Relations (see Love[*], p. 56)

$$\epsilon r = \frac{\partial u}{\partial r} \;, \quad \epsilon \theta = \frac{1}{r}\frac{\partial v}{\partial \theta} + \frac{u}{r} \;, \quad \epsilon z = \frac{\partial w}{\partial z}$$

$$\epsilon \theta z = \frac{1}{r}\frac{\partial w}{\partial \theta} + \frac{\partial v}{\partial z} \;, \quad \epsilon zr = \frac{\partial u}{\partial z} + \frac{\partial w}{\partial r} \;, \quad \epsilon r\theta = \frac{\partial v}{\partial r} - \frac{v}{r} + \frac{1}{r}\frac{\partial u}{\partial \theta} \qquad (2)$$

[*] Love, A. E. H., "A Treatise on the Mathematical Theory of Elasticity", Dover Publ., New York, N. Y., 4th Ed.

where u, v, w are the radial, axial, and tangential displacements respectively, of a general point in the tube.

3.   Strain-Stress Relations

It is assumed that each lamination has symmetry about three axes, r, z, and θ, that is the material is orthotropic,

$$\epsilon_r = \frac{1}{E_r}\left[\sigma_r - \nu_{r\theta}\sigma_\theta - \nu_{rz}\sigma_z\right]$$

$$\epsilon_\theta = \frac{1}{E_\theta}\left[\sigma_\theta - \nu_{\theta z}\sigma_z - \nu_{\theta r}\sigma_r\right]$$

$$\epsilon_z = \frac{1}{E_z}\left[\sigma_z - \nu_{zr}\sigma_r - \nu_{z\theta}\sigma_\theta\right]$$

$$\epsilon_{\theta z} = \frac{1}{G_{\theta z}}\sigma_{\theta z} \tag{3}$$

$$\epsilon_{zr} = \frac{1}{G_{zr}}\sigma_{zr}$$

$$\epsilon_{r\theta} = \frac{1}{G_{r\theta}}\sigma_{r\theta}$$

In equations (3) there are 12 coefficients; however, only 9 are independent since

$$\frac{\nu_{r\theta}}{E_r} = \frac{\nu_{\theta r}}{E_\theta}$$

$$\frac{\nu_{rz}}{E_r} = \frac{\nu_{zr}}{E_z}$$

$$\frac{\nu_{\theta z}}{E_\theta} = \frac{\nu_{z\theta}}{E_z}$$

These follow from Maxwell's Reciprocal Relations.

Consider now a tube composed of n laminations. Shown in
Figure 1 are the inner, the outer and a general ith lamination. The radius r_i
does not have to be a constant but can be a function of the angle Θ. In this
way the effect of imperfections can be incorporated. It is assumed, without
any loss of generality, that the inside is at zero pressure and the outside of the
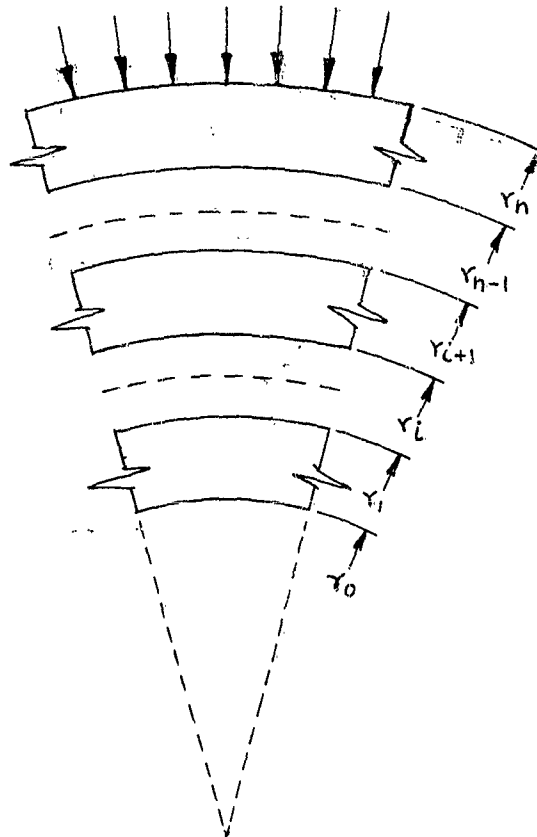tube is subject to a pressure p.

Figure 1

4. **Non-Dimensional Form of Equations**

For each lamination there will be a set of equations such as (1), (2), and (3). Furthermore for each lamination there will be in general nine elastic coefficients. To denote the quantities belonging to the ith lamination we introduce the subscript notation,

$$\sigma_{\theta i}, \quad \sigma_{r i}, \quad \sigma_{z i}, \quad \text{etc.}$$

$$\varepsilon_{r i}, \quad \varepsilon_{\theta i}, \quad \varepsilon_{z i}, \quad \text{etc.}$$

$$u_i, \quad v_i, \quad w_i$$

$$E_{r i}, \quad E_{\theta i}, \quad E_{z i}, \quad \nu_{r\theta i}, \quad \nu_{\theta z i}, \quad \nu_{z r i}$$

We now choose, arbitrarily, one particular length as a characteristic length. Let us take r_o, the inside radius, and write it

$$r_o = r_o' + r_o'' (\theta)$$

where r_o' is a constant

and $r_o'' (\theta)$ is a function of θ, allowing for possible initial deformation r_o' can be taken as our characteristic length, of course any other length could be used just as well. We also choose one elastic coefficient as characteristic quantity, for example take E_{r_o}

Non-dimensionalizing, put

$$r = \bar{r} \, r_o' \quad , \quad \theta = \bar{\theta} \quad , \quad z = \bar{z} \, r_o'$$

$$u_i = \bar{u}_i \, r_o' \quad , \quad v_i = \bar{v}_i \, r_o' \quad , \quad w_i = \bar{w}_i \, r_o'$$

$$E_{r i} = \bar{E}_{r i} \, E_{r o} \quad , \quad E_{\theta i} = \bar{E}_{\theta i} \, E_{r o} \, , \quad E_{z i} = \bar{E}_{z i} \, E_{r o}$$

B-9

Equations (1), (2), and (3) can not be rewritten in the non-dimensional form. By multiplying equations (1) by r_0, we get,

$$\frac{\partial \sigma_{ri}}{\partial \overline{r_i}} + \frac{1}{\overline{r}} \frac{\partial \sigma_{r\theta i}}{\partial \overline{\theta}} + \frac{\partial \sigma_{rzi}}{\partial \overline{z}} + \frac{\sigma_{ri} - \sigma_{\theta i}}{\overline{r}} = 0$$

$$\frac{\partial \sigma_{r\theta i}}{\partial \overline{r}} + \frac{1}{\overline{r}} \frac{\partial \sigma_{\theta i}}{\partial \overline{\theta}} + \frac{\partial \sigma_{\theta zi}}{\partial \overline{z}} + \frac{2\sigma_{r\theta i}}{\overline{r}} = 0 \qquad (4)$$

$$\frac{\partial \sigma_{rzi}}{\partial \overline{r}} + \frac{1}{\overline{r}} \frac{\partial \sigma_{\theta zi}}{\partial \overline{\theta}} + \frac{\partial \sigma_{zi}}{\partial \overline{z}} + \frac{\sigma_{rzi}}{\overline{r}} = 0$$

Strain-displacement relations, equations (2), become,

$$\epsilon_{ri} = \frac{\partial \overline{u}_i}{\partial \overline{r}} \quad , \quad \epsilon_{\theta i} = \frac{1}{\overline{r}} \frac{\partial \overline{v}_i}{\partial \overline{\theta}} + \frac{\overline{u}_i}{\overline{r}} \quad , \quad \epsilon_{zi} = \frac{\partial \overline{w}_i}{\partial \overline{z}}$$

$$\epsilon_{\theta zi} = \frac{1}{\overline{r}} \frac{\partial \overline{v}_i}{\partial \overline{\theta}} + \frac{\partial \overline{v}_i}{\partial \overline{z}} \quad , \quad \epsilon_{zri} = \frac{\partial \overline{u}_i}{\partial \overline{z}} + \frac{\partial \overline{w}_i}{\partial \overline{r}} \qquad (5)$$

$$\epsilon_{r\theta i} = \frac{\partial \overline{v}_i}{\partial \overline{r}} - \frac{\overline{v}_i}{\overline{r}} + \frac{1}{\overline{r}} \frac{\partial \overline{u}_i}{\partial \overline{\theta}}$$

Multiplying equations (3) by Er_0, we get

$$\epsilon_{ri} = \frac{1}{E_{ri}} \left[\sigma_{ri} - \nu_{r\theta i} \sigma_{\theta i} - \nu_{rzi} \sigma_{zi} \right]$$

$$\epsilon_{\theta i} = \frac{1}{E_{\theta i}} \left[\sigma_{\theta} - \nu_{\theta zi} \sigma_{zi} - \nu_{\theta ri} \sigma_{ri} \right]$$

$$\epsilon_{zi} = \frac{1}{E_{zi}} \left[\sigma_{zi} - \nu_{zri} \sigma_{ri} - \nu_{z\theta i} \sigma_{\theta i} \right] \qquad (6)$$

$$\epsilon_{\theta zi} = \frac{1}{G_{\theta zi}} \sigma_{\theta zi}$$

$$\epsilon_{zri} = \frac{1}{G_{zri}} \sigma_{zri}$$

$$\epsilon_{r\theta i} = \frac{1}{G_{r\theta i}} \sigma_{r\theta i}$$

By the use of equations (5) and (6) equation (4) can be expressed in terms of $\overline{u_i}, \overline{v_i}, \overline{w_i}$, and the non-dimensional elastic constants. Therefore, theoretically the three equations, for each lamination, can be solved for the non-dimensional displacements in terms of the non-dimensional elastic coefficients and the non-dimensional polar coordinates $\overline{r}, \overline{z}$, and $\overline{\theta}$. From equations (5) and (6) the dimensional stresses can be calculated and they are obviously dependent on non-dimensional coordinates and elastic coefficients only. The solution can be completed by matching the stresses and non-dimensional displacement on the boundaries between the laminations and at any axial stations where there are discontinuities.

It is obvious from the above discussion that any general elastic problem of the laminated shells can be formulated in terms of the non-dimensional elastic constants, and the dimensional stresses. Therefore, any set of geometric models having exactly the same non-dimensional configurations (all dimensions linearly scaled), the same non-dimensional elastic constants, and identical surface stresses, will have identical dimensional stress distribution, independent of actual size of the model.

The introduction of the general elastic equations in this section has been only for the purpose of illustrating how they can be made independent of actual size of the elastic model. Any actual solutions of these equations for a general laminated shell, loaded with arbitrary surface loads, is of course impossible, nor is it necessary for the present discussion.

LIST OF SYMBOLS

$$\left.\begin{array}{c} \sigma_r \\ \sigma_\theta \\ \sigma_z \\ \sigma_{r\theta} \\ \sigma_{\theta z} \\ \sigma_{z\theta} \end{array}\right\}$$ Six components of the stress in cylindrical coordinate system.

$$\left.\begin{array}{c} \epsilon_r \\ \epsilon_\theta \\ \epsilon_z \\ \epsilon_{r\theta} \\ \epsilon_{\theta z} \\ \epsilon_{zr} \end{array}\right\}$$ Six components of the strain in cylindrical coordinate system.

u Radial Displacement

v Circumferential Displacement

w Axial Displacement

r Radial Coordinate

θ Circumferential Coordinate

z Axial Coordinate

B-12

E_r Youngs modulus in the axial direction.

E_θ Youngs modulus in the circumferential direction.

E_z Youngs modulus in the axial direction.

$G_{r\theta}$ Shear modulus in the $\gamma - \theta$ plane.

$G_{\theta z}$ Shear modulus in the $\theta - z$ plane.

G_{zr} Shear modulus in the $z - \gamma$ plane.

$$\left. \begin{array}{l} \nu_{r\theta} \\ \nu_{\theta r} \\ \nu_{rz} \\ \nu_{zr} \\ \nu_{\theta z} \\ \nu_{z\theta} \end{array} \right\}$$ Poisson's ratios, the first index denotes the direction of the strain, the second denotes the direction of the stress.

i Indicates the quantity associated with the ith laminate.

B-13

DISTRIBUTION

	No. of Copies
Chief, Bureau of Ships (Code 634C) Navy Department Washington 25, D.C. Via: BuWepsRep., Azusa	9
Chief, Bureau of Ships (Code 335) Navy Department Washington 25, D.C. Via: BuWepsRep., Azusa	3
BuWepsRep., Azusa	1
Commanding Officer and Director David W. Taylor Model Basin (Mr. A. Willner - Code 735) Washington 7, D.C.	1
Commanding Officer and Director David W. Taylor Model Basin (Mr. J. Pulos - Code 731) Washington 7, D.C.	1
Commanding Officer and Director David W. Taylor Model Basin (Mr. J. Buhl - Code 727) Washington 7, D.C.	1
Commander, New York Naval Shipyard (Code 9350) Naval Base Brooklyn 1, New York	2
Chief, Bureau of Naval Weapons (RRMA) Navy Department Washington 25, D.C.	1
Chief, Bureau of Naval Weapons (RMMP-23) Navy Department Washington 25, D.C.	1
Commander, US Naval Ordnance Laboratory (Dr. A. Lightbody) Silver Spring, Md.	1

DISTRIBUTION (cont.)

No. of Copies

Commander, U.S. Naval Ordance Laboratory   1
(Mr. F. R. Barnet)
Silver Spring, Md.

Chief of Naval Research   1
(Dr. J. Shenk)
Navy Department
Washington 25, D.C.

Chief of Naval Research   1
(Dr. H. Liebowitz)
Navy Department
Washington 25, D.C.

Commanding General, Aeronautical   2
Systems Division (ASRCNC-1)
Wright Patterson Air Force Base, Ohio

Director, Plastics Technical Evaluation Center   2
Picatinny Arsenal
Dover, New Jersey

Director, U.S. Naval Research Laboratory   1
(Mr. J. Kies)
Washington 25, D.C.

Director, U.S. Naval Research Laboratory   1
(Mr. J. Cowling)
Washington 25, D.C.

Chief, Bureau of Naval Weapons   1
Special Projects Office (Mr. H. Bernstein)
Washington 25, D.C.

Commander U.S. Naval Ordnance Test Station   1
(Mr. S. Herzog - 5557)
China Lake, California

Armed Services Technical Information Agency   10
Arlington Hall Station
4000 Arlington Boulevard
Arlington 12, Virginia

DISTRIBUTION (cont.)

	No. of Copies
NARMCO Research & Development Division of Telecomputing Corporation (Mr. B. Duft) 3540 Aero Court San Diego 11, California	1
Armour Research Foundation (Dr. J. W. Dally) Illinois Institute of Technology 10 W. 35th Street Chicago 16, Illinois	1
General Motors Corporation (Dr. R. B. Costello) Defense Systems Division, Santa Barbara Laboratories Box T Santa Barbara, California	1
Battelle Memorial Institute (Dr. R. Leininger) 505 King Avenue Columbus, Ohio	1
H. I. Thompson Fiberglass (Mr. N. Meyers) 1600 W. 135th Street Gardena, California	1
Owens-Corning Fiberglas Corp. (Mr. R. J. Weaver) 806 Connecticut Avenue, N.W. Washington 6, D.C.	1
US Rubber Research Center (Mr. E. Francois, Jr.) Wayne, New Jersey	1
Shell Chemical Company (Mr. R. E. Bayes) Plastics & Resin Division 110 W. 51 Street New York 20, New York	1
North American Aviation Inc. (Mr. R. Gorcey) Rocketdyne Division 6633 Canoga Avenue Canoga Park, California	1

DISTRIBUTION (cont.)

	No. of Copies
Hercules Powder Company (Mr. J. A. Scherer) 910 Market Street Wilmington 99, Delaware	1
Brunswick Corporation (Mr. W. McKay) Marion, Virginia	1
Douglas Aircraft Corporation (Mr. J. H. Cunningham) Missile and Space Systems Division 3000 Ocean Park Boulevard Santa Monica, California	1
U.S. Naval Ordnance Test Station (Mr. J. L. Phillips - P-8082) 3202 E. Foothill Boulevard Pasadena, California	1
Goodyear Aircraft Corporation 1210 Massillon Road Akron, Ohio	1
A. O. Smith Corporation (Mr. W A. Deringer) Milwaukee 1, Wisconsin	1
University of Illinois (Prof. H. T. Corten) Dept. of T & AM Urbana, Illinois	1
AVCO Corporation (Undersea Projects Directorate) 201 Lowell Street Wilmington, Massachusetts	1
Union Carbide Plastics Corporation (Mr. Charles Platt) Brunswick, New Jersey	1
Internal	34